A Keldysh approach to shot noise in quantum point contacts

Submitted by
Andreas Tsevas

BACHELOR THESIS

Faculty of Physics
at Ludwig-Maximilians-Universität
Munich

Supervisor:
Prof. Dr. Jan von Delft

Munich, November 22, 2018

Untersuchung von Schrotrauschen in Quantenpunktkontakten mit dem Keldysh Formalismus

Vorgelegt von
Andreas Tsevas

BACHELORARBEIT

Fakultät für Physik
Ludwig-Maximilians-Universität
München

Betreuer:
Prof. Dr. Jan von Delft

München, November 22, 2018

Abstract

The topic of this thesis is the investigation of shot noise as a transport phenomenon in mesoscopic low-dimensional inhomogeneous systems, in particular quantum point contacts. After general considerations about noise in the framework of scattering theory and the system at hand, the Keldysh formalism is introduced as a way to calculate correlation functions in many-body systems. This formalism is used for the calculation of the necessary propagators as well as the derivation of the relevant physical observables. Interacting results are obtained numerically through the use of the functional Renormalization Group. Finally, these results are presented and compared to previous results from scattering theory along with experimental measurements, as a way of presenting the benefits of the new approach in the understanding of noise terms.

Contents

1 Introduction

1.1 Motivation

The last decades have seen the rise and refinement of new methods of describing quantum many-body systems. The Keldysh formalism has been established as a powerful alternative to the Matsubara formalism that comes with many benefits [Kam11]. Firstly, it avoids complications that arise from a transformation to imaginary time resulting in the necessity of an analytical continuation of the imaginary to the real axis, which is often quite bothersome. Furthermore, it is able to treat non-equilibrium systems. Of course, this comes at some cost: the introduction of a tensor structure to the propagators.

The extension of the functional Renormalization Group to Keldysh formalism is a relatively new emerging field, which allows for the handling of infrared divergences, non-linear dispersion models and out-of-equilibrium states, along with the ability to perform calculations at real frequencies and describe large systems [GPM07] [JPS10a] [JPS10b] [Sch18] [Jak10]. In a nutshell, it achieves its goal of calculating vertex functions up to a certain order by solving an infinite hierarchy of coupled differential equations and neglecting higher order terms.

The arrival and study of these methods presents us with the opportunity to apply them to known quantum systems with a double purpose: firstly, one wishes to study the application of these methods in a somewhat familiar environment with the goal of 'testing' them in the field, understanding their benefits and drawbacks, as well as refining and adapting them to ever-new situations. Secondly, we have the goal of gaining a deeper theoretical knowledge of the systems under investigation and using the new methods to their fullest extent, so as to be able to investigate completely new realms that were not accessible to us with previous methods.

In this case, we investigate specific transport properties of the so-called quantum point contact. It only became possible to construct such a system in the last few decades, following improvements in high-quality materials and micro-fabrication techniques [vKv⁺88]. In recent years there has been peaked interest in the study of this system, which boils down to a low-dimensional electrons gas imprinted with an external potential. Being on a mesoscopic scale, it combines a high particle number with the necessity of quantum treatment. While many effects, such as the quantization of the conductance [Lan57], were predicted decades ago, it took a long time to fully understand many of the transport properties of the system, such as the 0.7 anomaly, which is induced by interactions in the quantum point contact [Mic11] [BHS⁺13].

Noise is a useful fundamental feature since it is connected to properties of the system generating the noise and, thus, provides deeper knowledge about both its equilibrium and transport state. While there have been experimental measurements concerning noise [DZM⁺06] [BGG⁺05], up to now there has not yet been a theoretical treatment and understanding of the phenomenon in this specific context that goes beyond basic scattering theory and zero-frequency predictions and accounts for the effects of interactions. Thus, the goal of this thesis is the study of the noise properties of this system in the framework of the aforementioned formalism.

1.2   Outline of this thesis

Following the aim of analyzing noise within the Keldysh formalism, the necessary concepts and considerations are introduced step by step:

Firstly, there is an introduction into the system under consideration. The basic setup of the quantum point contact is described and an overview over some important experimental results is given, while the main assumptions about a theoretical model that is capable of describing such a system are analyzed. This is done in **section 2**.

Then we turn our attention to noise in general, its definition and an analysis of the different kinds of noise. The Schottky formula for shot noise is motivated at this point through various calculations. What follows is an overview over scattering theory and its predictions for our case. This is all realized in **section 3**.

The Keldysh formalism is a central concept to this thesis as a tool to calculate correlation functions in quantum many-body systems. The closed time contour, which is the basic concept of this framework, is introduced along with Greens functions, with no prior knowledge besides quantum mechanics required. Furthermore, Wick's theorem is motivated as the basic building block, which is the basis for most calculations within quantum field theory. A reference to the exact form of the fluctuation dissipation theorem in the Keldysh formalism is made. Afterwards, we turn our attention to the calculation of the Greens functions that have just been introduced. We find a closed expression for the free propagators in the Keldysh formalism through the infinitesimal limit of a discrete approach, while we describe the methodology of calculating exact propagators through Wick's theorem. This is done in **section 4**.

At this point, all the necessary tools have been introduced to perform specific calculations in our system. We motivate the exact choice of the Hamiltonian of the QPC and then proceed to express the current and the noise of the system in terms of Keldysh Greens functions in **section 5**.

Finally, we proceed with the presentation of our results. The calculations were implemented at the chair of Prof. von Delft at the LMU Munich with the use of the Leibniz Rechenzentrum. After an overview over the functional Renormalization Group, which is the cornerstone of the numeric simulation and which has been implemented by Lukas Weidinger, we delve into some intricacies of our implementation. Then, we proceed with the illustration of the results through various plots of the noise terms and we compare them to both experimental measurements and theoretical predictions of scattering theory. This is performed in **section 6**.

The results of this thesis are summarized in the **Conclusion**. Here the results of the thesis as well as the challenges that have been overcome are listed. At the end, an outlook on future challenges and goals is given, both on a theoretical and an implementation-wise level.

2 Quantum point contact

2.1 The setup

The system under consideration in this thesis is a quantum point contact (QPC). It can be realized experimentally by generating a two dimensional electron gas embedded in a plane between two semi-conductors (eg. GaAs - AlGaAs) and imprinting this gas with a potential generated by external gates. We assume that these gates are constructed in such a way that their field lines penetrate the semiconductors and split the electron gas into two baths which are connected by a narrow path. Depending on the form of the potential in this bath, the system is called either a quantum wire (if the potential is long and flat), a quantum dot (if localized states are possible, i.e. if the potential has a minimum) or a quantum point contact (if the potential has the form of a saddle).
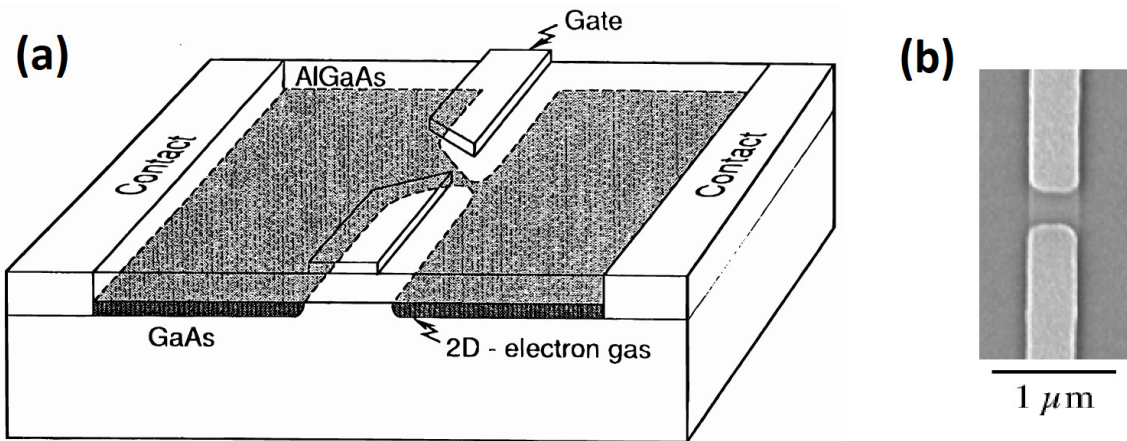
Figure 1: (a) Schematic cross-sectional view of a quantum point contact, defined in a high-mobility 2D electron gas at the interface of a GaAs–AlGaAs heterojunction [vHB05]. The point contact is formed when a negative voltage is applied to the gate electrodes on top of the AlGaAs layer. Transport measurements are made by employing contacts to the 2D electron gas at either side of the constriction. (b) Micrograph of a typical QPC [CLGG$^+$02].

Within this plane, the electrons may scatter off impurities, phonons or other electrons. In our case, we restrict ourselves to low temperatures and are thus able to neglect interactions with phonons. By assuming that the structure which we observe is smaller than the mean distance between impurities, we can also neglect the effects of impurities. As a result, we are only left with electron-electron interactions which are mediated through the Coulomb force. Since the region under consideration is small (mesoscopic scale), transport is phase coherent and a quantum mechanical description is required.

We call the two baths, which are connected through the QPC, reservoirs or leads. We assume that they are large enough to be characterized by temperatures T_L (left), T_R (right) and chemical potentials μ_L, μ_R. We assume the reservoirs to be large compared to the QPC, which only represents a small perturbation of the equilibrium systems.

On a mesoscopic scale, we can assume that the motions of the electrons longitudinal (along the narrow path) and transverse (across the path) are separable. Longitudinal eigen-

states are morally characterized by the continuous wave vector k_l with corresponding energy $E_l = \frac{\hbar^2 k_l^2}{2m}$, where $\hbar$ is the reduced Planck constant and m is the electron mass. The transverse motion is quantized and described by the discrete index n with corresponding energy E_n. Thus, for a given total energy $E = E_n + E_l$ only a finite amount of channels exists. By reducing the width of the quantum point contact through the external gates, it is even possible to eliminate all transverse states except one. Thus, such a system can be treated as one-dimensional, since there are no degrees of freedom in any direction except the longitudinal.

The form of the potential of a QPC along the longitudinal direction is simply an inverted parabola with a maximum at the center. The height of the potential barrier determines the magnitude of the current that flows between the two baths when applying a relative voltage between them; such a voltage is called source-drain bias voltage. If the source-drain bias voltage is zero and there is no temperature gradient, then no current will flow. The differential conductance G is a useful quantity to describe this phenomenon: it measures how much current can flow by increasing the source-drain bias voltage and is defined as the derivative of the current with the respect to the source-drain bias voltage:[1]

$$G = \frac{\partial I}{\partial V_{sd}}$$
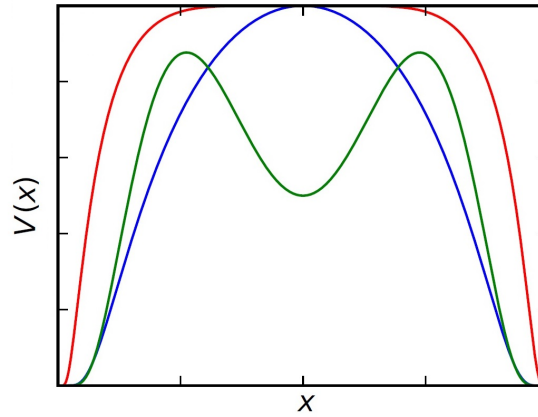
Figure 2: Potential along the longitudinal axis of the path. The blue parabola is a QPC, the red curve that flattens in the center is a quantum wire and the green curve is a quantum dot. [Sch18]

2.2 Experimental data

The quantization of the momentum in the transversal direction leads to a quantization of the conductance. Practically, the conductance counts the number of transmitting modes in units of e^2/h. In the case of no magnetic field, this number is increased by 2 each time a new transverse mode is added due to the spin degeneracy of electrons. In the presence of a

---

[1]Note that there is also the linear conductance, which is defined as the derivative of the current with respect to the source-drain bias voltage at zero voltage, i.e. $G_{\text{lin}} = \left. \frac{\partial I}{\partial V_{sd}} \right|_{V_{sd}=0}$. However, in this thesis we are often interested in the transport state of the system at $V_{sd} \neq 0$.

magnetic field, the up- and down-electrons can be regarded separately - each adding their own stepwise contributions to the conductance.

In this thesis, we focus mainly on a QPC with a single transverse mode, i.e. we are going to focus on the first conductance step from $G = 0$ to $G = 2e^2/h$.

We are interested in the changes in the conductance G under variation of our external parameters temperature T, external magnetic field B, gate voltage V_g and source-drain bias voltage V_{sd}.

Figure 3 shows the conductance as a function of the gate voltage while the magnetic field is varied. Note that the conductance step becomes increasingly asymmetrical as the magnetic field is increased. This irregularity can be attributed to the strong suppression of the conductance in the subopen regime (G at around $0.7 \times 2e^2/h$), hence the name 0.7 anomaly. This effect is caused by interactions between electrons. Practically, this shows that it does not suffice to model the electrons as free particles.
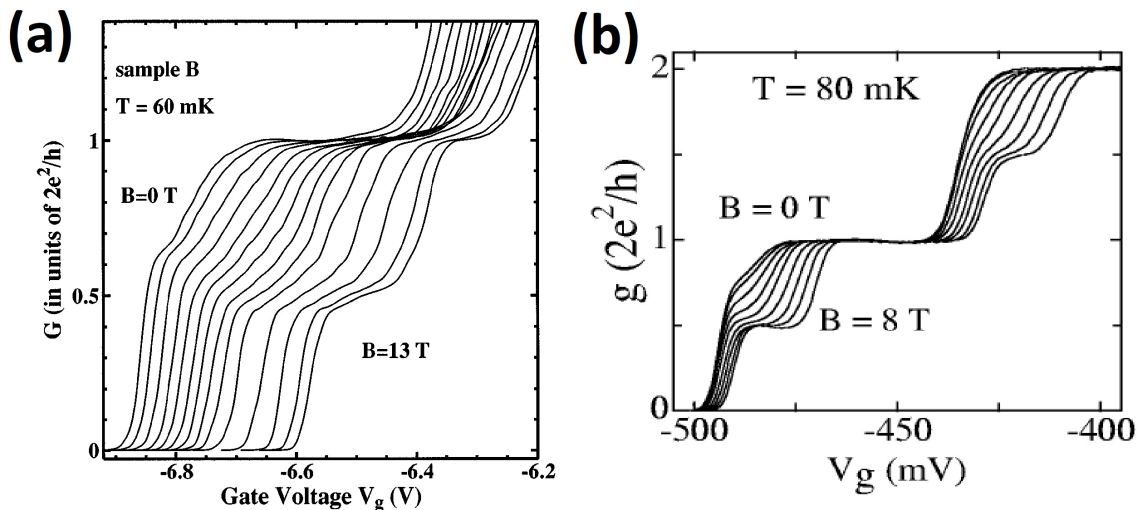
Figure 3: Experimental measurements of the conductance as a function of the gate voltage under variation of the magnetic field. (a) [TNS$^+$96] (b) [CLGG$^+$02].

Figure 4 shows the conductance as a function of the gate voltage with the temperature being varied this time. By increasing the temperature, the conductance step is flattened out. However, once again this flattening is highly asymmetric, as the conductance is strongly suppressed in the subopen regime; in fact, this suppression is much stronger than the thermal broadening. Once again, this can be attributed to interactions between electrons.
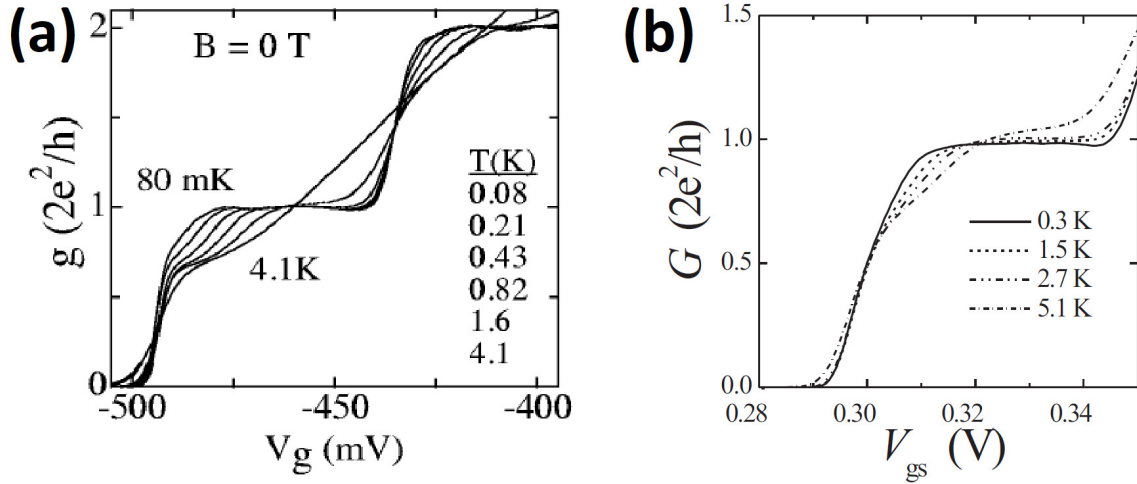
Figure 4: Experimental measurements of the conductance as a function of the gate voltage under variation of the temperature with no magnetic field. (a) [CLGG+02] (b) [KBH+00].

Figure 5 shows how the conductance changes when the source-drain bias voltage is varied at fixed temperature and magnetic field. Once again, this illustrates the step-like nature of the conductance in a QPC.
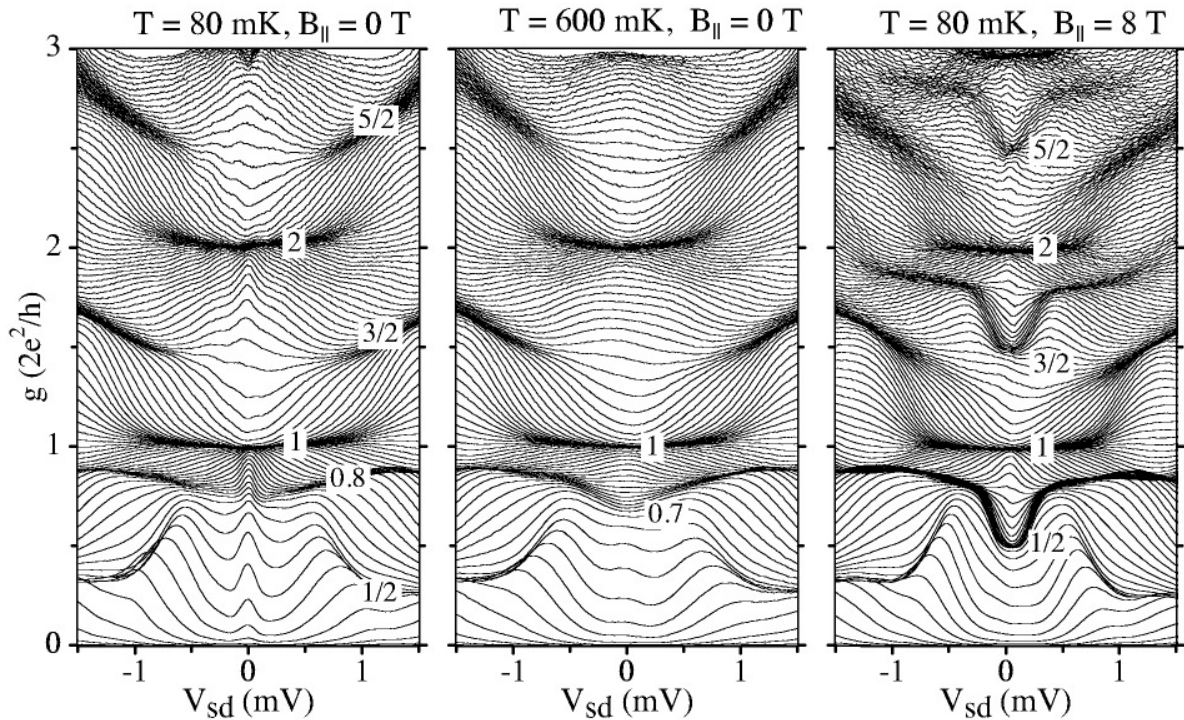
Figure 5: Experimental measurements of the conductance as a function of the source-drain bias voltage, at various temperatures, magnetic fields and gate voltages. [CLGG+02]

2.3 Our model

We model the QPC as a discrete one-dimensional tight-binding chain. The first and the last site in this chain are coupled to the respective leads. Since the leads are in equilibrium and we are interested in the QPC, we assume that the electrons in the leads are non-interacting and that the coupling between the leads and the QPC is also non-interacting. Basically, we are able to treat the two-dimensional electron gas in the leads as a Fermi liquid. However, this breaks down in the QPC and the resulting interaction in the narrow region has to be treated explicitly. Thus, only the Hamiltonian of the chain itself may contain terms that are not quadratic in creation/annihilation operators. Physically, the leads act as non-interacting baths for our system. With regard to practical calculations, this simply corresponds to additional terms in the Wick expansion of our interaction Hamiltonian. (see section (4.6))

We assume that the Coulomb-force is short ranged, since the assumption is often well-justified that the surrounding materials can rearrange so that the Coulomb interaction is sufficiently screened. Basically, we are interested in physics at timescales much larger than $\frac{\text{length of QPC}}{\text{speed of light in material}}$ and assume that the density of the materials is high enough to provide such a screening. With the simplifications above, there can only be the following kinds of terms in our QPC-Hamiltonian: those which describe the static potential at each site of the chain, those which describe the hopping of the electrons between adjacent sites and those that describe the interaction / coupling between two electrons.

After this brief overview about the basic concepts of a QPC, it is time to introduce some other basic concepts regarding noise and the Keldysh formalism.

3 Noise

When one applies a constant magnetic field and a constant voltage to a QPC, typically a stationary current arises, whose measurement gives us information about the system under consideration. However, one may notice the existence of time-dependent fluctuations of the current around its mean value. One would measure such fluctuations even with access to infinite precision measurements; thus, they are an intrinsic property of our system.

Generally, such fluctuations are called noise. Noise is an interesting feature because it is fundamentally connected to properties of the system that generate the noise. Formally speaking, noise is defined as the Fourier transform of the current-current correlation function. We distinguish two main types of noise: thermal noise and shot noise.

3.1 Thermal noise

At non-zero temperatures, there are thermal fluctuations. The occupation number n of electron states is fluctuating around its thermodynamic average $\langle n \rangle$, which is determined by the Fermi distribution. The mean-squared fluctuations $\langle (n - \langle n \rangle)^2 \rangle$ increase with higher temperatures and are determined by the Maxwell-Boltzmann distribution. This type of noise causes equilibrium current fluctuations, which can be shown[2] to be related to the conductance of the system, i.e. the conductance can be determined by equilibrium current fluctuation measurements.

3.2 Shot noise

Unlike thermal noise, shot noise cannot be measured at equilibrium; it arises in the transport state of the system. The origin of shot noise lies in the discrete nature of electronic charge. When measuring a low current with great accuracy, one can no longer neglect the fact that electrons are quantized; a detector, which registers each passing electron separately, will measure a fluctuating current that depends on how many electrons are detected at each individual moment in time.[3]

Shot noise can be understood and quantified by examining the underlying physics that is governing the emission and transport of electrons. The first prediction of this nature was made by Walter Schottky who coined the term in 1918. Shot noise is also often called Poisson noise; let us look at the following simple yet powerful example to understand why:

Let us assume that the particles we are interested in are emitted independently from one another and are non-interacting, i.e. each arrives independently in our detector. Let τ be the characteristic time scale of our measurement, in this case the mean time between the measurement of two such particles. We are looking for the probability $P_N(t)$ for detecting N particles during a time interval of length t.[4]

---

[2] [BB00]

[3] Historic remark: The term 'shot noise' originates from the sputtering sound that can be heard in an audio amplifier, which translates the random fluctuations of electrons emitted from a hot cathode into sound.

[4] We observe that $\tau = t/\langle N \rangle$.

The probability $P_0(t)$ to detect zero particles in time t satisfies

$$P_0(t + dt) = \left(1 - \frac{dt}{\tau}\right) P_0(t)$$

since $\left(1 - \frac{dt}{\tau}\right)$ is the probability of not detecting any particle in the infinitesimal time interval dt. This can be solved as

$$\left.\frac{dP_0}{dt}\right|_t \equiv \frac{P_0(t + dt) - P_0(t)}{dt} = -\frac{1}{\tau} P_0(t) \implies P_0(t) = e^{-t/\tau}$$

We now attempt to find P_N for $N > 0$. We can express P_N recursively through P_{N-1}, as follows:

$$P_N(t + dt) = \left(1 - \frac{dt}{\tau}\right) P_N(t) + \frac{dt}{\tau} P_{N-1}(t) + \left(\frac{dt}{\tau}\right)^2 P_{N-2}(t) + \dots$$

Since dt is infinitesimal, all terms of higher order than linear in dt can be set to zero. We proceed to get

$$\tau \left.\frac{dP_N}{dt}\right|_t \equiv \tau \frac{P_N(t + dt) - P_N(t)}{dt} = P_{N-1}(t) - P_N(t)$$

We multiply by $e^{t/\tau}$ and obtain

$$\frac{d}{d(t/\tau)} \left(P_N(t) e^{t/\tau}\right) = P_{N-1}(t) e^{t/\tau}$$

which by induction leads to

$$\frac{d^N}{d(t/\tau)^N} \left(P_N(t) e^{t/\tau}\right) = P_0(t) e^{t/\tau} = 1$$

This is solved by

$$P_N(t) = \frac{(t/\tau)^N}{N!} e^{-t/\tau} \tag{1}$$

which is a Poisson distribution in $N \in \mathbb{N}_0$. We obtained this general result by simply demanding independence of detection events, hence the term Poisson noise.

The mean value and variance of a Poisson distribution with parameter $t/\tau \in \mathbb{R}^+$ are given by

$$\langle N \rangle = t/\tau, \quad \text{Var}(N) \equiv \langle N^2 \rangle - \langle N \rangle^2 = \langle N \rangle = t/\tau$$

If we are interested in detecting electrons, then the mean measured current $\langle I \rangle$ satisfies $\langle I \rangle = q\langle N \rangle/t = q/\tau$. The noise S is proportional to the variance of the number of transmitted particles. With the correct proportionality factors, one obtains

$$S = \frac{2q^2}{t} \text{Var}(N) = 2q\langle I \rangle$$

The equation $S = 2q\langle I \rangle$ is a central characteristic of shot noise. We are going to examine it more closely in the following section:

3.3   Derivation through the Wiener-Khintchine theorem

Given a current $I(t)$, we define its autocorrelation function

$$R_I(\tau) := \langle I(t)I(t-\tau)\rangle = \lim_{T\to\infty} \frac{1}{T} \int_{-T/2}^{T/2} dt\, I(t)I(t-\tau)$$

which can be considered to be a measure of the current fluctuations. The noise is defined as its Fourier transform:

$$S(\omega) := \int_{-\infty}^{\infty} d\tau\, R_I(\tau)e^{i\omega\tau}$$

We can now make some basic integral calculations:

$$S(\omega) = \lim_{T\to\infty} \frac{1}{T} \int_{-T/2}^{T/2} dt \int_{-\infty}^{\infty} d\tau\, I(t)I(t-\tau)e^{i\omega\tau}$$

$$= \lim_{T\to\infty} \frac{1}{T} \int_{-T/2}^{T/2} dt \int_{-T/2}^{T/2} dt' \int_{-\infty}^{\infty} d\tau\, I(t)I(t')e^{i\omega\tau}\delta(t-t'-\tau)$$

$$= \lim_{T\to\infty} \frac{1}{T} \int_{-T/2}^{T/2} dt \int_{-T/2}^{T/2} dt' \int_{-\infty}^{\infty} d\tau\, I(t)I(t')e^{i\omega\tau} \int_{-\infty}^{\infty} \frac{d\omega'}{2\pi} e^{i\omega'(t-t'-\tau)}$$

By using $\int_{-\infty}^{\infty} d\tau\, e^{i(\omega-\omega')\tau} = 2\pi\delta(\omega-\omega')$ we obtain

$$S(\omega) = \lim_{T\to\infty} \frac{1}{T} \int_{-T/2}^{T/2} dt\, I(t)e^{i\omega t} \int_{-T/2}^{T/2} dt'\, I(t')e^{-i\omega t'}$$

This translates to

$$S(\omega) = \langle \tilde{I}(\omega)\tilde{I}^*(\omega)\rangle = \langle |\tilde{I}(\omega)|^2\rangle \tag{2}$$

where $\tilde{I}(\omega)$ is the Fourier transform of $I(t)$. Equation (2) is known as the Wiener-Khintchine theorem and is the basis for many calculations in statistics and signal processing. It states that the Fourier transform of the autocorrelation gives the power spectrum; knowledge of the one is equivalent to the other. Because of this relation, $S(\omega)$ is called the (two-sided) power spectral density (PSD).

We observe that $S(\omega) = S(-\omega)$. Thus, for $\omega \geq 0$ this gives rise to the definition

$$S_I(\omega) := S(\omega) + S(-\omega) = 2S(\omega) = 2\int_{-\infty}^{\infty} d\tau\, R_I(\tau)e^{i\omega\tau}$$

which is called the one-sided power spectral density or noise.

Now let us consider some simple examples for $I(t)$:

3.3.1   Sharp pulses

In the case that the electrons arrive independently from one another (Poisson process) and that the duration during which they arrive is negligible compared to the timespan between the arrival of successive electrons, we can model the current as

$$I(t) = q \sum_{n=1}^{N} \delta(t-t_n)$$

where $\{t_i\}$ are the independent arrival times of the electrons, uniformly randomly distributed in the interval $[-\frac{T}{2}, \frac{T}{2}]$. The average current $\langle I \rangle$ is given by $\langle I \rangle = \frac{qN}{T}$. The Fourier transform is given by

$$\tilde{I}(\omega) = q \int_{-\infty}^{\infty} dt e^{i\omega t} \sum_{n=1}^{N} \delta(t - t_n) = q \sum_{n=1}^{N} e^{i\omega t_n}$$

Thus, the one-sided power spectrum is

$$S_I(\omega) = 2\langle \tilde{I}(\omega)\tilde{I}^*(\omega) \rangle = \lim_{T\to\infty} \frac{2q^2}{T} \left(\sum_{n=1}^{N} e^{i\omega t_n} \sum_{m=1}^{N} e^{-i\omega t_m} \right)$$

The cross terms ($n \neq m$) vanish in the limit $T \to \infty$ because the $\{t_i\}$ are independent.[5] Thus, we are left with

$$S_I(\omega) = \lim_{T\to\infty} \frac{2q^2 N}{T} = 2q\langle I \rangle$$

Note that this corresponds exactly to the expected result for shot noise. The spectrum $2q\langle I \rangle$ is uniform in all frequencies, it is called white noise.

3.3.2 Rectangular pulses

Suppose that we can no longer neglect the duration of the arrival of the electrons, which is a more realistic assumption. Then we may model each arriving electron as a rectangular pulse in our current. Let

$$r(t) = \begin{cases} \frac{1}{\tau}, & \text{if } t \in [-\frac{\tau}{2}, \frac{\tau}{2}] \\ 0, & \text{otherwise} \end{cases}$$

for some electron tick duration $\tau > 0$ (note that the integral over each rectangular pulse is normed to 1) and

$$I(t) = q \sum_{n=1}^{N} r(t - t_n)$$

where $\{t_i\}$ are the independent arrival times of the electrons, uniformly randomly distributed in the interval $[-\frac{T}{2}, \frac{T}{2}]$. The Fourier transform is given by

$$\tilde{I}(\omega) = q \sum_{n=1}^{N} \int_{-\infty}^{\infty} dt e^{i\omega t} r(t - t_n) = \ldots = q \sum_{n=1}^{N} e^{i\omega t_n} \left[\frac{\sin(\omega\tau/2)}{\omega\tau/2} \right]$$

We continue as before

$$S_I(\omega) = 2\langle \tilde{I}(\omega)\tilde{I}^*(\omega) \rangle = \lim_{T\to\infty} \frac{2q^2}{T} \left[\frac{\sin(\omega\tau/2)}{\omega\tau/2} \right]^2 \left(\sum_{n=1}^{N} e^{i\omega t_n} \sum_{m=1}^{N} e^{-i\omega t_m} \right)$$

and obtain

$$S_I(\omega) = 2q\langle I \rangle \left[\frac{\sin(\omega\tau/2)}{\omega\tau/2} \right]^2$$

This noise is no longer white, but it still reproduces the expected result $S_I(0) = 2q\langle I \rangle$. It falls off to 0 for $\omega \gg 1$

---

[5]Heuristically, the expectation value of $\exp[i\omega(t_n - t_m)]$ vanishes, since this term describes a uniform distribution on the unit circle in the complex plane for $n \neq m$ and $T \to \infty$. The expectation value is the center of this circle, i.e. zero.

3.4   Scattering theory

This chapter only provides a brief overview of the main results of scattering theory that are of interest in our case; detailed derivations of the following results can be found in [BB00] and [BÿŸ92].

The idea of the scattering approach (also called Landauer approach) is to relate the fluctuation properties of the system to its scattering properties. We consider our model of the QPC: two baths / leads (left and right) being linked by a sample, which only allows for a single transverse mode. To this end, we introduce creation and annihilation operators: $a_L^\dagger(E)$, $a_L(E)$ create/annihilate electrons that are incoming from the left sample with energy E, while $b_L^\dagger(E)$, $b_L(E)$ create/annihilate electrons that are outgoing to the left lead with energy E. Similarly, we introduce operators for the right lead. They obey the usual fermionic anticommutation rules: let q be the set of all quantum numbers describing an electron, then

$$a_q^\dagger(E)a_{q'}(E') + a_{q'}(E')a_q^\dagger(E) = \delta_{q,q'}\delta(E - E')$$

while creation and annihilation operators anticommute with operators of the same nature respectively.
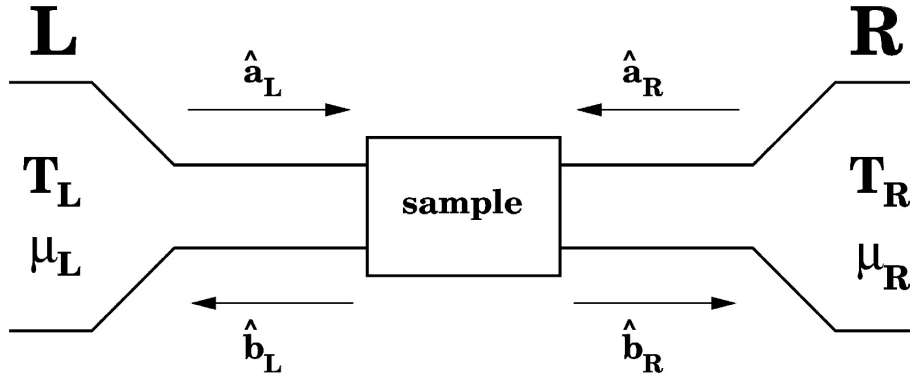
Figure 6: Two-terminal scattering with one transverse channel. [BB00]

The scattering matrix s relates the outgoing current amplitudes to the incoming ones:

$$\begin{pmatrix} b_L \\ b_R \end{pmatrix} = s \begin{pmatrix} a_L \\ a_R \end{pmatrix} , \text{ where } s \equiv \begin{pmatrix} s_{LL} & s_{LR} \\ s_{RL} & s_{RR} \end{pmatrix} = \begin{pmatrix} r & t \\ t' & r' \end{pmatrix}$$

The generalization to multiple transverse channels is straightforward: individual creation / annihilation operators are introduced for each channel and the entries $r, t, \ldots$ of the scattering matrix s are no longer complex numbers but block matrices.

Intuitively speaking, the current leaving the left bath is given by the difference between the number of outgoing electrons ($a_L^\dagger a_L$) and incoming electrons ($b_L^\dagger b_L$). Under the assumption that the electron velocities vary quite slowly with energy, while the energies of the incoming and outgoing electrons are relatively close to each other, it can be shown that the current operator is given by

$$\hat{I}_L(t) = \frac{e}{2\pi\hbar} \int dE\big(a_L^\dagger(E)a_L(E) - b_L^\dagger(E)b_L(E)\big) = \frac{e}{2\pi\hbar} \sum_{\alpha,\beta} \int dE\big(a_\alpha^\dagger(E)A_{\alpha\beta}(E)a_\beta(E)\big)$$

with $A_{\alpha\beta} = \delta_{L\alpha}\delta_{L\beta} - s_{L\alpha}^* s_{L\beta}$, where we used the definition of the s-matrix. We wish to calculate the mean current by using the fact that $\langle a_\alpha^\dagger(E) a_\beta(E') \rangle = \delta_{\alpha\beta}\delta(E - E')f_\alpha(E)$, where f_α is the equilibrium fermionic distribution function

$$f_\alpha(E) = \frac{1}{\exp\left(\frac{E - \mu_\alpha}{k_B T}\right) + 1}$$

In scattering theory, one additional crucial assumption is made. We assume that our description includes all possible physical states, which implies that the scattering matrix s is unitary as each incoming state is transformed into a superposition of our list of outgoing states. However, this assumption neglects inelastic scattering; for example, an incoming electron being transformed into two outgoing electrons and one outgoing hole is not part of this description. Thus, we have to keep in mind that the results of scattering theory are only exact in the non-interacting regime and in the zero-temperature limit of the interacting regime.

To this end, chapter 7.4.1 of [Sch18] analyzes this loss of 'one-particle probability'. Generally speaking, our assumption is correct when the chemical potentials are far from the peak of the potential barrier. The subopen regime, where the chemical potentials are near to the maximum of the barrier, is problematic and requires more careful treatment due to the domination of inelastic processes.

From the unitarity of s we obtain $|r|^2 + |t|^2 = 1$ and thus

$$\begin{aligned}\langle \hat{I}_L(t) \rangle &= \frac{e}{2\pi\hbar} \int dE \left\langle a_L^\dagger a_L - |r|^2 a_L^\dagger a_L - |t|^2 a_R^\dagger a_R - r^* t a_L^\dagger a_R - rt^* a_R^\dagger a_L \right\rangle \\ &= \frac{e|t|^2}{2\pi\hbar} \int dE \left(f_L(E) - f_R(E) \right)\end{aligned} \tag{3}$$

We used the fact that $\langle a_L^\dagger a_R \rangle = \langle a_R^\dagger a_L \rangle = 0$, as mentioned above.

Here we ignored the energy dependence of the s-matrix, as we are mainly interested in the relatively narrow energy range at the Fermi level. In fact, the term in the integral vanishes for energies far from the Fermi level, which makes this a reasonable approximation. In order to obtain the conductance, we take the derivative of the mean current with respect to $V_{sd} = \Delta\mu/e$. In the zero-temperature limit, the fermionic distribution functions are step functions with the step at μ_L (and μ_R respectively). We obtain

$$G = \frac{e^2}{2\pi\hbar}|t|^2 \tag{4}$$

This reproduces the expected result, i.e. that the conductivity is given in units of $\frac{e^2}{h}$ at low temperatures. Note that it is multiplied with $|t|^2$, which can be interpreted as the transmission probability of a single particle; it is the factor by which the amplitude of the squared norm of the wave function of an incoming electron is multiplied after being transmitted through the sample. In the case of multiple transverse channels, the transmission probability $|t|^2$ is replaced with $\text{Tr}[t^\dagger t]$, i.e. the sum of all eigenvalues of the transmission matrix $t^\dagger t$.

Once again, we are interested in the noise term. Using the definition $\Delta\hat{I}_\alpha(t) \equiv \hat{I}_\alpha(t) - \langle \hat{I}_\alpha \rangle$, the autocorrelation function is defined as

$$S_{\alpha\beta}(t - t') = \frac{1}{2} \left\langle \Delta\hat{I}_\alpha(t)\Delta\hat{I}_\beta(t') + \Delta\hat{I}_\beta(t')\Delta\hat{I}_\alpha(t) \right\rangle$$

Note that it only depends on the difference $(t - t')$ of the times, since we are in a stationary state. In order to calculate the noise, which is its Fourier transform

$$2\pi\delta(\omega + \omega')S_{\alpha\beta}(\omega) = \left\langle \Delta\hat{I}_\alpha(\omega)\Delta\hat{I}_\beta(\omega') + \Delta\hat{I}_\beta(\omega')\Delta\hat{I}_\alpha(\omega) \right\rangle$$

we employ expressions for the quantum statistical expectation value of the product of four operators a. We obtain for zero-frequency noise $S \equiv S_{LL}(0) = S_{RR}(0) = -S_{LR}(0) = -S_{RL}(0)$,[6] which is our main point of interest, the following result:

$$
\begin{aligned}
S &= \frac{e^2}{2\pi\hbar} \sum_{\gamma\delta} \int dE \, A_{\gamma\delta}(E)A_{\delta\gamma}(E)\Big(f_\gamma(E)\big(1 - f_\delta(E)\big) + f_\delta(E)\big(1 - f_\gamma(E)\big)\Big) \\
&= \frac{e^2}{\pi\hbar} \int dE \, \left\{ |t|^2\Big(f_L\big(1 - f_L\big) + f_R\big(1 - f_R\big)\Big) - |t|^2(1 - |t|^2)\big(f_L - f_R\big)^2 \right\}
\end{aligned}
\tag{5}
$$

In the last line of the equation above, the first term in the integral (proportional to $|t|^2$) is the equilibrium noise contribution, while the last term (which is second order in the Fermi distribution functions) is the non-equilibrium or shot noise.[7]

Let us now consider some interesting cases in order to apply this result.

3.4.1 Equilibrium noise

In the case of an equilibrium $T_L = T_R$ and $\mu_L = \mu_R$ (thus $V_{sd} = \Delta\mu/e = 0$) we obtain $f_\gamma = f_\delta$ and the noise can be calculated to be merely a multiple of equation (4):

$$S = 4k_B T G \tag{6}$$

Note that this result can also be proven in a more general context where we do not assume an invariant scattering matrix. [BB00]

3.4.2 Zero temperature noise

In the case that $T_L = T_R = 0$, the fermionic distribution functions become step functions and the calculation of equation (5) is straightforward and leaves us with the result

$$S = \frac{e^3 V_{sd}}{\pi\hbar} |t|^2(1 - |t|^2) \tag{7}$$

In the case of low transparency $(1 - |t|^2) \approx 1$, we use that the integral in equation (3) simply gives $\Delta\mu = eV_{sd}$ and obtain the classic result by Schottky

$$S_{\text{cl}} = \frac{e^3 V_{sd}}{\pi\hbar} |t|^2 = 2e\langle I \rangle$$

The Fano factor $F = S/S_{\text{cl}} = (1 - |t|^2) \in [0, 1]$ is a measure of whether the noise is Poissonian $(F = 1)$ or whether the sample is transparent $(F = 0)$.

---

[6]These equalities follow from current conservation, as explained in [BB00].

[7]In the equilibrium case, $f_L = f_R$, which implies that the shot noise term vanishes.

3.4.3   Constant scattering matrix

In the case that $|t|$ in equation (5) is energy-independent,[8] the remaining integral can be calculated analytically and the noise term simplifies to

$$S = \frac{e^2}{\pi\hbar}\left[2k_BT|t|^2 + eV_{sd}\coth\left(\frac{eV_{sd}}{2k_BT}\right)|t|^2(1 - |t|^2)\right] \tag{8}$$

This is consistent with the previous results, as it reduces to equation (6) in the equilibrium case $V_{sd} \to 0$ and to equation (7) in the zero temperature case $T \to 0$.

---

[8]This is well-justified if the temperature and applied voltage are not on the same scale as the scale of the energy dependence of s.

4 Keldysh formalism

We employ the (Schwinger-) Keldysh formalism in our description of the QPC, which is able to treat arbitrary out-of-equilibrium many-body systems. Our goal is to employ an approach, which will allow us to calculate correlations between physical quantities, i.e. we wish to evaluate the expectation values of arbitrary observables.

Note that from here on $\hbar = 1$ for reasons of simplicity.

4.1 Basic introduction to the closed time contour

Let us consider a quantum many-body system, which is governed by a time-dependent Hamiltonian $\hat{H}(t) = \hat{H}_0(t) + \hat{V}(t)$, which we decoupled into a single-particle part $\hat{H}_0(t)$ and a part $\hat{V}(t)$, describing the interactions and couping between particles.[9] We assume that in the distant past $t = -\infty$ the system is in equilibrium, i.e. there are no interactions between particles, while it is described by the density matrix $\rho \equiv \rho(-\infty)$. We are interested in the behavior under time evolution, which generally drives the system away from equilibrium.

Operators $\hat{O}_H(t)$ in the Heisenberg picture evolve in time given by $\hat{O}_H(t) = \hat{U}(t_0, t)\hat{O}_S\hat{U}(t, t_0)$, where $\hat{U}(t, t_0)$ is the unitary[10] time evolution operator.[11] As the Hamiltonian operators evaluated at different moments in time do not necessarily commute with each other, $\hat{U}(t, t_0)$ should be understood as an infinite product of evolution operators with instantaneously constant Hamiltonians

$$
\begin{aligned}
\hat{U}(t, t_0) &= \lim_{N \to \infty} e^{-i\hat{H}(t-\delta t)\delta t} e^{-i\hat{H}(t-2\delta t)\delta t} \cdots e^{-i\hat{H}(t-N\delta t)\delta t} e^{-i\hat{H}(t_0)\delta t} \\
&= \mathbb{1} + (-i)\int_{t_0}^t dt'\hat{H}(t') + (-i)^2 \int_{t_0}^t \int_{t_0}^{t'} dt'dt''\mathbb{T}\hat{H}(t')\hat{H}(t'') \\
&\quad + (-i)^3 \int_{t_0}^t \int_{t_0}^{t'} \int_{t_0}^{t''} dt'dt''dt'''\mathbb{T}\hat{H}(t')\hat{H}(t'')\hat{H}(t''') + \ldots \\
&\equiv \mathbb{T}\exp\left(-i\int_{t_0}^t dt'\hat{H}(t')\right)
\end{aligned}
\tag{9}
$$

where $\delta t = (t - t_0)/N$ is the infinitesimal time step and $\mathbb{T}$ denotes time ordering, i.e. the earlier in time an operator is evaluated the further to the right it stands.

The evolution of the density matrix $\rho(t)$ is described by the von Neumann Equation

$$
\partial_t \rho(t) = -i[\hat{H}(t), \rho(t)]
$$

By using the identities $\partial_t \hat{U}(t, t_0) = -i\hat{H}(t)\hat{U}(t, t_0)$ and $\partial_{t_0}\hat{U}(t, t_0) = i\hat{U}(t, t_0)\hat{H}(t)$, one observes that the equation above is solved by

$$
\rho(t) = \hat{U}(t, -\infty)\rho(-\infty)\hat{U}(-\infty, t)
\tag{10}
$$

We assume $\text{Tr}[\rho] = 1$, which is satisfied if ρ is the density matrix of a physical system. If ρ describes a system in equilibrium, it is given by $\rho = \frac{1}{Z}e^{-\beta\hat{K}}$, where $\beta = \frac{1}{k_B T}$ and $Z =$

---

[9]The Heisenberg picture will be employed, where operators evolve in time, while wavefunctions are t-independent.

[10]$[\hat{U}(t, t_0)]^\dagger = \hat{U}(t_0, t)$

[11]The Schrödinger equation takes the form $\partial_t\hat{O}(t) = -i[\hat{O}_H(t), \hat{H}(t)]$ in this convention.

$\text{Tr}[e^{-\beta \hat{K}}]$. In the case of the canonical ensemble $\hat{K} = \hat{H}$, while in the case of the grand canonical ensemble $\hat{K} = \hat{H} - \mu\hat{N}$. The expectation value of some observable $\hat{O}$ at time t is defined as

$$\langle \hat{O} \rangle(t) \equiv \text{Tr}[\hat{O}\rho(t)]$$

Using the invariance of the trace under cyclic permutations, equation (10) and the fact that $\hat{U}(-\infty, +\infty)\hat{U}(+\infty, t) = \hat{U}(-\infty, t)$ and trivially $U(-\infty, t)\hat{U}(t, -\infty) = \mathbb{1}$, one can show

$$\begin{aligned}
\langle \hat{O}_S \rangle(t) &= \text{Tr}[\hat{O}\hat{U}(t, -\infty)\rho\hat{U}(-\infty, t)] \\
&= \text{Tr}[\hat{U}(-\infty, t)\hat{O}_S\,\hat{U}(t, -\infty)\rho] \\
&= \text{Tr}[\hat{O}_H(t)\rho] \\
&= \langle \hat{O}_H(t) \rangle \\
&= \text{Tr}[\hat{U}(-\infty, +\infty)\hat{U}(+\infty, t)\hat{O}_S\,\hat{U}(t, -\infty)\rho]
\end{aligned} \tag{11}$$

Read from right to left, the last line corresponds to evolving the initial state forward from $-\infty$ to t, acting on it with the operator $\hat{O}$, evolving it forward again to $+\infty$ and, finally, evolving it backwards in time to $-\infty$, as illustrated in figure 7.

Figure 7: Graphic representation of the Keldysh contour with a single operator $\hat{O}$, which is evaluated at time t (on the forward branch) with initial density matrix ρ.

Evolution along this closed time contour $\mathcal{C}$ is a keystone of the Keldysh formulation. Note that the operator $\hat{O}$ could also equivalently have been inserted on the backwards branch of the contour(i.e. the branch which is evolving backwards in time) by writing

$$\hat{U}(-\infty, +\infty)\hat{U}(+\infty, t)\hat{O}\hat{U}(t, -\infty)\rho = \hat{U}(-\infty, t)\hat{O}\hat{U}(t, +\infty)\hat{U}(+\infty, -\infty)\rho$$

This alternative representation is illustrated in figure 8 and is completely equivalent to the first representation.

In general, we are interested in the evolution operator along this closed contour $\hat{U}_{\mathcal{C}} = \hat{U}(-\infty, +\infty)\hat{U}(+\infty, -\infty)$. In the case that the Hamiltonian is the same on the forward and backward branch, the forward-backward evolution brings the system back exactly to the initial state; we obtain $\hat{U}_{\mathcal{C}} \equiv \mathbb{1}$. By modifying the Hamiltonian to include different contributions on the forward and backward branch (e.g. $\hat{H}^{\pm}(t) = \hat{H}_0(t) \pm \hat{O}(t)V(t)$) $\hat{U}_{\mathcal{C}}$ becomes nontrivial.
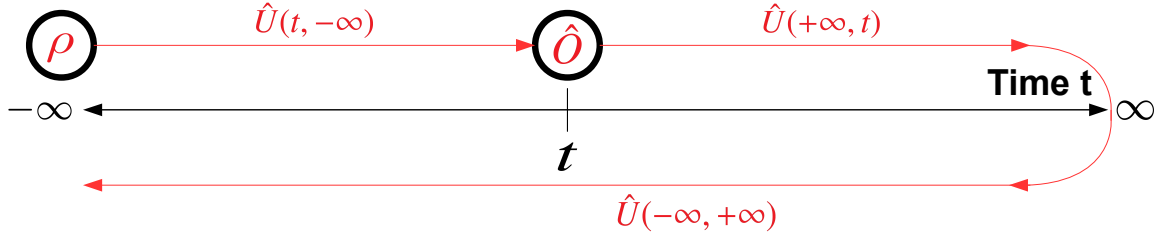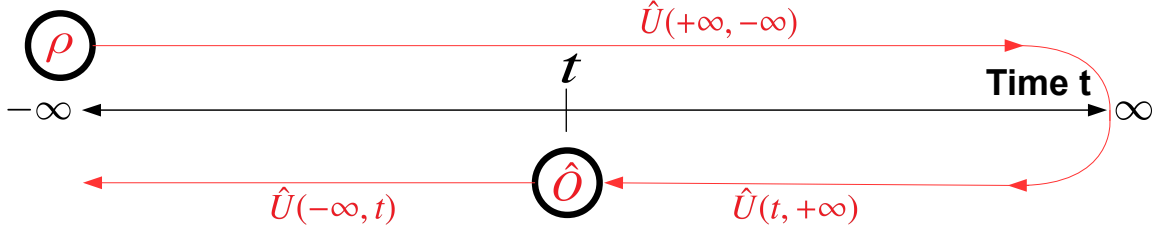
Figure 8: Graphic representation of the Keldysh contour with a single operator $\hat{O}$, which is evaluated at time t (on the backward branch) with initial density matrix ρ.

4.2   General correlation functions

We are interested in calculating correlation functions, which depend on more than one point in time. To that end, let $\hat{O}_H(t_1, \ldots, t_n)$ be an arbitrary operator, composed of creation and annihilation operators, each acting at either of the times $t_1, \ldots, t_n$. Our goal is to calculate its expectation value. First, we make the simplification that $\hat{O}$ is of the form $\hat{O}_{\tilde{\mathbb{T}}}(\{t_i\})\hat{O}_{\mathbb{T}}(\{t_i\})$, where $\hat{O}_{\mathbb{T}}$ is internally time ordered[12], while $\hat{O}_{\tilde{\mathbb{T}}}$ is internally anti-time ordered[13]. For example, if $t_1 > t_2 > t_3 > t_4$, then

$$\hat{O} = c^\dagger(t_4)c(t_2)c(t_1)c^\dagger(t_2)c(t_3)$$

has the desired form, with c and $c^\dagger$ being annihilation and creation operators respectively. By applying the previous notions, we obtain (assuming for simplicity $t_1 > t_2 > \ldots > t_n$):

$$
\begin{aligned}
\langle \hat{O}_H(\{t_i\}) \rangle &= \mathrm{Tr}[\hat{O}'_n(t_n) \cdots \hat{O}'_2(t_2)\hat{O}'_1(t_1)\hat{O}_1(t_1)\hat{O}_2(t_2) \cdots \hat{O}_n(t_n)\rho] \\
&= \mathrm{Tr}[\hat{U}(-\infty, t_n)\hat{O}'_n\hat{U}(t_n, t_{n-1}) \cdots \hat{U}(t_3, t_2)\hat{O}'_2\hat{U}(t_2, t_1)\hat{O}'_1\hat{U}(t_1, +\infty) \\
&\quad \hat{U}(+\infty, t_1)\hat{O}_1\hat{U}(t_1, t_2)\hat{O}_2\hat{U}(t_2, t_3) \cdots \hat{U}(t_{n-1}, t_n)\hat{O}_n\hat{U}(t_n, -\infty)\rho]\hat{O}'_{n-1}
\end{aligned}
$$

Thus, reading the equation from right to left we are again following the contour C on the complex plain($-\infty \rightarrow +\infty \rightarrow -\infty$). The operators $\hat{O}_1, \ldots, \hat{O}_n$ are evaluated on the forward branch, while the operators $\hat{O}'_1, \ldots, \hat{O}'_n$ are evaluated on the backward branch. This is illustrated in figure 9.

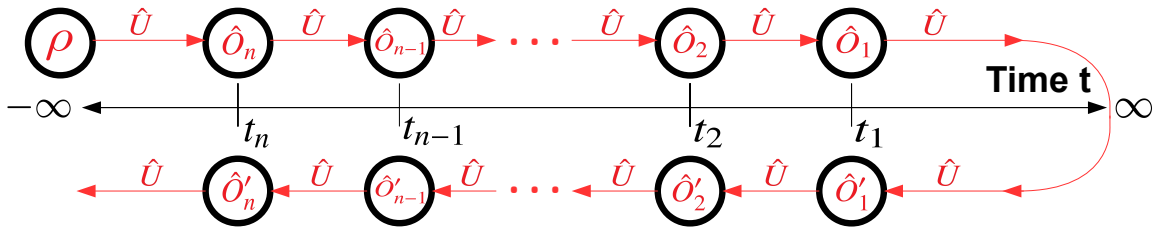Figure 9: Graphic representation of the Keldysh contour with operators $\hat{O}_1, \ldots, \hat{O}_n$ evaluated on the forward branch at times $t_1 > \ldots > t_n$ and operators $\hat{O}'_1, \ldots, \hat{O}'_n$ evaluated on the forward branch at times $t_1 > \ldots > t_n$ with initial density matrix ρ.

---

[12]$\mathbb{T}$: earlier times go to the right
[13]$\tilde{\mathbb{T}}$: later times go to the right

One observes that our request for $\hat{O}$ to have a specific form can easily be dropped, since one can always bring the operator to the desired contour-ordered form $\mathbb{T}_C \hat{O} = \hat{O}_{\tilde{\mathbb{T}}}(\{t_i\}) \hat{O}_{\mathbb{T}}(\{t_i\})$ by using the elementary (anti-)commutator relations of the creation and annihilation operators.[14] Only in the fermionic case, one may pick up a relative minus sign if an uneven amount of exchanges of creation-annihilation pairs is necessary, while the relative sign is conserved is the bosonic case.

The methods described up to now are very general and powerful, since we never assumed to stay in equilibrium under time evolution. Thus, they can be used to describe Hamiltonians with explicit time dependence, such as in the case of boundary conditions and external fields. Also, time in Keldysh formalism always stays on the real axis, without ever taking imaginary values. Both of these properties are in stark contrast to the Matsubara formalism, which is used to describe many-body systems in equilibrium.

4.3 Greens functions and Keldysh rotation

We introduce the contour indexes - and + to denote if an operator is acting on the forward branch (c^-) or on the backward branch (c^+) of C respectively. Given contour indexes j_i and times t_i we define the one-particle Green's function as

$$G^{j_1|j_2}(t_1|t_2) \equiv -i\langle \mathbb{T}_C c^{j_1}(t_1) c^{j_2\dagger}(t_2)\rangle \tag{12}$$

Specifically, the following relations hold true:

$$G^{+|+}(t_1|t_2) = -i\langle \mathbb{T}_C c^+(t_1) c^{+\dagger}(t_2)\rangle = -i\langle \tilde{\mathbb{T}} c(t_1) c^\dagger(t_2)\rangle$$
$$G^{+|-}(t_1|t_2) = -i\langle \mathbb{T}_C c^+(t_1) c^{-\dagger}(t_2)\rangle = -i\langle c(t_1) c^\dagger(t_2)\rangle$$
$$G^{-|+}(t_1|t_2) = -i\langle \mathbb{T}_C c^-(t_1) c^{+\dagger}(t_2)\rangle = -i\sigma\langle c^\dagger(t_2) c(t_1)\rangle$$
$$G^{-|-}(t_1|t_2) = -i\langle \mathbb{T}_C c^-(t_1) c^{-\dagger}(t_2)\rangle = -i\langle \mathbb{T} c(t_1) c^\dagger(t_2)\rangle$$

where the relative sign $\sigma = 1$ for bosons and $\sigma = -1$ for fermions is picked up from the (anti-)commutator relations. We get

$$
\begin{aligned}
G^{+|+}&(t_1|t_2) + G^{-|-}(t_1|t_2) - G^{+|-}(t_1|t_2) - G^{-|+}(t_1|t_2) \\
&= -i\langle (\mathbb{T} + \tilde{\mathbb{T}})(c(t_1) c^\dagger(t_2)) - c(t_1) c^\dagger(t_2) - \sigma c^\dagger(t_2) c(t_1)\rangle \\
&= -i\langle \left(c(t_1) c^\dagger(t_2) + \sigma c^\dagger(t_2) c(t_1)\right) - c(t_1) c^\dagger(t_2) - \sigma c^\dagger(t_2) c(t_1)\rangle \\
&= 0
\end{aligned}
\tag{13}
$$

This linear relation satisfied by the four Greens functions illustrates a redundancy in our description. This motivates the choice of another basis, in which the redundant degree of freedom is eliminated:

$$c^c = \frac{1}{\sqrt{2}}(c^- + c^+), \quad c^q = \frac{1}{\sqrt{2}}(c^- - c^+)$$

---

[14]Under $\mathbb{T}_C$ operators are ordered in the sequence, in which they are transversed in the complex contour C.

Here we replaced the contour indices $+$ and $-$ by the Keldysh indices classical (c) and quantum (q).[15] By performing the substitutions using the definitions above, we obtain

$$G^K \equiv G^{c|c}(t_1|t_2) \equiv -i\langle \mathbb{T}_C c^c(t_1) c^{c\dagger}(t_2)\rangle = \frac{1}{2}\Big(G^{+|+} + G^{-|-} + G^{+|-} + G^{-|+}\Big) = G^{+|-} + G^{-|+}$$

$$G^R \equiv G^{c|q}(t_1|t_2) = \cdots = \frac{1}{2}\Big(G^{+|+} - G^{-|-} + G^{+|-} - G^{-|+}\Big) = \theta(t_1 - t_2)\Big(G^{+|-} - G^{-|+}\Big)$$

$$G^A \equiv G^{q|c}(t_1|t_2) = \cdots = \frac{1}{2}\Big(G^{+|+} - G^{-|-} - G^{+|-} + G^{-|+}\Big) = \theta(t_2 - t_1)\Big(G^{-|+} - G^{+|-}\Big)$$

and finally $G^{q|q}(t_1|t_2) = \frac{1}{2}\Big(G^{+|+} + G^{-|-} - G^{+|-} - G^{-|+}\Big) = 0$

The superscripts K, R and A stand for Keldysh, retarded and advanced respectively. The causality structure is such that the advanced component vanishes for $t_1 > t_2$, while the retarded component vanishes in the case $t_1 < t_2$.

The last equality in the second and third line holds only for $t_1 \neq t_2$. The case $t_1 = t_2$ presents some technical complications[16].

We observe that $G^R + G^A = G^{+|+} - G^{-|-}$ from above equations. By observing that time ordering $\mathbb{T}$ and anti-time ordering $\tilde{\mathbb{T}}$ coincide at equal times, we obtain the useful identity

$$G^R(t|t) + G^A(t|t) = 0 \tag{14}$$

In practice, we will usually be able to neglect the case of equal times in our calculations. Finally, one can use the (anti)commutation rules to show that for $t_1 \neq t_2$:

$$\Big[G^{+|-}(t_1|t_2)\Big]^* = \Big[-i\langle c(t_1)c^\dagger(t_2)\rangle\Big]^* = i\langle c(t_2)c^\dagger(t_1)\rangle = i\sigma\langle c^\dagger(t_1)c(t_2)\rangle = -G^{-|+}(t_2|t_1)$$

which leads to

$$\begin{aligned}
\Big[G^R(t_1|t_2)\Big]^* &= \Big[\theta(t_1 - t_2)\Big(G^{+|-}(t_1|t_2) - G^{-|+}(t_1|t_2)\Big)\Big]^* \\
&= \theta(t_1 - t_2)\Big(G^{-|+}(t_2|t_1) - G^{+|-}(t_2|t_1)\Big) \\
&= G^A(t_2|t_1)
\end{aligned}$$

This observation leads to the fact that knowledge of G^R leads to full knowledge of G^A.

4.4   General Greens functions

Let us now consider a general multi-particle system. A particle with quantum number i has a corresponding creation operator $c_i^\dagger$ and annihilation operator c_i.[17] The canonical commutation relation $c_i c_i^\dagger - \sigma c_i^\dagger c_i = \delta_{ij}$ holds. It will prove useful to define the multi-particle Greens functions:

$$G_{s|s'}^{j|j'}(t|t') = (-i)^n \Big\langle \mathbb{T}_C c_{s_1}^{j_1}(t_1) \cdots c_{s_n}^{j_n}(t_n) c_{s_n'}^{j_n'\dagger}(t_n') \cdots c_{s_1'}^{j_1'\dagger}(t_1')\Big\rangle$$

---

[15]The names 'classical' and 'quantum' stem from the following fact: in a purely classical configuration the action on the forward part of the branch is canceled by that on the backward part. This corresponds to a vanishing quantum component $c^q = 0$, which implies $c^+ = c^-$, as one would expect in the classical case.

[16]We can resolve the ordering ambiguity of creation and annihilation operators acting at the same time by using the definition $\mathbb{T}c^\dagger(t)c(t) = \frac{1}{2}c^\dagger(t)c(t) + \frac{1}{2}\sigma c(t)c^\dagger(t)$ of the continuous time formalism.

[17]In this context, i is the set of all quantum numbers necessary to specify the creation or annihilation operator of the particle.

where j, j' are n-component vectors whose entries are either $+$ or $-$ (this determines on which part of the contour C the corresponding operator is inserted on), s, s' are n-component vectors containing the quantum numbers of the operators and t, t' are n-component vectors specifying the times at which the operators act. In this case, we only considered operators that contain an equal number of creation and annihilation operators, which is sufficient for the description of the QPC.

Analogous to the one-particle case, we can generalize the notion of the Keldysh rotation, which is going to prove quite useful. Let Greek letters $\alpha \in \{c, q\}^n$ denote n-component vectors of Keldysh indices, while Latin letters $j \in \{+, -\}^n$ denote n-component vectors of real indexes. In the one-particle case ($n = 1$), we had defined the transformation

$$G^{\alpha|\beta} = \sum_{j,k \in \{+,-\}^n} (D^{-1})^{\alpha|j} G^{j|k} D^{k|\beta} \tag{15}$$

where

$$D^{+|q} = -\frac{1}{\sqrt{2}}, \quad D^{-|q} = D^{\pm|c} = \frac{1}{\sqrt{2}}$$

$$(D^{-1})^{q|+} = -\frac{1}{\sqrt{2}}, \quad (D^{-1})^{q|-} = (D^{-1})^{c|\pm} = \frac{1}{\sqrt{2}}$$

The generalization of this transformation is the implicit summation over all internal indices

$$D^{j|\alpha} = \prod_{k=1}^{n} D^{j_k|\alpha_k}$$

where equation (15) still applies.

Let us consider two characteristic examples of the inverse transformation, which is going to be useful later on[18]:

$$G^{-|+} = \sum_{\alpha,\beta \in \{c,q\}} D^{-|\alpha} G^{\alpha|\beta} (D^{-1})^{\beta|+} = \frac{1}{2}(G^{c|c} - G^{c|q} + G^{q|c} - G^{q|q}) = \frac{1}{2}(G^K - G^R + G^A - 0)$$

$$G^{--|++} = \sum_{\alpha,\alpha' \in \{1,2\}^2} D^{--|\alpha} G^{\alpha|\beta} (D^{-1})^{\alpha'|++} = \sum_{\alpha_1,\alpha_2,\alpha_3,\alpha_4} D^{-|\alpha_1} D^{-|\alpha_2} G^{\alpha_1\alpha_2|\alpha_3\alpha_4} (D^{-1})^{\alpha_3|+} (D^{-1})^{\alpha_4|+}$$

$$= \frac{1}{2} \sum_{\alpha_3,\alpha_4} G^{\alpha_1\alpha_2|\alpha_3\alpha_4} (D^{-1})^{\alpha_3|+} (D^{-1})^{\alpha_4|+} = \frac{1}{4} \sum_{\alpha_1,\alpha_2,\alpha_3,\alpha_4} (-1)^{\alpha_3+\alpha_4} G^{\alpha_1\alpha_2|\alpha_3\alpha_4}$$

The generalized Keldysh rotation again has the benefit of transforming our correlation functions into a basis with useful properties. Recall: in the one-particle case we had $G^{q|q} = 0$. More generally, the ordering of operators under contour ordering $\mathbb{T}_C$ does not change if the operator corresponding to the largest time is moved between the $+$ and $-$ branch. Since the quantum Keldysh component takes the difference between the $+$ and $-$ contour, it vanishes whenever the largest time is quantum. As a result, $G^{q\cdots q|q\cdots q} = 0$ and, furthermore, $G^{cq\cdots q|q\cdots q}$ is retarded, i.e. it is only non-zero if t_1 is the largest time.

Another useful property of our description up to this point stems from the fact that the initial state ρ is stationary, since it describes the system in equilibrium. Hence, it obeys time

---

[18]We denote $(-1)^{\alpha+\beta} \equiv \begin{cases} 1 & \text{, if } \alpha = \beta \\ -1 & \text{, if } \alpha \neq \beta \end{cases}$

translational invariance, which implies that an expression such as $\langle \mathbb{T}_C c^{j_1}(t_1) c^{j_2 \dagger}(t_2) \rangle$ depends only on the time interval $(t_1 - t_2)$ rather than the concrete values of t_1 and t_2. Generally, the n-particle Greens function depends on $2n-1$ time arguments. Thus, the single-particle Greens function satisfies

$$G(t|t') = G(t - t'|0) =: G(t - t')$$

As a result, we obtain for the Fourier transform

$$
\begin{aligned}
G^{j|j'}_{s|s'}(\omega|\omega') &:= \iint dt dt' \, e^{i(\omega t - \omega' t')} G^{j|j'}_{s|s'}(t|t') \\
&= \iint dt dt' \, e^{i(\omega t - \omega' t')} G^{j|j'}_{s|s'}(t - t') \\
&= 2\pi\delta(\omega - \omega') \int dt G^{j|j'}_{s|s'}(t) =: 2\pi\delta(\omega - \omega') G^{j|j'}_{s|s'}(\omega)
\end{aligned}
\tag{16}
$$

4.5   Interaction picture

Now our goal is the development a diagrammatic language, which will allow us to easily calculate the Greens functions defined above for any Hamiltonian $\hat{H} = \hat{H}_0 + \hat{V}$. To this end, we employ the interaction picture of quantum mechanics. In the interaction picture, wavefunctions and operators evolve according to

$$|\psi_I(t)\rangle = \hat{U}_I(0, t)|\psi_S(t)\rangle$$
$$\hat{O}_I(t) = \hat{U}_I(t_0, t)\hat{O}_S \hat{U}_I(t, t_0),$$
$$\text{with } \hat{U}_I(t, t_0) = \exp\left(-iH_0(t - t_0)\right) \text{ unitary}^{[19]}$$

where $|\psi_S(t)\rangle$ is the wavefunction in the Schrödinger picture. Thus

$$|\psi_I(t)\rangle = \hat{U}_I(0, t)|\psi_S(t)\rangle = \hat{U}_I(0, t)\hat{U}(t, t_0)|\psi_S(t_0)\rangle = \hat{U}_I(0, t)\hat{U}(t, t_0)\hat{U}_I(t_0, 0)|\psi_I(t_0)\rangle$$

i.e. the evolution of the wave function is given by $\hat{u}(t, t_0) := \hat{U}_I(0, t)\hat{U}(t, t_0)\hat{U}_I(t_0, 0)$ and $|\psi_I(t)\rangle = \hat{u}(t, t_0)|\psi_I(t_0)\rangle$. From the definition of $\hat{u}$ follow several interesting properties:

- $\hat{u}$ is unitary, i.e. $[\hat{u}(t, t_0)]^\dagger = \hat{u}(t_0, t)$

- $\hat{u}(t_1, t_2)\hat{u}(t_2, t_3) = \hat{u}(t_1, t_3)$

- $\hat{u}(t_1, t_2)\hat{u}(t_2, t_1) = \mathbb{1}$

Now we derive the equation of motion of $|\psi_I(t)\rangle$ from the Schrödinger equation:[20]

$$
\begin{aligned}
i\partial_t |\psi_I(t)\rangle &= i\partial_t \left(e^{iH_0 t}|\psi_S(t)\rangle\right) \\
&= -H_0 e^{iH_0 t}|\psi_S(t)\rangle + e^{iH_0 t} i\partial_t|\psi_S(t)\rangle \\
&= -H_0 e^{iH_0 t}|\psi_S(t)\rangle + e^{iH_0 t}(H_0 + V_S)|\psi_S(t)\rangle \\
&= e^{iH_0 t} V_S|\psi_S(t)\rangle \\
&= e^{iH_0 t} V_S e^{-iH_0 t}|\psi_I(t)\rangle \\
\implies i\partial_t|\psi_I(t)\rangle &= V_I(t)|\psi_I(t)\rangle
\end{aligned}
$$

---

[19] $[\hat{U}_I(t, t_0)]^\dagger = \hat{U}_I(t_0, t)$

[20] Note that $\hat{H}_0$ is time-independent in the interaction picture. This follows from the fact that $\hat{H}_0$ commutes with $\hat{U}_I$ and $\hat{U}_I(t_0, t)\hat{U}_I(t, t_0) = \mathbb{1}$.

By inserting $|\psi_I(t)\rangle = \hat{u}(t, t_0)|\psi_I(t_0)\rangle$ into the last equation we obtain

$$i\partial_t \hat{u}(t, t_0) = \hat{V}_I(t)\hat{u}(t, t_0)$$

This equation is solved by the infinite series (compare comprehensive notation to equation (9)):[21]

$$\hat{u}(t, t_0) = \mathbb{T}\exp\left(-i\int_{t_0}^t dt'\, \hat{V}_I(t')\right)$$

By using $\rho(t) = \hat{U}(t, -\infty)\rho(-\infty)\hat{U}(-\infty, t)$ (equation (10)) and the fact that ρ and H_0 commute if H_0 contains no interaction terms, it follows (compare with equation (11)):

$$
\begin{aligned}
\langle\hat{O}\rangle(t) &= \langle\hat{O}_H(t)\rangle = \mathrm{Tr}[\hat{U}(-\infty, t)\hat{O}_S\,\hat{U}(t, -\infty)\rho] \\
&= \mathrm{Tr}[\hat{U}(-\infty, t)\hat{U}_I(t, 0)\hat{O}_I(t)\hat{U}_I(0, t)\hat{U}(t, -\infty)\rho] \\
&= \mathrm{Tr}\left[\left(\hat{U}_I(-\infty, 0)\hat{U}_I(0, -\infty)\right)\hat{U}(-\infty, t)\hat{U}_I(t, 0)\hat{O}_I(t)\hat{U}_I(0, t)\hat{U}(t, -\infty)\rho\right] \\
&= \left\langle\hat{U}_I(0, -\infty)\hat{U}(-\infty, t)\hat{U}_I(t, 0)\hat{O}_I(t)\hat{U}_I(0, t)\hat{U}(t, -\infty)\hat{U}_I(-\infty, 0)\right\rangle \\
&= \left\langle\hat{u}(-\infty, t)\hat{O}_I(t)\hat{u}(t, -\infty)\right\rangle \\
&= \left\langle\hat{u}(t, -\infty)^\dagger\hat{O}_I(t)\hat{u}(t, -\infty)\right\rangle \\
&= \left\langle\left[\tilde{\mathbb{T}}\exp\left(+i\int_{-\infty}^t dt'\,\hat{V}_I(t')\right)\right]\hat{O}_I(t)\left[\mathbb{T}\exp\left(-i\int_{-\infty}^t dt'\,\hat{V}_I(t')\right)\right]\right\rangle
\end{aligned}
$$

Having two different time orderings in the last equation follows from the fact that we have a forward and a backward evolution in time. Once again, we are free to choose our contour indices $-$ and $+$ in order to get

$$
\begin{aligned}
\langle\hat{O}\rangle(t) &= \left\langle\left[\tilde{\mathbb{T}}\exp\left(+i\int_{-\infty}^t dt'\,\hat{V}_I^+(t')\right)\right]\hat{O}_I^-(t)\left[\mathbb{T}\exp\left(-i\int_{-\infty}^t dt'\,\hat{V}_I^-(t')\right)\right]\right\rangle \\
&= \left\langle\mathbb{T}_C\left[\exp\left(+i\int_{-\infty}^t dt'\,\hat{V}_I^+(t')\right)\hat{O}_I^-(t)\exp\left(-i\int_{-\infty}^t dt'\,\hat{V}_I^-(t')\right)\right]\right\rangle \\
&= \left\langle\mathbb{T}_C\left[\exp\left(+i\int_{-\infty}^\infty dt'\,\hat{V}_I^+(t') - i\int_t^\infty dt'\,\hat{V}_I^-(t')\right)\hat{O}_I^-(t)\exp\left(-i\int_{-\infty}^t dt'\,\hat{V}_I^-(t')\right)\right]\right\rangle \\
&= \left\langle\mathbb{T}_C\left[\exp\left\{-i\left(\int_\infty^{-\infty} dt'\,\hat{V}_I^+(t') + \int_{-\infty}^\infty dt'\,\hat{V}_I^-(t')\right)\right\}\hat{O}_I^-(t)\right]\right\rangle
\end{aligned}
$$

We could also have chosen $+$ as the contour index of $\hat{O}_I(t)$ and would then have made a similar calculation to the right side of the operator.

The most suggestive way to write the last line is

$$\langle\hat{O}\rangle(t) = \frac{\left\langle\mathbb{T}_C\left[\exp\left\{-i\left(\int_\infty^{-\infty} dt'\,\hat{V}_I^+(t') + \int_{-\infty}^\infty dt'\,\hat{V}_I^-(t')\right)\right\}\hat{O}_I^-(t)\right]\right\rangle}{\left\langle\mathbb{T}_C\left[\exp\left\{-i\left(\int_\infty^{-\infty} dt'\,\hat{V}_I^+(t') + \int_{-\infty}^\infty dt'\,\hat{V}_I^-(t')\right)\right\}\right]\right\rangle} \tag{17}$$

---

[21]This can be easily checked by inserting the solution directly into $i\partial_t|\psi_I(t)\rangle = V_I(t)|\psi_I(t)\rangle$ and comparing the terms with the same power of $\hat{V}$ on both sides.

where the term in the denominator is equal to 1. Equation (17) has a diagrammatic interpretation, which is going to be discussed in the following section.

4.6 Wick's theorem

We may expand equation (17) in the powers of the interaction to obtain

$$\langle \hat{O} \rangle(t) = \sum_{n=0}^{\infty} \frac{(-i)^n}{n!} \sum_{j \in \{+,-\}^n} (-j_1) \cdots (-j_n) \int_{-\infty}^{\infty} dt_n \cdots dt_1 \left\langle \mathbb{T}_C \hat{V}_I^{j_n}(t_n) \cdots \hat{V}_I^{j_1}(t_1) \hat{O}_I^-(t) \right\rangle \qquad (18)$$

A powerful tool to calculate such expectation values as in the above expression is Wick's Theorem.

To that end, one needs to introduce a few concepts first. We can express the operators $\hat{V}_I(t)$ and $O_I(t)$ in terms of creation and annihilation operators $\left[c_s^j \right]_I(t)$, $\left[c_s^{j\dagger} \right]_I(t)$. Each such substitution yields block of creation and annihilation operators with identical time argument. We may define contour ordering $\mathbb{T}_C$ so that the internal ordering of such blocks of operators is left unchanged.

Let $\tilde{c}_s^j$ be either a creation or an annihilation operator. The contraction between two operators is defined as

$$\underbracket{\left[\tilde{c}_s^j\right](t)\left[\tilde{c}_{s'}^{j'}\right]}(t') := \left\langle \mathbb{T}_C \left[\tilde{c}_s^j\right](t)\left[\tilde{c}_{s'}^{j'}\right](t') \right\rangle$$

We observe that the contraction between two creation or two annihilation operators vanishes if our dynamics conserve the particle number, which is the case for most applications. We define the total pairing $\mathbb{P}$ as the sum over all permutations of complete pairwise contractions

$$\mathbb{P}(\tilde{c}_1 \cdots \tilde{c}_n) := \left(\underbracket{\tilde{c}_1 \tilde{c}_2} \underbracket{\tilde{c}_3 \tilde{c}_4} \cdots \underbracket{\tilde{c}_{n-2} \tilde{c}_{n-1}} \tilde{c}_n \right) + \left(\underbracket{\tilde{c}_1 \tilde{c}_2 \tilde{c}_3 \tilde{c}_4} \cdots \underbracket{\tilde{c}_{n-2} \tilde{c}_{n-1}} \tilde{c}_n \right) + \ldots$$

Simple combinatorics shows us that there are a total of $n(n-1)/2$ such permutations in this sum. Before evaluating above expression, the operators in each summand have to be permuted in such a way that operators which are contracted to each other are adjacent. In the fermionic case one picks up a relative (-1) sign for odd permutations.

Wick's theorem (in the special case of applying the vacuum expectation value) connects the contour ordered expectation value of arbitrary creation and annihilation operators to their total pairing:

$$\left\langle \mathbb{T}_C \left[\tilde{c}_{s1}^j\right](t_1) \cdots \left[\tilde{c}_{sn}^j\right](t_n) \right\rangle = \mathbb{P}\left(\left[\tilde{c}_{s1}^j\right](t_1) \cdots \left[\tilde{c}_{sn}^j\right] \right) \qquad (19)$$

This allows us to calculate $\langle \hat{O} \rangle(t)$ from equation (18) by applying the diagram rules resulting from Wick's theorem. These so-called diagram rules are just a helpful way of visualizing terms from the powers of the interaction Hamiltonian (see equation (18)). Let us examine some examples:

Time dependence will not be explicitly denoted for the rest of this section, while all operators are assumed to be evaluated in the interaction picture, i.e. all creation and annihilation operators are evolved under the free Hamiltonian, which includes no interactions. The diagrammatic representation of $G^{-|+} = -i \langle \mathbb{T}_C c^- c^{+\dagger} \rangle = -i \underbracket{c^- c^{+\dagger}}$ is a line between an incoming $-$ annihilation operator to an outgoing $+$ creation operator. By convention, arrows are directed

from annihilation to creation operators. Similarly, $G^{+|-}$ corresponds to a line between an incoming $+$ line and an outgoing $-$ line, while $G^{+|+}$ corresponds to an incoming and outgoing $+$ line. This diagrammatic way of thinking can also be applied to operators with Keldysh indices. For example, $G^R = G^{c|q}$ corresponds to a vertex between an incoming classical line and an outgoing quantum line.

Now let us examine an interaction Hamiltonian of the form

$$\hat{V}(t) = \frac{g}{2}(c^{c\dagger}c^{q\dagger}c^c c^c + c^{c\dagger}c^{c\dagger}c^c c^q + c^{q\dagger}c^{c\dagger}c^q c^q + c^{q\dagger}c^{q\dagger}c^q c^c) \tag{20}$$

For example, the first summand corresponds to a vertex with two incoming classical lines, one outgoing classical line and one outgoing quantum line, while the second summand corresponds to a vertex with one incoming classical line, one incoming quantum line and two outgoing classical lines. $g/2$ is called the vertex factor of each of these vertices. Some examples of this diagrammatic way of thinking are illustrated in figure 10.
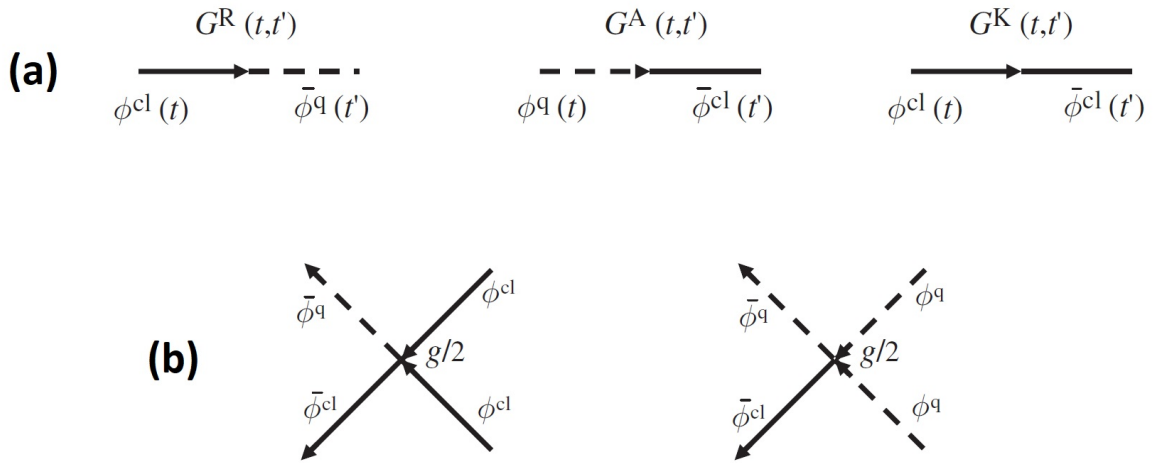

Figure 10: [Kam11] (a) Graphic representation of G^R, G^A and G^K. Full lines represent classical field components ϕ^{cl}, while dashed lines represent the quantum components ϕ^q. Arrows are directed from annihilation operators towards the the creation ones, i.e. from ϕ to $\bar{\phi}$. (b) Graphic representation of the first two vertices in equation (20), including vertex factors. The last two terms correspond to the same diagrams under complex conjugation, i.e. with the direction of all arrows reversed.

It is simple to check that $\langle \mathbb{T}_C \hat{V} \rangle = 0$. Firstly, the contour ordered expectation value of the last two terms vanishes because $\langle \mathbb{T}_C c^q c^{q\dagger} \rangle = 0$. By applying the definitions of the Greens functions and Wick's Theorem to the first two terms, we obtain

$$\left\langle \mathbb{T}_C c^{c\dagger} c^{q\dagger} c^c c^c \right\rangle = 2G^R(t|t)G^K(t|t) \quad \text{and} \quad \left\langle \mathbb{T}_C c^{c\dagger} c^{c\dagger} c^c c^q \right\rangle = 2G^A(t|t)G^K(t|t)$$

The sum of these two terms vanishes because of the identity in equation (14).

One can calculate the higher powers of the interaction term in a similar manner, for example $\langle \mathbb{T}_C \hat{V}(t_1)\hat{V}(t_2) \rangle = 0$. In fact, it can be shown that $\langle \mathbb{T}_C V^n \rangle = 0$ for all $n \in \mathbb{N}$.[22]

---

[22]Chapter 5, [Kam11]

To sum up, one notices that the diagram rules in this formalism are completely analogous to the Feynman rules in other quantum field theories. The main difference lies in the existence of an additional contour index $j \in \{+, -\}$ for each internal vertex. To evaluate such a diagram, we sum over all possible permutations of contractions. This corresponds to a summation over all possible internal indices in the diagrammatic representation.

It is important to note that no disconnected[23] diagrams contribute to our infinite sum. The denominator in equation (17) plays the role of canceling out all such diagrams.

After this introduction, let us consider how the non-interacting baths from section 2.3 can be included in our expansion, which up to now only treats the interaction Hamiltonian of our system, the QPC. We assume that the baths are coupled to the outer sites of the tight-binding chain with a coupling constant τ, which corresponds to an electron traveling between the bath and the chain. Let the Greens function describing the free evolution of electrons in the baths be G_{lead}. We now construct the complete set of diagrams of both the baths and the QPC, by starting from the diagrams of the QPC as constructed above and adding additional diagrams in powers of τ. Since there are no interactions in the bath, all diagrams linear in τ are irrelevant, as they describe electrons escaping the system. At second order in τ, one Greens function G^0_{QPC} from our existing diagrams is respectively changed to $G^0_{\text{QPC}} \tau G_{\text{lead}} \tau G^0_{\text{QPC}}$, which corresponds to propagation in the QPC, hopping to the lead, propagation in the lead, hopping to the QPC and, finally, propagation in the QPC. All orders are implemented by exchanging G^0_{QPC} with $\sum_n G^0_{\text{QPC}} (\tau G_{\text{lead}} \tau G^0_{\text{QPC}})^n$. This is a geometric sum, i.e. we replace G^0_{QPC} with $G^0_{\text{QPC}} (\mathbb{1} - \tau G_{\text{lead}} \tau G^0_{\text{QPC}})^{-1}$. Equivalently this corresponds to replacing G^0_{QPC} with $(G^0_{\text{QPC}}{}^{-1} - \tau G_{\text{lead}} \tau)^{-1}$. This simple replacement is all we need to do here to take the interaction with the baths into account.

4.7   Fluctuation dissipation theorem

The FDT is a general and powerful property of physical systems. It connects the response of a system to perturbations to its equilibrium fluctuation properties. Heuristically speaking, the response of a system to fluctuations is similar to its response to small perturbations from the equilibrium state. Specifically, it gives a relation between the response and correlation functions of a system in thermodynamical equilibrium.

In our formalism, for fermionic particles it takes the form

$$G^K(\omega) = \tanh\left(\frac{\omega - \mu}{2T}\right)\left(G^R(\omega) - G^A(\omega)\right) \tag{21}$$

Note that this equation only holds in the equilibrium case, i.e. only if the temperatures and chemical potentials of the baths surrounding the QPC are the same. A complete derivation that only relies on the conventions and definitions which are used in this thesis can be found in [Jak10].

4.8   Free and exact propagators

It is very important to distinguish in the definition of the Greens functions whether the operators are evaluated in the Heisenberg picture or in the interaction picture. In the former,

---

[23]A disconnected diagram is a diagram with two or more connected components.

the full interaction Hamiltonian is factored into the time evolution of the operators, while in the latter case the operators do not 'see' the interactions between particles. Thus, the free one-particle Greens function, also called the free propagator, is defined as

$$\hat{g}_{s_1|s_2}^{j_1|j_2}(t_1|t_2) \equiv -i\left\langle \mathbb{T}_C\left[c_{s_1}^{j_1}\right]_I(t_1)\left[c_{s_2}^{j_2\,\dagger}\right]_I(t_2)\right\rangle$$

while the full / dressed / exact Greens function is defined as

$$\hat{G}_{s_1|s_2}^{j_1|j_2}(t_1|t_2) \equiv -i\left\langle \mathbb{T}_C\left[c_{s_1}^{j_1}\right]_H(t_1)\left[c_{s_2}^{j_2\,\dagger}\right]_H(t_2)\right\rangle$$

In order to obtain this exact propagator, which is an object of central interest for our considerations, one must first calculate the free propagator. This is done thoroughly in Appendix A. It is shown that the free propagator of a fermionic system in frequency space is given by

$$\begin{aligned}
\hat{g}^R(\epsilon) &= \frac{1}{\epsilon - \epsilon_0 + i0} \\
\hat{g}^A(\epsilon) &= \frac{1}{\epsilon - \epsilon_0 - i0} \\
\hat{g}^K(\epsilon) &= -2\pi i(1 - 2n_F(\epsilon_0))\delta(\epsilon - \epsilon_0)
\end{aligned} \tag{22}$$

where $n_F(\epsilon_0) = (e^{\beta(\epsilon_0 - \mu)} + 1)^{-1}$ is the fermionic equilibrium distribution function and the infinitesimal term $\pm i0$ is to be understood as a prescription for calculations involving integration through the residue theorem.

Now we turn our attention to the derivation of the exact propagator. Since interactions can no longer be neglected, it does not suffice to only consider the bare action of the system (i.e. the action that does not include any interactions). Instead, the interaction action which stems from the interaction Hamiltonian has to be added to the total action. This is treated formally in Appendix B.

From here on, our argumentation will mainly be diagrammatic, since this is the most intuitive and fast approach. Note that the rigorous definition of the diagrammatic language makes this approach self-contained and not any less rigorous than any other approach. For further reading, books like [Neg18] and [FW03] are recommended.

4.8.1 Dyson equation

The one-particle irreducible diagrams are defined as the Feynman diagrams which can't be cut into two disconnected parts by removing a single line from the interior of the digram. The self-energy $\hat{\Sigma}$ is defined as the sum of the inner parts of all one-particle irreducible propagator diagrams (with the two external legs cut off). The self-energy is an extremely important quantity, since calculating the self-energy allows us to evaluate the exact propagator.

One can express the exact propagator diagrammatically in terms of the free-propagator and the self-energy, as demonstrated in figure 11.

Translated into an equation, this means

$$\hat{G} = \hat{g} + \hat{g} \circ \hat{\Sigma} \circ \hat{g} + \hat{g} \circ \hat{\Sigma} \circ \hat{g} \circ \hat{\Sigma} \circ \hat{g} + \dots$$

The $\circ$ symbol stands for a convolution of space-time coordinates along with a multiplication of the respective (2×2) Greens matrices (indexed by the Keldysh indices 1 and 2). We
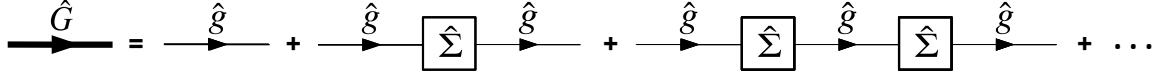
Figure 11: Diagrammatic Dyson series of the full Greens function. The self-energy blocks $\hat{\Sigma}$ are to be understood as the sum of all one-particle irreducible diagrams.

observe that the equation above simplifies to

$$\hat{G} = \hat{g} + \hat{g} \circ \hat{\Sigma} \circ \hat{G}$$

which, written explicitly, is the same as

$$G_{s|s'}^{j|j'}(t|t') = g_{s|s'}^{j|j'}(t|t') + \sum_{i,i'} \int_{u,u'} \iint d\tau \, d\tau' \, g_{s|u}^{j|i}(t|\tau) \Sigma_{u|u'}^{i|i'}(\tau|\tau') G_{u'|s'}^{i'|j'}(\tau'|t')$$

This equation is the famous Dyson equation. We solve it by bringing $\hat{G}$ to the left side and obtain

$$\hat{G} = \left(\hat{g}^{-1} - \hat{\Sigma}\right)^{-1} \tag{23}$$

with the convention that $^{-1}$ means inversion of the Greens matrix. The Greens matrix $\hat{G}$ has the structure (2×2) in Keldysh components, while the sub-matrices G^R, G^A and G^K may be arbitrarily complicated.

By using the results from the calculation of the free propagator and by evaluating the self-energy through Wick's theorem, we are thus able to calculate the exact one-particle propagator.

4.8.2 Multiple particles

Similar to the one-particle propagator, whose diagrammatic representation consists of one incoming and one outgoing line, we are also interested in multi-particle Greens functions. For example, a two-particle Greens function $G_{i_1 i_2|i_3 i_4}^{\alpha_1 \alpha_2|\alpha_3 \alpha_4}(t_1, t_2|t_3, t_4) = -\left\langle \mathbb{T}_C c_{i_1}^{\alpha_1}(t_1) c_{i_2}^{\alpha_2}(t_2) c_{i_3}^{\alpha_3 \dagger}(t_3) c_{i_4}^{\alpha_4 \dagger}(t_4) \right\rangle$ consists of two external and two internal legs, with the the two-particle interaction in between.

Similar to the self-energy in the one-particle case, we define the two-particle vertex function $\gamma_{i_1 i_2|i_3 i_4}^{\alpha_1 \alpha_2|\alpha_3 \alpha_4}(t_1, t_2|t_3, t_4)$ as the sum of all one-particle irreducible diagrams, which have two incoming and two outgoing legs that have been cut off. Our goal is to connect γ and G.

To that end, consider the object

$$G_{c_{i_1 i_2|i_3 i_4}}^{\alpha_1 \alpha_2|\alpha_3 \alpha_4}(t_1, t_2|t_3, t_4) = -i \cdot G_{i_1|j_1}^{\alpha_1|\beta_1}(t_1) G_{i_2|j_2}^{\alpha_2|\beta_2}(t_2) \gamma_{j_1 j_2|j_3 j_4}^{\beta_1 \beta_2|\beta_3 \beta_4}(t_1, t_2|t_3, t_4) G_{j_3|i_3}^{\beta_3|\alpha_3}(t_3) G_{j_4|i_4}^{\beta_4|\alpha_4}(t_4) \tag{24}$$

where summation over all double indices β and j is implicit. Essentially, we have connected two incoming and two outgoing one-particle propagators to the vertex function (which in itself has had its external legs cut off) and summed over all possible combinations of such legs, given external indices α and i. The resulting object G_c is called the 'connected Greens function'; by definition it is the sum of all one-particle irreducible diagrams with two incoming and two outgoing legs.

The full Greens function contains more diagrams than the connected one. It contains the diagrams in which the first incoming leg is connected to the first outgoing leg, while the second incoming leg is connected to the second outgoing leg - without these two connections being joined together through any vertices. Additionally, it also contains the diagrams, in which the first incoming leg is connected to the second outgoing leg, while the second incoming leg is connected to the first outgoing leg. By adding these two types of diagrams to G_c, we obtain the full two-particle Greens function. Translated into a formula, this means

$$G^{\alpha_1\alpha_2|\alpha_3\alpha_4}_{i_1i_2|i_3i_4}(t_1,t_2|t_3,t_4) = G^{\alpha_1\alpha_2|\alpha_3\alpha_4}_{c\,i_1i_2|i_3i_4}(t_1,t_2|t_3,t_4) + \left(G^{\alpha_1|\alpha_3}_{i_1|i_3}(t_1|t_3)G^{\alpha_2|\alpha_4}_{i_2|i_4}(t_2|t_4) - G^{\alpha_1|\alpha_4}_{i_1|i_4}(t_1|t_4)G^{\alpha_2|\alpha_3}_{i_2|i_3}(t_2|t_3)\right)$$

The minus sign in the equation above comes from the anti-commutativity of fermions under the exchange of two external legs. The more intuitive diagrammatic representation of this equation can be seen in figure 12.
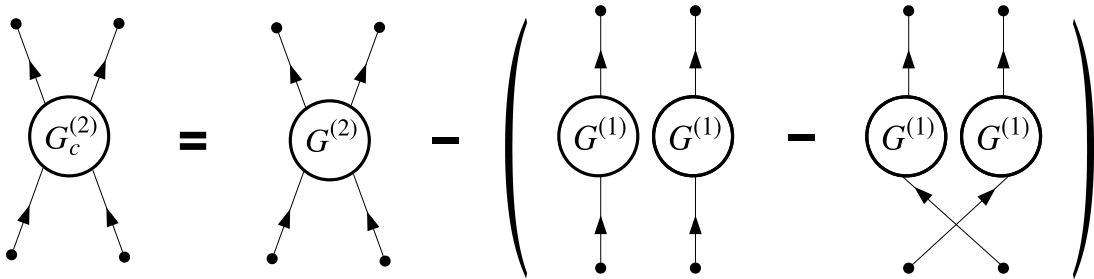
Figure 12: Diagrammatic representation of the connected two-particle Greens function in terms of the two- and one-particle Greens functions

For more than two particles, exactly the same diagrammatic argument can be made by defining the n-particle vertex function and expressing the full n-particle Greens function through $(n-1)$-particle Greens functions and the connected n-particle Greens function.

Thus, we can calculate any n-particle Greens function by evaluating the n-particle vertex function.

5 Description of physical observables

The goal of this chapter is the derivation of expressions for the various physical observables of a QPC in the framework of the Keldysh formalism.

5.1 The Hamiltonian

In section 2.3 we already briefly discussed our basic assumptions about the QPC, namely our neglect of phonons and impurities, the short-ranged nature of the Coulomb force and our modeling of the QPC as a one dimensional tight-binding chain with N discrete sites, while the sites indexed 1 and N are coupled to the leads that are in equilibrium.

Let $c_j^\dagger$ be the creation operator of an electron at site j and c_j the corresponding annihilation operator. The additional index $\sigma \in \{\uparrow, \downarrow\}$ denotes spin. We are interested in the case of a single transverse mode.

Our general QPC-Hamiltonian[24] under the presence of no magnetic field[25] is thus given by

$$\hat{H}_{QPC} = \sum_{j,j',\sigma} t_{j'j,\sigma} c_{j',\sigma}^\dagger c_{j,\sigma} + \sum_{j,j'} v_{jj'} c_{j,\uparrow}^\dagger c_{j,\uparrow} c_{j',\downarrow}^\dagger c_{j',\downarrow} \tag{25}$$

where we have used the same conventions as in [Sch18].

The first term describes the binding between two adjacent sites and thus models the external potential along the QPC.

$$t_{j'j,\sigma} = \tau_{j'} \delta_{jj'+1} + \tau_j \delta_{j+1j'}$$

where τ_j is the hopping parameter between the sites $j - 1$ and j.

The second term in the Hamiltonian describes the electron-electron interaction and is modeled by

$$v_{jj'} = \delta_{jj'} U_j$$

where U_j is the interaction strength.

5.2 The current

We define the site-resolved current at site j as the change in particle number in the system to the left of site $j + 1$:

$$\hat{I}_j := -e \sum_{i \leq j} \dot{n}_i \tag{26}$$

Note that this expression is independent of j in theory. For reasons of clarity, we assume implicit summation over spin indices from this point, whenever they are omitted.

---

[24]Here we do not include the interaction with the baths, which is considered and fully accounted for in section 4.6.

[25]We are mainly interested in the case of a vanishing magnetic field $h = 0$ in this thesis. In the case $h \neq 0$, the term $\left(- \sum_{j,\sigma} \frac{\sigma h}{2} c_{j,\sigma}^\dagger c_{j,\sigma}\right)$ has to be added to the Hamiltonian, so that the energy contribution from the magnetic field is accounted for.

Using the Hamiltonian, one obtains

$$\sum_{i \le j} \dot{n}_i = \frac{i}{\hbar}\Big[\hat{H}_{QPC}, \sum_{i \le j} n_i\Big]$$

$$= \frac{i}{\hbar}\Big[t_{j+1j}c_{j+1}^\dagger c_j + t_{jj+1}c_j^\dagger c_{j+1} \,,\, \sum_{i \le j} n_i\Big] + \frac{iU_i}{\hbar}\Big[c_{i,\uparrow}^\dagger c_{i,\uparrow} c_{i,\downarrow}^\dagger c_{i,\downarrow}, \sum_{i \le j} n_i\Big]$$

where we used the fact that the sum of all particles which are left of site $j+1$ commutes with terms that describe the hopping of particles left of that site, since it is invariant under such hoppings. Thus, only the only hopping term remaining is the one connecting the sites j and $j+1$. We also observe that the product of two identical fermionic operators vanishes because of the anti-commutation rules, i.e. $c_q c_q = c_q^\dagger c_q^\dagger = 0$. This implies that the entire second term vanishes. By applying this identity and the fermionic anti-commutation rules in each step, we are left with[26]

$$\sum_{i \le j} \dot{n}_i = \frac{i\tau_j}{\hbar}\Big[c_{j+1}^\dagger c_j + c_j^\dagger c_{j+1} \,,\, n_j\Big]$$

$$= \frac{i\tau_j}{\hbar}\Big(c_{j+1}^\dagger c_j c_j^\dagger c_j - c_j^\dagger c_j c_{j+1}^\dagger c_j + c_j^\dagger c_{j+1} c_j^\dagger c_j - c_j^\dagger c_j c_j^\dagger c_{j+1}\Big)$$

$$= \frac{i\tau_j}{\hbar}\Big(c_{j+1}^\dagger c_j - 2c_j^\dagger c_j c_{j+1}^\dagger c_j + 2c_j^\dagger c_{j+1} c_j^\dagger c_j - c_j^\dagger c_{j+1}\Big)$$

$$= \frac{i\tau_j}{\hbar}\Big(c_{j+1}^\dagger c_j - 0 + 0 - c_j^\dagger c_{j+1}\Big)$$

Thus, the site-resolved current in terms of creation and annihilation operators is given by

$$\hat{I}_j = -\frac{ie\tau_j}{\hbar}\Big(c_{j+1}^\dagger c_j - c_j^\dagger c_{j+1}\Big) \tag{27}$$

In order the calculate the mean current, we introduce contour indices so as to express everything in terms of Greens functions:

$$\langle \hat{I}_j \rangle = \frac{ie\tau_j}{\hbar}\Big\langle c_j^\dagger c_{j+1} - c_{j+1}^\dagger c_j \Big\rangle$$

$$= \frac{ie\tau_j}{\hbar}\Big\langle c_j c_{j+1}^\dagger - c_{j+1} c_j^\dagger \Big\rangle$$

$$= \frac{ie\tau_j}{\hbar}\Big\langle \mathbb{T}_C\Big(c_j^- c_{j+1}^{+\,\dagger} - c_{j+1}^{-} c_j^{+\,\dagger}\Big)\Big\rangle$$

$$= -\frac{e\tau_j}{\hbar}\Big(G_{j|j+1}^{-|+} - G_{j+1|j}^{-|+}\Big)$$

By performing the Keldysh rotation $G^{-|+} = (G^K + G^A - G^R)/2$ and transforming to Fourier space, we obtain

$$\langle \hat{I}_j \rangle = -\frac{e\tau_j}{2\hbar}\int \frac{d\omega}{2\pi}\Big(G_{j|j+1}^K(\omega) + G_{j|j+1}^A(\omega) - G_{j|j+1}^R(\omega) + G_{j+1|j}^K(\omega) + G_{j+1|j}^A(\omega) - G_{j+1|j}^R(\omega)\Big)$$

---

[26]Additionally, note that any contributions from a magnetic field $h \ne 0$ in the Hamiltonian vanish, since particle number operators commute.

5.3 The noise

Our main goal is the calculation and description of the noise term in the QPC. Given the current operators $\hat{I}_j(t_j)$ and $\hat{I}_k(t_k)$ at two distinct sites (j and k) and times (t_j and t_k), the autocorrelation function of the current is defined as

$$S_{jk} = \frac{1}{2}\langle \Delta\hat{I}_j\Delta\hat{I}_k + \Delta\hat{I}_k\Delta\hat{I}_j \rangle \tag{28}$$

where $\Delta\hat{I} = \hat{I} - \langle\hat{I}\rangle$. Note that the autocorrelation is defined in such a way that it is the expectation value of a self-adjoint operator.

First, let us assume that $j \notin \{k-1, k, k+1\}$. This restriction ensures that all annihilation and creation operators with j-indices anti-commute with operators containing a k-index. By using this fact and our previous calculations about the site-resolved current, we obtain

$$
\begin{aligned}
S_{jk} =&\frac{1}{2}\Big\langle \Delta\hat{I}_j\Delta\hat{I}_k + \Delta\hat{I}_k\Delta\hat{I}_j \Big\rangle = \frac{1}{2}\Big\langle \hat{I}_j\hat{I}_k + \hat{I}_k\hat{I}_j \Big\rangle - \Big\langle\hat{I}_j\Big\rangle\Big\langle\hat{I}_k\Big\rangle \\
=&-\frac{e^2\tau_j\tau_k}{2\hbar^2}\Big\langle (c_jc_{j+1}^\dagger - c_{j+1}c_j^\dagger)(c_kc_{k+1}^\dagger - c_{k+1}c_k^\dagger) + (c_kc_{k+1}^\dagger - c_{k+1}c_k^\dagger)(c_jc_{j+1}^\dagger - c_{j+1}c_j^\dagger) \Big\rangle - \Big\langle\hat{I}_j\Big\rangle\Big\langle\hat{I}_k\Big\rangle \\
=&-\frac{e^2\tau_j\tau_k}{\hbar^2}\Big\langle (c_jc_{j+1}^\dagger - c_{j+1}c_j^\dagger)(c_kc_{k+1}^\dagger - c_{k+1}c_k^\dagger) \Big\rangle - \Big\langle\hat{I}_j\Big\rangle\Big\langle\hat{I}_k\Big\rangle \\
=&-\frac{e^2\tau_j\tau_k}{\hbar^2}\Big\langle c_jc_{j+1}^\dagger c_kc_{k+1}^\dagger + c_{j+1}c_j^\dagger c_{k+1}c_k^\dagger - c_jc_{j+1}^\dagger c_{k+1}c_k^\dagger - c_{j+1}c_j^\dagger c_kc_{k+1}^\dagger \Big\rangle - \Big\langle\hat{I}_j\Big\rangle\Big\langle\hat{I}_k\Big\rangle \\
=&\frac{e^2\tau_j\tau_k}{\hbar^2}\Big\langle c_{k+1}c_jc_{j+1}^\dagger c_k^\dagger + c_kc_{j+1}c_j^\dagger c_{k+1}^\dagger - c_kc_jc_{j+1}^\dagger c_{k+1}^\dagger - c_{k+1}c_{j+1}c_j^\dagger c_k^\dagger \Big\rangle - \Big\langle\hat{I}_j\Big\rangle\Big\langle\hat{I}_k\Big\rangle \\
=&\frac{e^2\tau_j\tau_k}{\hbar^2}\Big\langle c_k^\dagger c_{j+1}^\dagger c_jc_{k+1} + c_{k+1}^\dagger c_j^\dagger c_{j+1}c_k - c_{k+1}^\dagger c_{j+1}^\dagger c_jc_k - c_k^\dagger c_j^\dagger c_{j+1}c_{k+1} \Big\rangle - \Big\langle\hat{I}_j\Big\rangle\Big\langle\hat{I}_k\Big\rangle
\end{aligned}
$$

Now it is time to insert contour indices in order to introduce Greens functions:

$$
\begin{aligned}
S_{jk} =&\frac{e^2\tau_j\tau_k}{\hbar^2}\Big\langle \mathbb{T}_C\Big(c_k^{+\dagger}c_{j+1}^{+\dagger}c_j^- c_{k+1}^- + c_{k+1}^{+\dagger}c_j^{+\dagger}c_{j+1}^- c_k^- - c_{k+1}^{+\dagger}c_{j+1}^{+\dagger}c_j^- c_k^- - c_k^{+\dagger}c_j^{+\dagger}c_{j+1}^- c_{k+1}^-\Big)\Big\rangle - \Big\langle\hat{I}_j\Big\rangle\Big\langle\hat{I}_k\Big\rangle \\
=&\frac{e^2\tau_j\tau_k}{\hbar^2}\Big\langle \mathbb{T}_C\Big(c_{k+1}^- c_j^- c_{j+1}^{+\dagger}c_k^{+\dagger} + c_k^- c_{j+1}^- c_j^{+\dagger}c_{k+1}^{+\dagger} - c_k^- c_j^- c_{j+1}^{+\dagger}c_{k+1}^{+\dagger} - c_{k+1}^- c_{j+1}^- c_j^{+\dagger}c_k^{+\dagger}\Big)\Big\rangle - \Big\langle\hat{I}_j\Big\rangle\Big\langle\hat{I}_k\Big\rangle
\end{aligned}
$$

and thus, by using the definition of the Greens function and equation (27), we obtain the following result:

$$
\begin{aligned}
S_{jk} =& -\frac{e^2\tau_j\tau_k}{\hbar^2}\Big(G_{k+1,j|k,j+1}^{--|++} + G_{k,j+1|k+1,j}^{--|++} - G_{k,j+1|k,j+1}^{--|++} - G_{k+1,j+1|k,j}^{--|++}\Big) \\
&-\frac{e^2\tau_j\tau_k}{\hbar^2}\Big(G_{j|j+1}^{-|+} - G_{j+1|j}^{-|+}\Big)\Big(G_{k|k+1}^{-|+} - G_{k+1|k}^{-|+}\Big)
\end{aligned} \tag{29}
$$

Recall the result $S_{LL} = S_{RR} = -S_{LR} = -S_{RL}$ from scattering theory (section 3.4). Assuming we model our QPC as a tight binding chain with sites indexed by $0, 1, 2, \ldots, N$, this translates to $S_{00} = S_{NN} = -S_{0N} = -S_{N0}$. Qualitatively, this means that one would expect the case $j = k$ to lead to a similar result as in equation (29). After some calculations, which

require the careful application of the anti-commutation rules and which are performed in Appendix C, one obtains

$$S_{kk} = -\frac{e^2\tau_k^2}{\hbar^2}\Big(G_{k+1,k|k,k+1}^{--|++} + G_{k,k+1|k+1,k}^{--|++} - G_{k,k|k+1,k+1}^{--|++} - G_{k+1,k+1|k,k}^{--|++}\Big)$$
$$-\frac{e^2\tau_k^2}{\hbar^2}\Big(G_{k|k+1}^{-|+} - G_{k+1|k}^{-|+}\Big)\Big(G_{k|k+1}^{-|+} - G_{k+1|k}^{-|+}\Big) + \frac{e^2\tau_k^2}{\hbar^2}\Big(iG_{k|k}^{-|+} + iG_{k+1|k+1}^{-|+} - 2\Big)$$

which is exactly equal to the previous case in equation (29) with an additional third term.

Note that we are mainly interested in the noise, which is the Fourier transform of the autocorrelation function. A Greens function of the form $G_{k|k}$ is constant in time, since it only depends on the difference of its time arguments $(t_k|t_k)$, as already shown.[27] Thus, the entire additional term is time-independent and, therefore, only adds a $\delta(\omega)$ contribution to the noise term, which we will neglect for now. As a result, the case $j = k$ is qualitatively the same for our purposes and we can continue our derivation of the noise term with equation (29).

The second line in equation (29) (which comes from the product of the mean currents) is also constant in time, following exactly the same argumentation. This also makes sense from a physical standpoint, as the mean current is time-invariant.

We are now going to express the two-particle Greens functions in terms of connected Greens functions (see section 4.8.2):

$$\begin{aligned}
S_{jk} = &-\frac{e^2\tau_j\tau_k}{\hbar^2}\Big(G_{c k+1,j|k,j+1}^{--|++} + G_{k+1|k}^{-|+}G_{j|j+1}^{-|+} - G_{k+1|j+1}^{-|+}G_{j|k}^{-|+} + G_{c k,j+1|k+1,j}^{--|++} \\
&+ G_{k|k+1}^{-|+}G_{j+1|j}^{-|+} - G_{k|j}^{-|+}G_{j+1|k+1}^{-|+} - G_{c k,j|k+1,j+1}^{--|++} - G_{k|k+1}^{-|+}G_{j|j+1}^{-|+} \\
&+ G_{k|j+1}^{-|+}G_{j|k+1}^{-|+} - G_{c k+1,j+1|k,j}^{--|++} - G_{k+1|k}^{-|+}G_{j+1|j}^{-|+} + G_{k+1|j}^{-|+}G_{j+1|k}^{-|+}\Big) \\
&-\frac{e^2\tau_j\tau_k}{\hbar^2}\Big(G_{j|j+1}^{-|+}G_{k|k+1}^{-|+} + G_{j+1|j}^{-|+}G_{k+1|k}^{-|+} - G_{j+1|j}^{-|+}G_{k|k+1}^{-|+} - G_{j|j+1}^{-|+}G_{k+1|k}^{-|+}\Big) \\
= &-\frac{e^2\tau_j\tau_k}{\hbar^2}\Big(G_{c k+1,j|k,j+1}^{--|++} + G_{c k,j+1|k+1,j}^{--|++} - G_{c k,j|k+1,j+1}^{--|++} - G_{c k+1,j+1|k,j}^{--|++} \\
&+ G_{k|j+1}^{-|+}G_{j|k+1}^{-|+} + G_{k+1|j}^{-|+}G_{j+1|k}^{-|+} - G_{k+1|j+1}^{-|+}G_{j|k}^{-|+} - G_{k|j}^{-|+}G_{j+1|k+1}^{-|+}\Big)
\end{aligned}\tag{30}$$

and are left with a far more simplified result, where no more constant terms are left. Physically, the subtraction of the product of the mean currents eliminated all contributions that were constant in time. Once again, we note that all Greens functions in the term above do not depend on the individual times t_j and t_k, but only on the difference $(t_j - t_k)$.[28]

We are interested in calculating the noise

$$S_{jk}(\omega) = \int d(t_j - t_k)e^{i\omega(t_j - t_k)}S_{jk}\tag{31}$$

which is the Fourier transform of the autocorrelation function with respect to its time argument. We consider the contributions from the two-particle Greens functions and the one-particle functions separately, i.e. from here on we denote[29]

$$S_{jk}(\omega) \equiv \mathcal{T}_{jk}^1(\omega) + \mathcal{T}_{jk}^2(\omega)$$

---

[27]see section 4.4.

[28]see section 4.4.

[29]$\mathcal{T}^2$ includes all terms that consist of G_c, while $\mathcal{T}^1$ includes the rest of the terms. Note that $\mathcal{T}^2 = 0$ by definition if we consider a non-interacting system.

Each of these two terms will now be treated individually. Generally, we wish to transform everything to frequency space, as we have already done in section 4.8.

5.3.1 One-particle contribution

From equation (30) we obtain that the one-particle term of the noise is given by

$$
\mathcal{T}_{jk}^1(\omega) = \frac{e^2 \tau_j \tau_k}{\hbar^2} \int d(t_j - t_k) e^{i\omega(t_j - t_k)} \Big\{ G_{k+1|j+1}^{-|+}(t_k|t_j) G_{j|k}^{-|+}(t_j|t_k) + G_{k|j}^{-|+}(t_k|t_j) G_{j+1|k+1}^{-|+}(t_j|t_k)
$$
$$
- G_{k|j+1}^{-|+}(t_k|t_j) G_{j|k+1}^{-|+}(t_j|t_k) - G_{k+1|j}^{-|+}(t_k|t_j) G_{j+1|k}^{-|+}(t_j|t_k) \Big\}
$$

By transforming all Greens functions to Fourier space we obtain

$$
\mathcal{T}_{jk}^1(\omega) = \frac{e^2 \tau_j \tau_k}{\hbar^2} \int d(t_j - t_k) \int \frac{d\omega_1}{2\pi} \int \frac{d\omega_2}{2\pi} \int \frac{d\omega_3}{2\pi} \int \frac{d\omega_4}{2\pi} e^{i\omega(t_j - t_k)} e^{-i\omega_1 t_k} e^{-i\omega_2 t_j} e^{i\omega_3 t_k} e^{i\omega_4 t_j}
$$
$$
\Big\{ G_{k+1|j+1}^{-|+}(\omega_1|\omega_4) G_{j|k}^{-|+}(\omega_2|\omega_3) + G_{k|j}^{-|+}(\omega_1|\omega_4) G_{j+1|k+1}^{-|+}(\omega_2|\omega_3)
$$
$$
- G_{k|j+1}^{-|+}(\omega_1|\omega_4) G_{j|k+1}^{-|+}(\omega_2|\omega_3) - G_{k+1|j}^{-|+}(\omega_1|\omega_4) G_{j+1|k}^{-|+}(\omega_2|\omega_3) \Big\}
$$
$$
= \frac{e^2 \tau_j \tau_k}{\hbar^2} \int d(t_j - t_k) \int \frac{d\omega_1}{2\pi} \int \frac{d\omega_2}{2\pi} \int \frac{d\omega_3}{2\pi} \int \frac{d\omega_4}{2\pi} e^{i\omega(t_j - t_k)} e^{-i\omega_1 t_k} e^{-i\omega_2 t_j} e^{i\omega_3 t_k} e^{i\omega_4 t_j}
$$
$$
2\pi\delta(\omega_1 - \omega_4) \cdot 2\pi\delta(\omega_2 - \omega_3) \Big\{ G_{k+1|j+1}^{-|+}(\omega_1) G_{j|k}^{-|+}(\omega_2) + G_{k|j}^{-|+}(\omega_1) G_{j+1|k+1}^{-|+}(\omega_2)
$$
$$
- G_{k|j+1}^{-|+}(\omega_1) G_{j|k+1}^{-|+}(\omega_2) - G_{k+1|j}^{-|+}(\omega_1) G_{j+1|k}^{-|+}(\omega_2) \Big\}
$$

where we used equation (16). This leads to

$$
\mathcal{T}_{jk}^1(\omega) = \frac{e^2 \tau_j \tau_k}{\hbar^2} \int d(t_j - t_k) \int \frac{d\omega_1}{2\pi} \int \frac{d\omega_2}{2\pi} \exp\{i(\omega + \omega_1 - \omega_2)(t_j - t_k)\} \Big\{ G_{k+1|j+1}^{-|+}(\omega_1) G_{j|k}^{-|+}(\omega_2)
$$
$$
+ G_{k|j}^{-|+}(\omega_1) G_{j+1|k+1}^{-|+}(\omega_2) - G_{k|j+1}^{-|+}(\omega_1) G_{j|k+1}^{-|+}(\omega_2) - G_{k+1|j}^{-|+}(\omega_1) G_{j+1|k}^{-|+}(\omega_2) \Big\}
$$

Finally, we use the fact that

$$
\int d(t_j - t_k) \exp\{i(\omega + \omega_1 - \omega_2)(t_j - t_k)\} = 2\pi\delta(\omega + \omega_1 - \omega_2)
$$

and, by eliminating the ω_2-integral, we conclude

$$
\mathcal{T}_{jk}^1(\omega) = \frac{e^2 \tau_j \tau_k}{\hbar^2} \int \frac{d\omega_1}{2\pi} \Big\{ G_{k+1|j+1}^{-|+}(\omega_1) G_{j|k}^{-|+}(\omega_1 + \omega) + G_{k|j}^{-|+}(\omega_1) G_{j+1|k+1}^{-|+}(\omega_1 + \omega)
$$
$$
- G_{k|j+1}^{-|+}(\omega_1) G_{j|k+1}^{-|+}(\omega_1 + \omega) - G_{k+1|j}^{-|+}(\omega_1) G_{j+1|k}^{-|+}(\omega_1 + \omega) \Big\}
$$

$$(32)$$

5.3.2 Two-particle contribution

Similarly, equation (30) implies

$$
\mathcal{T}_{jk}^2(\omega) = \int d(t_j - t_k) e^{i\omega(t_j - t_k)} \Big(G_{c_{k,j|k+1,j+1}}^{--|++} + G_{c_{k+1,j+1|k,j}}^{--|++} - G_{c_{k+1,j|k,j+1}}^{--|++} - G_{c_{k,j+1|k+1,j}}^{--|++} \Big)(t_k, t_j | t_k, t_j)
$$

$$
= \frac{e^2 \tau_j \tau_k}{\hbar^2} \int d(t_j - t_k) \int \frac{d\omega_1}{2\pi} \int \frac{d\omega_2}{2\pi} \int \frac{d\omega_3}{2\pi} \int \frac{d\omega_4}{2\pi} e^{i\omega(t_j - t_k)} e^{-i\omega_1 t_k} e^{-i\omega_2 t_j} e^{i\omega_3 t_k} e^{i\omega_4 t_j}
$$

$$
\Big(G_{c_{k,j|k+1,j+1}}^{--|++} + G_{c_{k+1,j+1|k,j}}^{--|++} - G_{c_{k+1,j|k,j+1}}^{--|++} - G_{c_{k,j+1|k+1,j}}^{--|++} \Big)(\omega_1, \omega_2 | \omega_3, \omega_4)
$$

As before, we use the fact that G_c only depends on three frequencies and denote this as

$$
G_c(\omega_1, \omega_2 | \omega_3, \omega_4) = 2\pi \delta(\omega_1 + \omega_2 - \omega_3 - \omega_4) G_c(\omega_1, \omega_2, \omega_3)
$$

By eliminating the ω_4-integral, we are left with

$$
\mathcal{T}_{jk}^2(\omega) = \frac{e^2 \tau_j \tau_k}{\hbar^2} \int d(t_j - t_k) \int \frac{d\omega_1}{2\pi} \int \frac{d\omega_2}{2\pi} \int \frac{d\omega_3}{2\pi} \exp\{i(\omega + \omega_1 - \omega_3)(t_j - t_k)\}
$$

$$
\Big(G_{c_{k,j|k+1,j+1}}^{--|++} + G_{c_{k+1,j+1|k,j}}^{--|++} - G_{c_{k+1,j|k,j+1}}^{--|++} - G_{c_{k,j+1|k+1,j}}^{--|++} \Big)(\omega_1, \omega_2, \omega_3)
$$

The time integral yields a δ-distribution, which allows us to eliminate the ω_3-integral. Finally, we are left with

$$
\mathcal{T}_{jk}^2(\omega) =
$$
$$
\frac{e^2 \tau_j \tau_k}{\hbar^2} \int \frac{d\omega_1}{2\pi} \int \frac{d\omega_2}{2\pi} \Big(G_{c_{k,j|k+1,j+1}}^{--|++} + G_{c_{k+1,j+1|k,j}}^{--|++} - G_{c_{k+1,j|k,j+1}}^{--|++} - G_{c_{k,j+1|k+1,j}}^{--|++} \Big)(\omega_1, \omega_2, \omega + \omega_1)
$$
$$
\tag{33}
$$

5.4 General properties of the noise

We will now prove several general and useful properties of the physical quantities under consideration:

- Recall the definition of the autocorrelation function and the fact that it only depends on the difference of its time arguments:

$$
S_{jk}(t - t') := S_{jk}(t|t') = \frac{1}{2} \langle \Delta \hat{I}_j(t) \Delta \hat{I}_k(t') + \Delta \hat{I}_k(t') \Delta \hat{I}_j(t) \rangle
$$

From this we obtain

$$
S_{jk}(t) = \frac{1}{2} \langle \Delta \hat{I}_j(t) \Delta \hat{I}_k(0) + \Delta \hat{I}_k(0) \Delta \hat{I}_j(t) \rangle = \frac{1}{2} \langle \Delta \hat{I}_k(0) \Delta \hat{I}_j(t) + \Delta \hat{I}_j(t) \Delta \hat{I}_k(0) \rangle = S_{kj}(-t)
$$

Thus, we have shown the following general identity for the noise:

$$
\boxed{S_{jk}(\omega) = S_{kj}(-\omega)} \tag{34}
$$

- We have already shown in section 4.3:

$$\left[G_{j|k}^{-|+}(t_j|t_k)\right]^* = -G_{k|j}^{-|+}(t_k|t_j)$$

By applying this result to the one-particle contribution in equation (30), one obtains

$$\left[\mathcal{T}_{jk}^1(t_j|t_k)\right]^* = -\frac{e^2\tau_j\tau_k}{\hbar^2}\left(G_{k|j+1}^{-|+}G_{j|k+1}^{-|+} + G_{k+1|j}^{-|+}G_{j+1|k}^{-|+} - G_{k+1|j+1}^{-|+}G_{j|k}^{-|+} - G_{k|j}^{-|+}G_{j+1|k+1}^{-|+}\right)^*$$

$$= -\frac{e^2\tau_j\tau_k}{\hbar^2}\left(G_{j+1|k}^{-|+}G_{k+1|j}^{-|+} + G_{j|k+1}^{-|+}G_{k|j+1}^{-|+} - G_{j+1|k+1}^{-|+}G_{k|j}^{-|+} - G_{j|k}^{-|+}G_{k+1|j+1}^{-|+}\right)$$

$$= \mathcal{T}_{jk}^1(t_j|t_k)$$

Note that all time arguments in the equation above are implicit.[30] This translates to

$$\left[\mathcal{T}_{jk}^1(t)\right]^* = \mathcal{T}_{jk}^1(t)$$

Thus, in Fourier space, we obtain

$$\boxed{\left[\mathcal{T}_{jk}^1(\omega)\right]^* = \mathcal{T}_{jk}^1(-\omega)} \tag{35}$$

- One can use the basic definition of the Greens functions to derive the following identity:[31]

$$\left[G_{ab|cd}^{--|++}(t_a, t_b|t_c, t_d)\right]^* = G_{cd|ab}^{--|++}(t_c, t_d|t_a, t_b)$$

By applying this to equation (30) we obtain

$$\left[\mathcal{T}_{jk}^2(t_j, t_k)\right]^* = -\frac{e^2\tau_j\tau_k}{\hbar^2}\left[\left(G_{ck+1,j|k,j+1}^{--|++} + G_{ck,j+1|k+1,j}^{--|++} - G_{ck,j|k+1,j+1}^{--|++} - G_{ck+1,j+1|k,j}^{--|++}\right)(t_k, t_j|t_k, t_j)\right]^*$$

$$= -\frac{e^2\tau_j\tau_k}{\hbar^2}\left[\left(G_{ck,j+1|k+1,j}^{--|++} + G_{ck+1,j|k,j+1}^{--|++} - G_{ck+1,j+1|k,j}^{--|++} - G_{ck,j|k+1,j+1}^{--|++}\right)(t_k, t_j|t_k, t_j)\right]$$

$$= \mathcal{T}_{jk}^2(t_j, t_k)$$

In Fourier space, this becomes

$$\boxed{\left[\mathcal{T}_{jk}^2(\omega)\right]^* = \mathcal{T}_{jk}^2(-\omega)} \tag{36}$$

- By combining equations (35) and (36), we conclude

$$\boxed{\left[S_{jk}(\omega)\right]^* = S_{jk}(-\omega)} \tag{37}$$

Note that this serves as a self-consistency check for our calculations. This identity also follows immediately from the fact that $S_{jk}(t)$ is real, since it is defined as the expectation value of a self-adjoint operator.

---

[30] An index j corresponds to time t_j and an index k corresponds to time t_k.
[31] see [Jak10]

- In the case of an equilibrium, i.e. $\mu_L = \mu_R$ and $T_L = T_R$, and if the potential barrier in the QPC is symmetric, then all physical observables are invariant under parity transformations. In particular, the identity $S_{1N}(\omega) = S_{N1}(\omega)$ holds. By combining this with equations (34) and (37), one immediately obtains

$$\boxed{S_{1N}(\omega) = S_{1N}(-\omega) = [S_{1N}(\omega)]^* \text{ in equilibrium case}} \tag{38}$$

  i.e. the noise between the left and right lead is real and symmetric around $\omega = 0$ in equilibrium.

- In section 3.3.2 we demonstrated that shot noise is non-white under the assumption that the arrival times of the individual electrons cannot be neglected. Specifically, under the assumption that the electron detection events can be modelled as rectangular pulses, we showed

$$\text{Shot noise } = 2e\langle \hat{I} \rangle \left[\frac{\sin(\omega t_0/2)}{\omega t_0/2} \right]^2 \tag{39}$$

  where t_0 is a constant corresponding to the pulse duration of an individual electron. This equation should be understood as a qualitative classical expectation rather than an exact result that can be applied to our specific setup.

6 Implementation and results

For the purpose of simplicity, plots of physical quantities throughout this section will contain dimensionless parameters. To this end, we use the convention $k_B = \hbar = e = 1$ and express everything in terms of the bandwidth 4τ of the QPC. For example, $T = 2$ stands for $T = 2\tau/k_B$ in SI units, while $\omega = 2$ stands for $\omega = 2\tau/\hbar$.

6.1 Modelling the system

The system is modeled as a one-dimensional tight binding chain consisting of N sites (indexed $1, \ldots, N$) with constant lattice spacing and a bandwidth of 4τ, ranging from -2τ to 2τ. In the case of a chemical potential μ the Fermi energy level lies at $\epsilon_F = 2\tau + \mu$.[32]

The potential barrier of the QPC is modeled through the hopping parameters, using the same conventions as in [Sch18]:

$$\tau_j = \tau - \frac{1}{4} V_g \exp\left(-\frac{x_j^2}{1 - x_j^2}\right), \text{ where } x_j = 2\frac{j-1}{N-2} - 1 \text{ for } j \in \{1, \ldots, N-1\}$$

where V_g is a parameter for the gate voltage. The height of the potential $V(x)$ is given by $2V_g$. This describes an almost parabolic potential which is centered around the middle ($j = N/2$) and which becomes constant at the flanks of the barrier region. The parabolic shape can be observed in the expansion

$$\tau_j = \tau - \frac{1}{4} V_g + \frac{1}{4} V_g x_j^2 + O(x_j^4)$$

The shape of the barrier is determined entirely by its curvature parameter Ω_x. In this case

$$\Omega_x = \frac{4\sqrt{\tau \cdot 2V_g}}{N-1}$$

For the on-site interactions the form used in [BHS+13], [BHvD14], [WBvD17] and [Sch18] respectively is implemented:

$$U_j = U_0 \exp\left(-\frac{l_j^6}{1 - l_j^2}\right), \text{ where } l_j = 2\frac{j-1}{N-1} - 1 \text{ for } j \in \{1, \ldots, N\}$$

It is approximately constant and almost equal to the interaction strength parameter U_0 in the center of the QPC and drops to zero at the flanks of the barrier region.

For the purpose of specific calculations in this thesis the conventions

$$N = \begin{cases} 61 & \text{in equilibrium case} \\ 41 & \text{in non-equilibrium case} \end{cases}$$

$$U_0 = 0.55$$

$$V_g = 0.25$$

$$\mu = \begin{cases} -1.475 & \text{open regime} \\ -1.5 & \text{subopen regime} \\ -1.55 & \text{closed regime} \end{cases}$$

---

[32]In this thesis: $\mu < 0$

are used. Thus, the curvature parameter in units of τ is given by

$$\Omega_x = \begin{cases} 0.04714 & \text{in equilibrium case} \\ 0.07071 & \text{in non-equilibrium case} \end{cases}$$

The temperature is varied between 0 and 0.005 in our calculations, which corresponds to ≈ 1.45K in SI units. The frequencies are discretizised in such a way that they are more densely packed around the center of the band, which lies at frequency zero. Specifically, we use about 1600 discrete frequency values, out of whom 50% lie between -3τ and 3τ. Our exact choice of the discretization procedure is described in [Sch18], Chapter 8.

6.2   The functional Renormalization Group

The functional Renormalization Group (fRG) is a powerful method of computing correlation functions in quantum systems, which are too large and complex to be fully described or solved analytically. In our case, we wish to solve a system consisting of at least 40 to 60 sites and two semi-infinite leads.[33] Additionally, we cannot make the assumption of an equilibrium or linear electron dispersion in our system, since we wish to model a quadratic barrier and non-zero source-drain bias voltage. All these requirements call for a treatment with fRG within the Keldysh formalism, since it is a numerically relatively cheap albeit powerful method.

The main idea of fRG is the introduction of an artificial parameter Λ into the system. For $\Lambda = +\infty$ the system becomes trivial and can be solved analytically, while for $\Lambda = 0$ one obtains the actual physical system. Then one computes how the solution of the system behaves under evolution of the flow parameter Λ from $+\infty$ to 0 with the goal of obtaining a solution to the actual physical system.

In terms of practical calculations, Λ may be introduced in the generating functional of correlation functions of the system (thus directly changing the action), it may be introduced in the generating functional of one-particle irreducible vertices for example or, more conveniently, it may be introduced directly in the free propagator g.

To illustrate this, one straightforward way of implementing the flow parameter would be

$$g^\Lambda(\omega) = \theta(|\omega| - \Lambda)g(\omega)$$

i.e. simply cutting off all frequencies above Λ, so that $g^{\Lambda=\infty} = 0$, which has a trivial solution.

Generally, by making the free propagator $g = g^\Lambda$ depend on Λ, this changes the value of all Feynman diagrams $d_n = d_n^\Lambda$ of order $n \in \mathbb{N}$, which in turn makes the vertex functions depend on Λ, $\gamma_n = \gamma_n^\Lambda$.[34] Specifically, now also the the self-energy depends on the flow parameter and, thus, the full propagator which is calculated by solving the Dyson equation (23) also depends on Λ. Our goal is to calculate how the solution of our system changes with respect to Λ, which means that we need to calculate the derivative of the vertex functions with respect to Λ.

---

[33]If we use less sites, the barrier is no longer as smooth and we obtain artifacts of the discretization in our computations.

[34]The order of a Feynman diagram refers the amount of incoming / outgoing particles, e.g. a dressed two-particle Greens function is an infinite sum of Feynman diagrams of second order.

The most intuitive approach is once again the diagrammatic one. If we consider a Feynman diagram d_n^Λ of order n, then we denote d'^Λ_n as the same diagram, where exactly one internal leg (i.e. internal free propagator g^Λ) is replaced by its derivative with respect to Λ (i.e. with $\partial g^\Lambda/\partial\Lambda$). By the product rule we obtain

$$\frac{\partial\gamma_n^\Lambda}{\partial\Lambda} = \sum_{\substack{d_n^\Lambda \text{ contributing} \\ \text{to } \gamma_n^\Lambda}} \frac{\partial d_n^\Lambda}{\partial\Lambda} = \sum_{\substack{d_n^\Lambda \text{ contributing} \\ \text{to } \gamma_n^\Lambda}} \sum_{\substack{d'^\Lambda_n \text{ contributing} \\ \text{to } \partial d_n^\Lambda/\partial\Lambda}} d'^\Lambda_n \tag{40}$$

The computation of the sum above is a combinatoric diagrammatic exercise, which is performed thoroughly in [Jak10]. The newly arising problem lies within the fact that that the Feynman diagram d'^Λ_n can contain all vertices up to order $n + 1$.[35] Thus, equation (40) corresponds to an infinite coupled hierarchy of differential equations, where the flow $\partial\gamma_n^\Lambda/\partial\Lambda$ is given as a function of $\Sigma^\Lambda, \gamma_2^\Lambda, \gamma_3^\Lambda, \ldots, \gamma_{n+1}^\Lambda$.

A straightforward way to solve this system is to neglect the flow of the higher order vertices, i.e. to fix an $m \in \mathbb{N}$, such that all vertex functions of higher order are set equal to their starting value, i.e. $\forall n > m : \gamma_n^\Lambda \equiv \gamma_n^{\Lambda=\infty}$. This is a reasonable approximation since the contribution of higher order Feynman diagrams is negligible compared to ones of lower order. What remains is a system of coupled ordinary differential equations in Λ, which can be solved numerically.

In our case, we choose $m = 2$ and the starting point $g^{\Lambda=\infty} = 0$, which yields the trivial solution $\Sigma^{\Lambda=\infty} = 0$, $\gamma_2^{\Lambda=\infty} = \bar{u}$ and $\forall n \geq 3 : \gamma_n^{\Lambda=\infty} = 0$, where $\bar{u}$ is the value of the bare two-particle interaction vertex, given our Hamiltonian. Theoretically, the exact choice of the flow parameter is irrelevant as one should always obtain the same solution to the system for $\Lambda = 0$. However, our neglect of higher order vertices and the numerical nature of our solution to the system of differential equations yields inaccuracies, which have to be contained.

In theory, the set of systems described by $0 < \Lambda < \infty$ has no physical meaning and may thus violate physical principles and identities. For example, there could be a Λ, such that $g^R(t) \neq 0$ for $t < 0$, thus violating causality; or there could be a Λ, for which the fluctuation dissipation theorem is violated. However, one should keep in mind that the truncated flow equations only describe a part of the flow due to our approximation, which implies that the solution at $\Lambda = 0$ still incorporates some parts of the solutions at $\Lambda \neq 0$. Thus, it makes sense to implement Λ in such a way that no physical principles and symmetries are ever violated during the flow, so as to ensure their validity in the solution of the actual system.

Finally, the calculation of the conductance requires the calculation of the derivative of the current with respect to the voltage, which is analyzed in [Sch18], Chapter 5.4 for the equilibrium case, where the gradient of the voltage can be assumed to be symmetric. The non-equilibrium case is more complicated and requires more careful treatment.

In conclusion, this brief overview sums up the basic notions of Keldysh fRG for our purposes. The ordinary differential equation flow is solved by a sixth-order Runge-Kutta algorithm with adaptive step-size[36] and a Gaussian quadrature algorithm based on Patterson sets. These algorithms were implemented by Florian Bauer, Jan Heyder, Dennis Hank Schimmel

---

[35]By differentiating one leg of d_n^Λ with respect to Λ, this leg can essentially be treated as an external leg connected to a diagram of higher order.

[36]The system changes far more drastically for $\Lambda <$ bandwidth than for $\Lambda \to \infty$, which has to be reflected in the algorithm.

and Lukas Weidinger at the chair of Professor Jan von Delft at the LMU Munich. A more in depth analysis on fRG and a detailed derivation of the flow equations can be found in [Jak10], Chapter 4, [Sch18], Chapters 4 & 8 and [WBvD17].

6.3 Tackling the integration

In order to calculate the noise, one still needs to handle the task of evaluating integrals such as the ones in equations (32) and (33). The main difficulty here lies within the fact that two-particle Greens functions are very expensive to calculate. Solving the fRG flow provides us with the values of the two-particle vertices γ_2. However, in order to obtain the connected Greens functions, all possible permutations of external legs have to be attached to γ_2, leaving us with[37]

$$G_{c_{i_1 i_2 | i_3 i_4}}^{\alpha_1 \alpha_2 | \alpha_3 \alpha_4}(\omega_1, \omega_2 | \omega_3, \omega_4) = -i \cdot G_{i_1 | j_1}^{\alpha_1 | \beta_1}(\omega_1) G_{i_2 | j_2}^{\alpha_2 | \beta_2}(\omega_2) \gamma_{j_1 j_2 | j_3 j_4}^{\beta_1 \beta_2 | \beta_3 \beta_4}(\omega_1, \omega_2 | \omega_3, \omega_4) G_{j_3 | i_3}^{\beta_3 | \alpha_3}(\omega_3) G_{j_4 | i_4}^{\beta_4 | \alpha_4}(\omega_4)$$

This expression is a quadruple sum over Keldysh indices β within a quadruple sum over $N = 61$ site indices j. In order to evaluate the double noise integral in equation (33) for a single value of ω, we have to calculate four such connected Greens functions and integrate twice over $N_f \approx 1600$ frequencies, keeping in mind our discretization. Assuming one were to calculate each G_c individually and then perform the double integral using the trapezoidal rule naively, one would have to sum over

$$4 \cdot 2^4 \cdot N^4 \cdot N_f^2 \approx 2 \cdot 10^{15} \text{ terms.}$$

We use the following facts and methods in order to reduce this vast number of terms:

- We already have theoretical knowledge about specific combinations of Keldysh indices, e.g. $G_c^{qq|qq} = 0$.

- The indices of the vertex function γ_2 are separate from the indices of G_c due to the summation. Thus, at given frequencies each integrand only consists of $2^4 \cdot N^4$ different vertex function terms.

- Several well-motivated approximations and simplifications in our fRG flow allow us to neglect the vertex function if all its site indices are different,[38] thus effectively turning the quadruple sum over sites into a triple sum.

- We use the fact that $G^{(1)} \sim 1/\omega$ and similarly $G_c^{(2)} \sim 1/\omega^2$ for large ω. Thus, we expect, the integrand not to fluctuate much outside of the bandwidth and can use this knowledge to dynamically adjust the step size during the integration, i.e. outside the bandwidth we only evaluate the integrand at a certain subset of points in each step and then adjust the fineness of the next step according to the fluctuations of these values. In practice, this corresponds to the choice of a certain tolerance threshold, where we make the assumption that integrand fluctuations below this threshold can be neglected.

---

[37]Recall equation (24).
[38] [Sch18]

- All results of the fRG flow (specifically the dressed propagators and the vertex functions) are pre-computed and stored as custom C++ objects, which are specifically designed to guarantee quick reading access. Thus, the calculation of each individual summand is greatly optimized.

6.4   Local density of states

Keeping in mind that the free propagator is given by $g^R(\omega) = (\omega - \omega_0 + i0)^{-1}$, the local density of states $\mathcal{A}$ of a system is defined through the relation

$$G^R(\omega) = \int dz \frac{\mathcal{A}(z)}{\omega - z + i0}$$

where G^R is the full propagator and dz denotes integration over the complex plane. In the case of a homogeneous system with energy ω_0 we obtain the expected result $\mathcal{A}(\omega) = \delta(\omega - \omega_0)$. Intuitively, $\mathcal{A}$ is a useful measure of which energies can occupied the most in a given system.

By using the Kramers-Kronig relations, the integral expression above can be solved for $\mathcal{A}$ and one obtains[39]

$$\mathcal{A}(\omega) = -\frac{1}{\pi} \mathrm{Im} G^R(\omega)$$

Thus, given a site j and a frequency ω, the local density of states is given by

$$\mathcal{A}_j(\omega) = -\frac{1}{\pi} \mathrm{Im} G^R_{j|j}(\omega)$$

It is very instructive to utilize this result in order to visualize and understand the system at hand. In our case, the maximum of the potential barrier lies at the center of the QPC. If the value of the Fermi energy $\epsilon_F = -2\tau - \mu$ is above the peak of the barrier, then the system is open and electrons with high energies are almost free to pass the QPC with little resistance, resulting in a high transmission probability and high conductance. On the other hand, a Fermi energy level below the peak of the barrier leads a so-called closed system, where electrons can only cross the barrier through quantum tunneling. This results in a low transmission rate and low conductance. Finally, it is useful to distinguish the subopen regime, where the Fermi level and the barrier peak approximately coincide. As already mentioned in section 2, this case has the most interesting and 'non-classical' properties, as the transmission probability is medium and electron-electron interactions govern the physics of the QPC.[40]

By plotting the local density of states as a function of site index (i.e. location in the QPC) and electron frequency[41] in figures 13 and 14, the exact shape of the barrier can be studied. It can be observed that most states are quenched into the energy levels around the potential barrier.[42] As one would expect, a low temperature leads to a denser accumulation of the states, while raising the temperature increases thermal fluctuations in the system, which leads to a reduction in the sharpness of the density of states.

---

[39]This requires $G^R(\omega) \sim 1/|\omega|$ for large ω and $G^R(\omega)$ has to be analytic in the upper half complex plane. Both of these are fulfilled, since $G^R(t)$ grows sufficiently slowly in time.

[40]Recall that in this regime the 0.7 anomaly appears, which cannot be explained by a non-interacting model.

[41]corresponding to electron energy

[42]Note that one can ignore the upper portion of these figures. While the density of states at positive energies also has certain maxima, these can realistically never be occupied by the electrons in our system, as it has a negative Fermi energy.
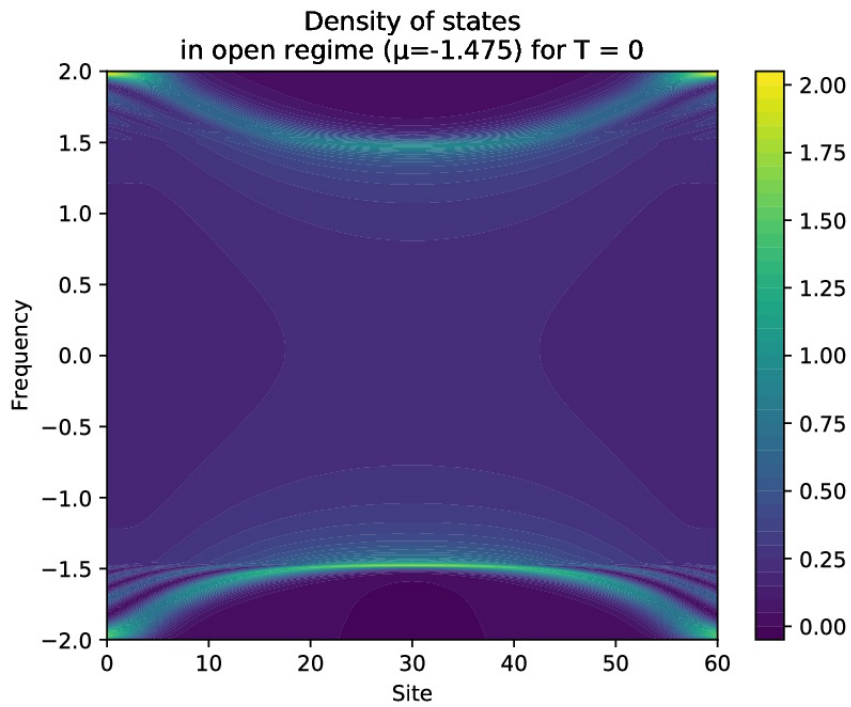
Figure 13: Local Density of states $\mathcal{A}_j(\omega)$ in equilibrium in the open regime ($\mu = -1.475$) with temperature $T = 0$ and magnetic field $h = 0$.
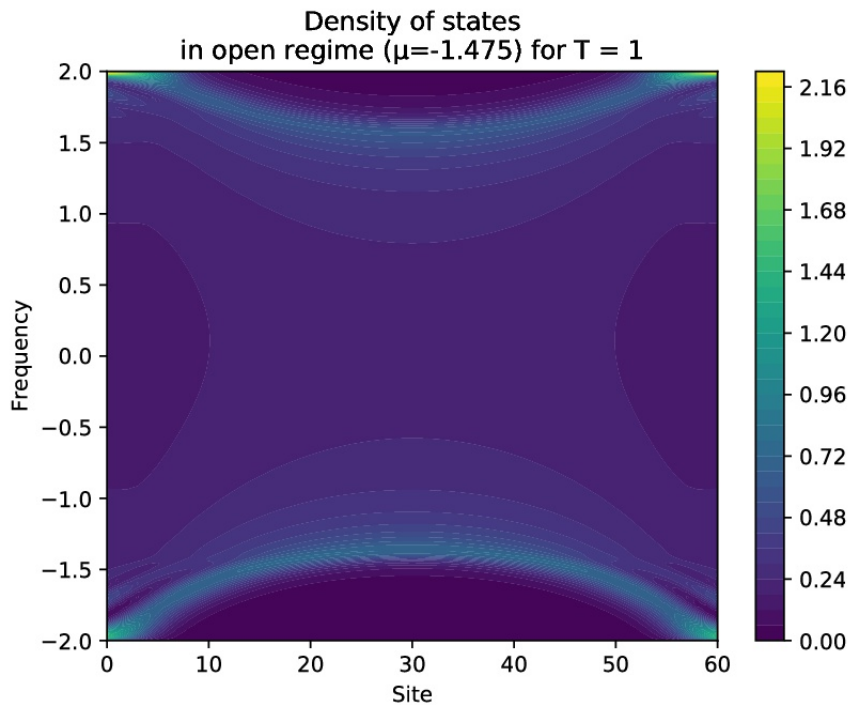

Figure 14: Local Density of states $\mathcal{A}_j(\omega)$ in equilibrium in the open regime ($\mu = -1.475$) with temperature $T = 1 = 21.213\,\Omega_x$ and magnetic field $h = 0$.

6.5 Noise

Our main point of interest in this thesis is the analysis of the properties of the noise term $S_{jk}(\omega)$. Recall our derivation of this term and the fact that it can be split into two contributions: the one-particle contribution $\mathcal{T}_{jk}^1(\omega)$ (equation (32)), which is numerically quite cheap to calculate, and the two-particle contribution $\mathcal{T}_{jk}^2(\omega)$ (equation (33)).

We assume that most of the times, the predominant term is the one-particle one, especially for chemical potentials that are far from the subopen regime, i.e. in regimes where interaction phenomena are not predominant. Thus, it is quite useful to neglect the interaction term at a first approach and to examine the QPC in the approximation $\mathcal{T}_{jk}^2(\omega) \ll \mathcal{T}_{jk}^1(\omega)$. Of course, this approach does not yield exact results but it can be used to estimate the correctness of this approximation and of the computations, to illustrate whether physical identities are fulfilled and to compare the results of this thesis to other publications.

6.5.1 Equilibrium noise: one-particle contribution

First, we start with the equilibrium case, i.e. we assume that $\mu_L = \mu_R$ and $T_L = T_R$, which implies that no current flows between the two leads. This case is far easier to treat, describe and implement in the context of the fRG flow, since the system has additional symmetries. Specifically, it is invariant under parity transformations, which leads to the symmetry $G_{j|k}^{\alpha_1|\alpha_2} = G_{k|j}^{\alpha_1|\alpha_2}$ for generic site indices j, k and Keldysh indices α_1, α_2. Furthermore, the fluctuation dissipation theorem holds:

$$G^K(\omega) = \tanh\left(\frac{\omega - \mu}{2T}\right)\left(G^R(\omega) - G^A(\omega)\right) \tag{21 revisited}$$

We have already shown that $\left[G_{s_1|s_2}^R(t_1|t_2)\right]^* = G_{s_2|s_1}^A(t_2|t_1)$ holds in a general context,[43] which implies that knowledge about the retarded Greens function suffices to calculate the object of our interest, $\mathcal{T}_{jk}^1(\omega)$, from equation (32).

6.5.1.1 Noise as a function of frequency

In order to obtain some intuition behind the noise, we consider some plots of $\mathcal{T}_{1N}^1(\omega)$ in the different regimes (by varying μ) and for different temperatures T and magnetic fields h. To that end, observe figures 15, 16, 17 and 18. Classically, $\mathcal{T}_{1N}^1(\omega)$ can be interpreted as $S_{LR}(\omega)$, i.e. the noise term corresponding to the correlation between the left and the right lead. We make the following observations:

- The noise is non-white, as it takes its maximum around the zero-frequency domain and falls off for high frequencies.[44] This comes as no surprise, as thermal noise does not have an infinite spectrum. Physically, this means that the detection of one electron is correlated to other electrons, if they arrive not too far apart in time.

- Equilibrium noise has to be real and symmetric around the frequency $\omega = 0$, as proven in equation (38). We observe that all plots satisfy the first condition exactly as the imaginary part vanishes within machine accuracy. Furthermore, the noise is approximately

---

[43]See section 4.3.

[44]In this case, $\omega = 1$ corresponds to $\omega = \tau/h \approx 6$ THz in SI units, which is extremely high and justifies the sudden apparent drop of the noise outside the central frequency domain.

symmetric with slight inaccuracies, which can most likely be attributed to numerical errors during the integration.

- An increase in temperature leads to an increase of the value of the peak noise, which occurs at $\omega = 0$. This is in accordance with classical scattering theory, as analyzed in section 6.5.1.2. Intuitively, this makes sense, since the thermal fluctuations get increasingly stronger with higher temperatures.

- An increase in temperature leads to a narrower noise peak around $\omega = 0$. For very large temperatures one expects the noise to approach a δ-peak in frequency space, i.e. only the zero-frequency contribution becomes relevant.

In figure 19 one can observe some plots of $\mathcal{T}_{11}^1(\omega)$, i.e. the noise corresponding to the correlation between the currents measured at the same lead, $S_{LL}(\omega)$. In figure 20 the same physical quantities are plotted in the case of a strictly non-interacting system, i.e. $U_0 = 0$. Classical scattering theory predicts $S_{LR} = -S_{LL}$, as mentioned in section 3.4. However, the results of our computation violate this principle, as one can see in the plots: they look highly different from all previous plots and violate our expectation that the noise increases with higher temperatures, both in the interacting and non-interacting case. Heuristically, one could argue that the on-site noise term in the interacting case might contain larger numerical fRG errors than S_{LR}, since the latter contains propagation terms across the entire QPC, while the former only contains propagators spanning a single site. However, as of now there is no satisfying explanation of the behavior of the on-site noise term in the non-interacting case.
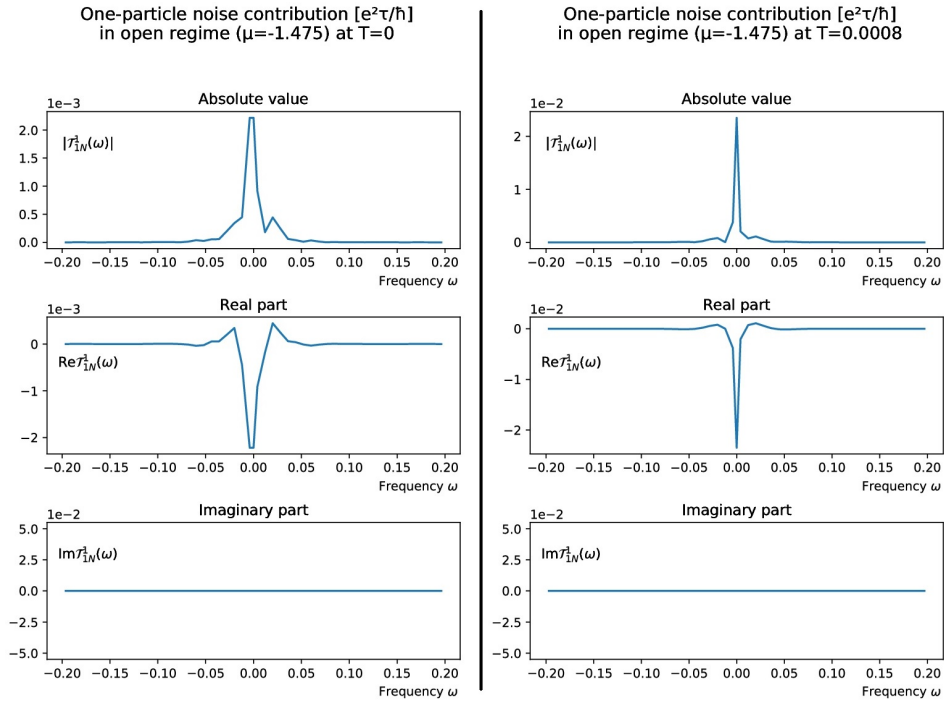

Figure 15: One-particle noise contribution $\mathcal{T}_{1N}^1(\omega)$ in open regime ($\mu = -1.475$) at temperatures $T = 0$ and $T = 0.0008 = 1.6971 \cdot 10^{-2}\, \Omega_x$, with no magnetic field

Figure 16: One-particle noise contribution $\mathcal{T}_{1N}^1(\omega)$ in subopen regime ($\mu = -1.5$) at temperatures $T = 0$ and $T = 0.0008 = 1.6971 \cdot 10^{-2} \, \Omega_x$, with no magnetic field
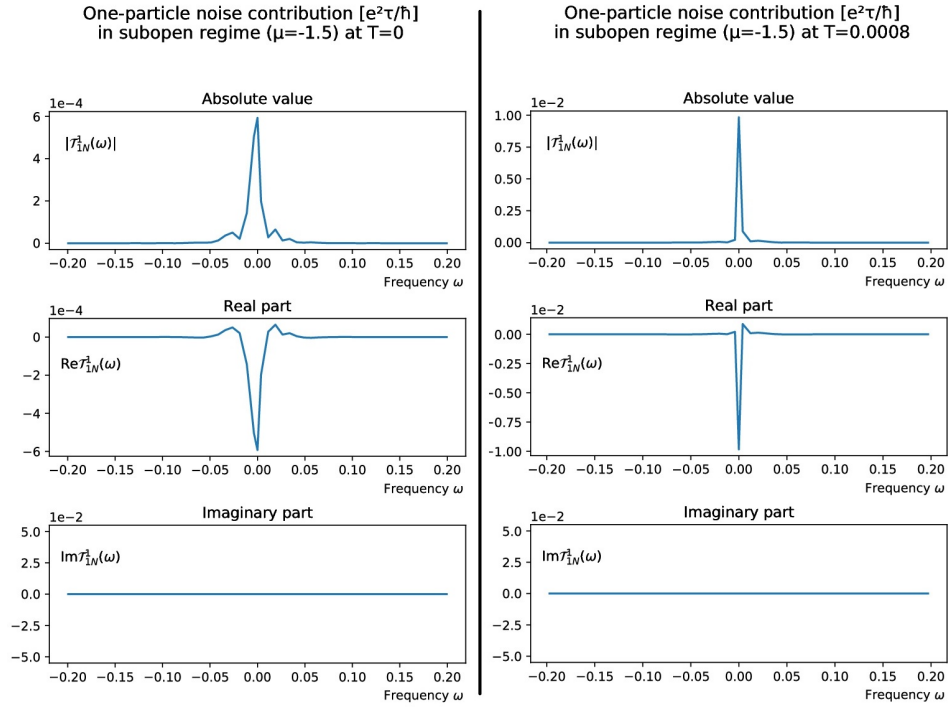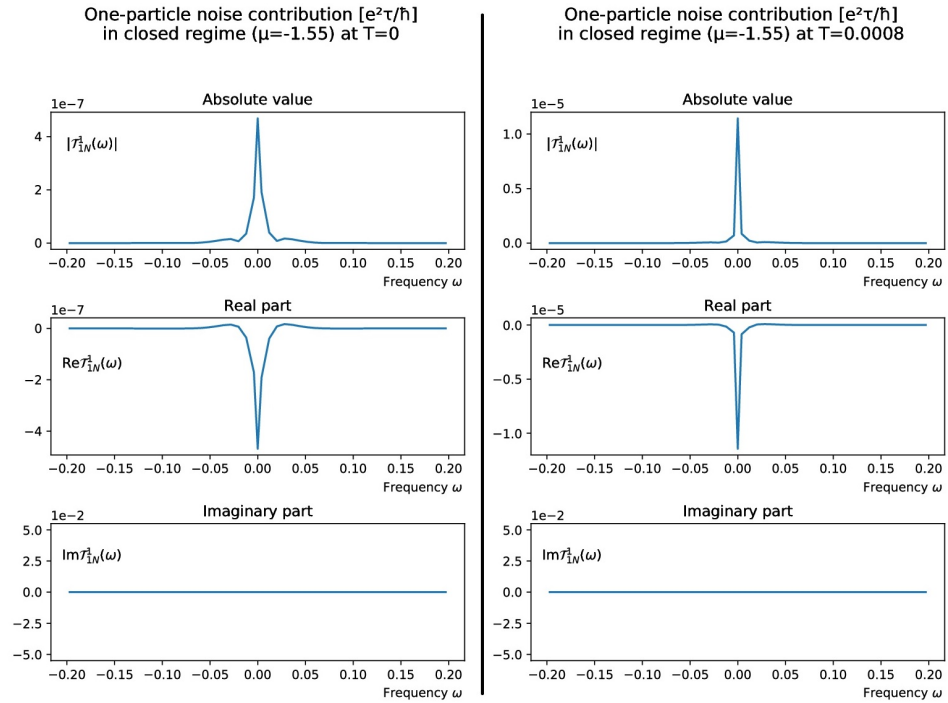

Figure 17: One-particle noise contribution $\mathcal{T}_{1N}^1(\omega)$ in closed regime ($\mu = -1.55$) at temperatures $T = 0$ and $T = 0.0008 = 1.6971 \cdot 10^{-2} \, \Omega_x$, with no magnetic field
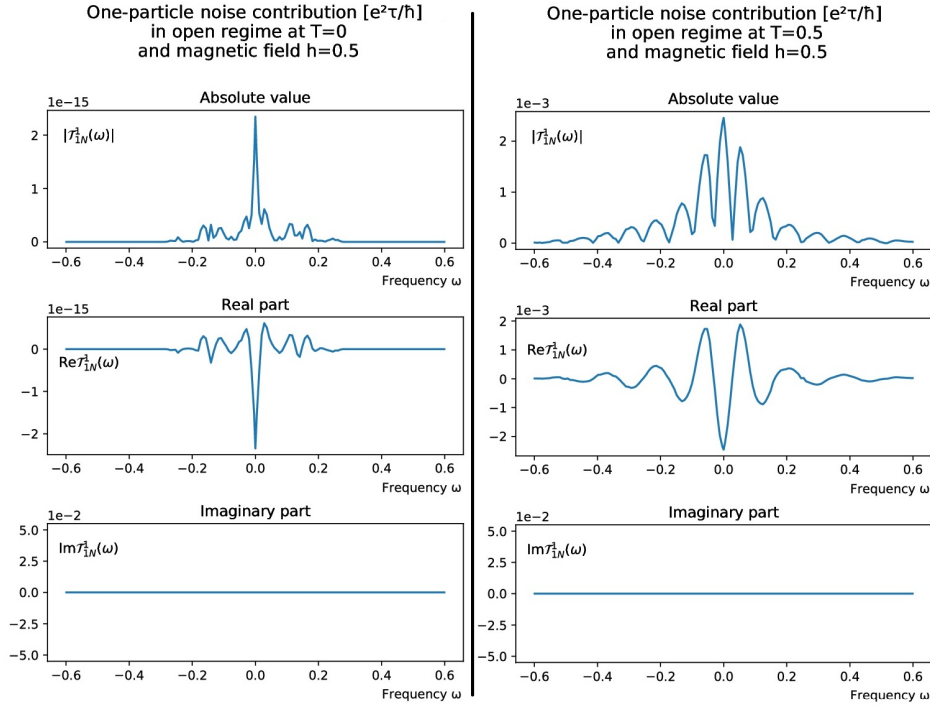
Figure 18: One-particle noise contribution $\mathcal{T}^1_{1N}(\omega)$ in open regime ($\mu = -1.475$) at temperatures $T = 0$ and $T = 0.5 = 10.6067\,\Omega_x$, with magnetic field $h = 0.5$
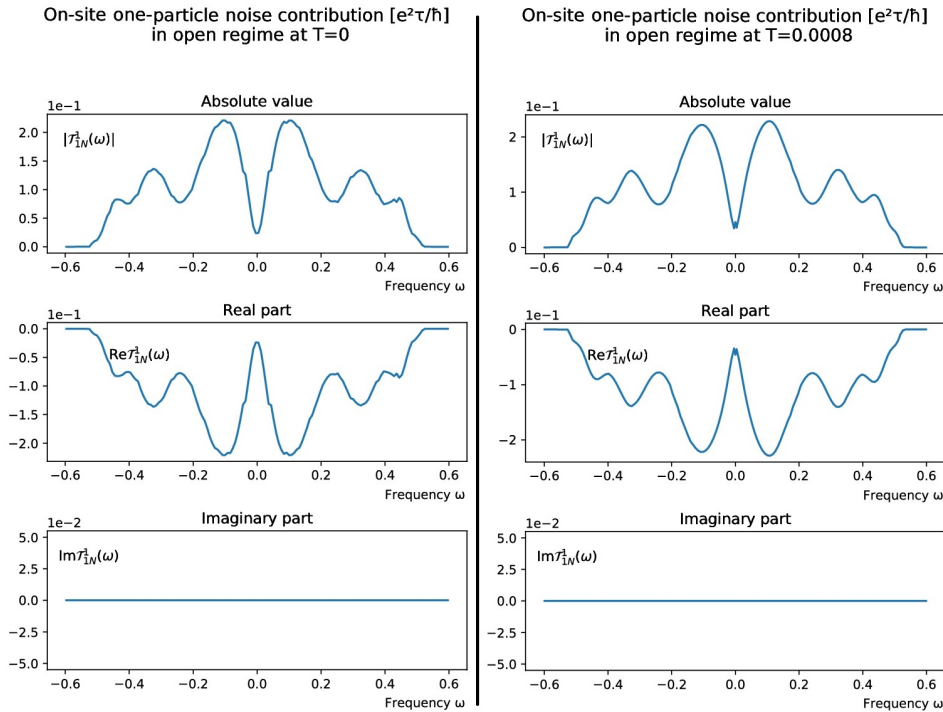
Figure 19: **On-site** one-particle noise contribution $\mathcal{T}^1_{11}(\omega)$ in open regime ($\mu = -1.475$) at temperatures $T = 0$ and $T = 0.0008 = 1.6971 \cdot 10^{-2}\,\Omega_x$, with no magnetic field

Figure 20: **On-site** one-particle noise contribution **in a strictly non-interacting system** $\mathcal{T}_{11}^{1}(\omega)$ in open regime ($\mu = -1.475$) at temperatures $T = 0$ and $T = 0.0008 = 1.6971 \cdot 10^{-2}$ Ω_x, with no magnetic field
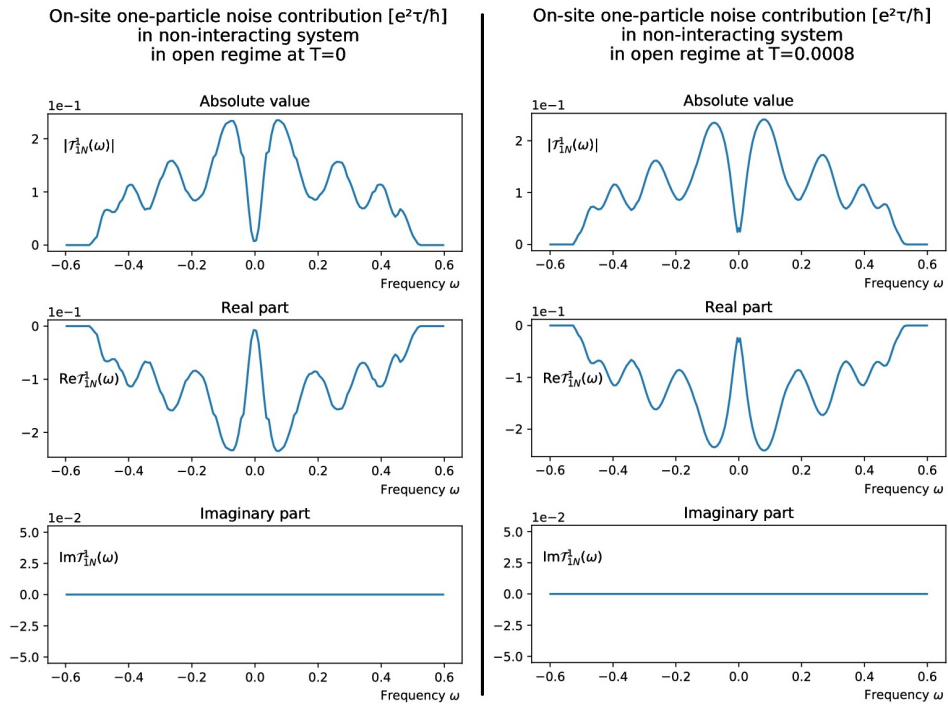
6.5.1.2   Comparison to scattering theory

It is rather interesting to compare the results of our calculations in the Keldysh formalism to classical scattering theory, so as to observe the similarities and the differences between the two approaches. To this end, we are going to base our considerations on the results of section 3.4 on scattering theory.

We showed that the following equation holds in the equilibrium case:

$$S = 4k_B T G \qquad\qquad (\text{6 revisited})$$

where S is the noise at zero frequency, corresponding to $\mathcal{T}_{1N}^1$ in our case. Thus, we expect the noise to be proportional to the product of the temperature and the calculated conductivity of the system.

To that end, figure 21 is a plot of the noise as a function of $T \cdot G$ at the various regimes. Additionally, figure 22 is exactly the same under the additional assumption that the system is strictly non-interacting, i.e. $U_0 = 0$. We make the following observations:

- In all cases, we observe that the proportionality holds for low temperatures, i.e. there is a linear regime where the prediction of scattering theory is almost exact and the linear fit is well justified. However, at higher temperatures, the ratio is no longer proportional and scattering theory breaks down.

- Since the axes are given in exactly the same units, one would expect the slope of the linear fits to be equal to 1. However, in our case, it ranges from 15 to 60 in the various plots. Thus, we are facing a severe scaling problem within the implementation.

Let us now consider each of the three regimes individually.

In the closed regime (shown as (c) in figures 21 and 22), both the interacting and the non-interacting system apparently severely violate the prediction from scattering theory for large temperatures $T > 0.001$. However, this can be attributed to the fact that we have extremely low confidence in our calculation of the conductivity. In this case, the conductivity lies at the magnitude $G = 10^{-4} \times 2e^2/h$, which is extremely low; thus, small absolute errors lead to huge relative errors for the value of G.

In the open regime (shown as (a) in figures 21 and 22), the comparison between the non-interacting system and scattering theory remains highly accurate up to high temperatures (besides some numerical errors). However, the prediction breaks down for large temperatures $(T > 0.001)$ in the interacting system. This can be attributed to the fact that we have neglected the interaction contribution $\mathcal{T}_{1N}^2$ and, more importantly, that the main assumption of scattering theory, namely the unitarity of the s-matrix is no longer valid in the interacting case at high temperatures. This leads to the insufficiency of scattering theory in the description of such systems.[45]

The subopen regime (shown as (b) in figures 21 and 22) shows some interesting unexpected features. In this case, the interacting system remains accurate up to high temperatures, while the non-interacting system deviates from scattering theory. This comes as a surprise, since the non-interacting case fulfills the unitarity of the s-matrix by definition and since the conductivity in the non-interacting case generally changes slower with regard to the variation of temperature than in the interacting case. Additionally, the interaction contribution to

---

[45]The fact that the s-matrix is highly non-unitary for finite temperatures is illustrated in [Sch18], Chapter 7.4.

noise vanishes in the case of no interactions. Thus, this result should be the subject of further investigation, including double-checking the numerical implementation for errors.
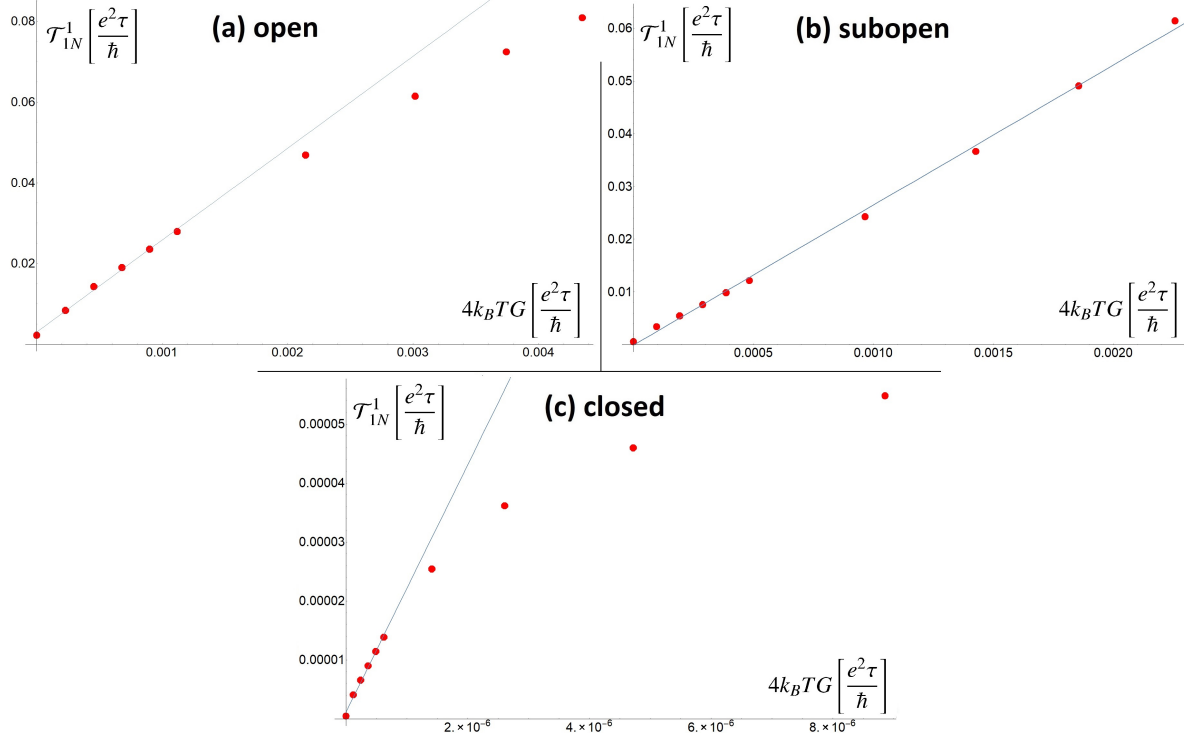

Figure 21: One-particle zero-frequency noise contribution $\mathcal{T}_{1N}^1$ as a function of temperature T times conductance G in open regime ($\mu = -1.475$), subopen regime ($\mu = -1.5$) and closed regime ($\mu = -1.55$) respectively (without magnetic field). The scatter plots were created at temperatures $T = 0, 0.0002, 0.0004, 0.0006, 0.0008, 0.001, 0.002, 0.003, 0.004$ and 0.005. In units of the curvature: $T = 0, 0.42427 \cdot 10^{-2} \, \Omega_x, 0.84854 \cdot 10^{-2} \, \Omega_x, 1.2728 \cdot 10^{-2} \, \Omega_x,$ $1.6971 \cdot 10^{-2} \, \Omega_x, 2.1213 \cdot 10^{-2} \, \Omega_x, 4.2427 \cdot 10^{-2} \, \Omega_x, 6.3640 \cdot 10^{-2} \, \Omega_x, 8.4854 \cdot 10^{-2} \, \Omega_x,$ $10.607 \cdot 10^{-2} \, \Omega_x$.

We wish to make a connection between the concept of the *s*-matrix in scattering theory and our formalism. To that end, it can be shown[46] that the *s*-matrix for our system is given by

$$s(\omega) = \begin{pmatrix} r(\omega) & t(\omega) \\ t'(\omega) & r'(\omega) \end{pmatrix} = \mathbb{1} - 2\pi i \rho(\omega) \tau^2 \begin{pmatrix} G_{11}^R(\omega) & G_{1N}^R(\omega) \\ G_{N1}^R(\omega) & G_{NN}^R(\omega) \end{pmatrix}$$

where $\rho(\omega) = \begin{cases} \frac{1}{2\pi\tau} \sqrt{4\tau^2 - \hbar^2\omega^2} & \text{, if } \hbar\omega \in [-2\tau, 2\tau] \\ 0 & \text{, else} \end{cases}$ is the density of states in the leads. This allows us, for example, to calculate the transmission probability in terms of the Greens function linking the first site to the last site.

We are going to use this relation in order to visualize this general result from scattering theory:

$$S = \frac{e^2}{2\pi\hbar} \sum_{\gamma\delta} \int dE \, A_{\gamma\delta}(E) A_{\delta\gamma}(E) \Big(f_\gamma(E)\big(1 - f_\delta(E)\big) + f_\delta(E)\big(1 - f_\gamma(E)\big) \Big) \qquad \text{(5 revisited)}$$
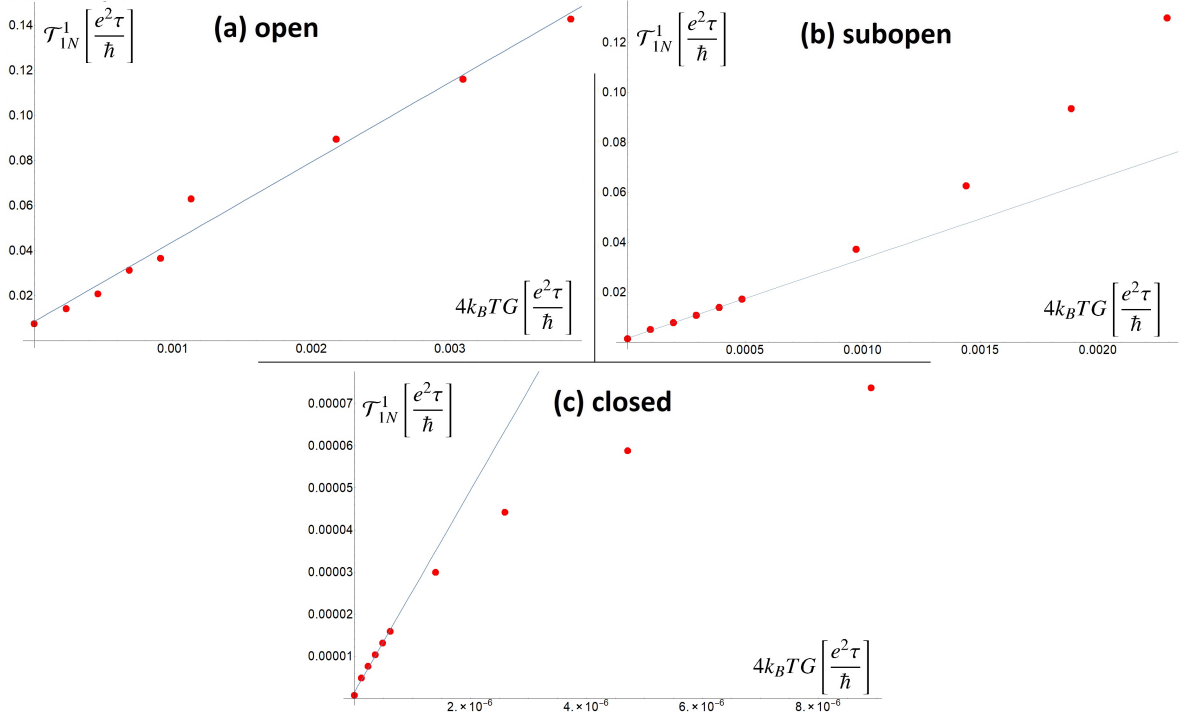
---

[46] see [Tay12]

Figure 22: One-particle zero-frequency noise contribution $\mathcal{T}_{1N}^1$ **in a strictly non-interacting system** as a function of temperature T times conductance G in open regime ($\mu = -1.475$), subopen regime ($\mu = -1.5$) and closed regime ($\mu = -1.55$) respectively (without magnetic field). The scatter plots were created at temperatures $T = 0, 0.0002, 0.0004, 0.0006, 0.0008$, $0.001, 0.002, 0.003, 0.004$ and 0.005. In units of the curvature: $T = 0, 0.42427 \cdot 10^{-2} \, \Omega_x$, $0.84854 \cdot 10^{-2} \, \Omega_x$, $1.2728 \cdot 10^{-2} \, \Omega_x$, $1.6971 \cdot 10^{-2} \, \Omega_x$, $2.1213 \cdot 10^{-2} \, \Omega_x$, $4.2427 \cdot 10^{-2} \, \Omega_x$, $6.3640 \cdot 10^{-2} \, \Omega_x$, $8.4854 \cdot 10^{-2} \, \Omega_x$, $10.607 \cdot 10^{-2} \, \Omega_x$.

This allows us to express the zero-frequency noise as an integral over all energies, specifically

$$S = \int d\omega_1 \zeta(\omega_1)$$

where $\zeta(\omega_1) := \dfrac{e^2}{2\pi} \sum_{\gamma\delta} A_{\gamma\delta}(\omega_1) A_{\delta\gamma}(\omega_1) \Big(f_\gamma(\omega_1)\big(1 - f_\delta(\omega_1)\big) + f_\delta(\omega_1)\big(1 - f_\gamma(\omega_1)\big) \Big)$ (41)

where ζ depends on the *s*-matrix and the Fermi functions at a given frequency. The Keldysh analogue to ζ can be found in our previous equation

$$\mathcal{T}_{jk}^1(\omega) = \frac{e^2 \tau_j \tau_k}{\hbar^2} \int \frac{d\omega_1}{2\pi} \Big\{ G_{k+1|j+1}^{-|+}(\omega_1) G_{j|k}^{-|+}(\omega_1 + \omega) + G_{k|j}^{-|+}(\omega_1) G_{j+1|k+1}^{-|+}(\omega_1 + \omega)$$

$$- G_{k|j+1}^{-|+}(\omega_1) G_{j|k+1}^{-|+}(\omega_1 + \omega) - G_{k+1|j}^{-|+}(\omega_1) G_{j+1|k}^{-|+}(\omega_1 + \omega) \Big\}$$

(32 revisited)

Thus, the zero-frequency noise can be expressed as

$$\mathcal{T}_{jk}^1(0) = \int d\omega_1 \sigma(\omega_1)$$

$$\text{where } \sigma(\omega_1) := \frac{e^2 \tau_j \tau_k}{\hbar^2} \Big\{ G_{k+1|j+1}^{-|+}(\omega_1) G_{j|k}^{-|+}(\omega_1) + G_{k|j}^{-|+}(\omega_1) G_{j+1|k+1}^{-|+}(\omega_1)$$

$$- G_{k|j+1}^{-|+}(\omega_1) G_{j|k+1}^{-|+}(\omega_1) - G_{k+1|j}^{-|+}(\omega_1) G_{j+1|k}^{-|+}(\omega_1) \Big\} \tag{42}$$

We wish to compare $\sigma(\omega_1)$ and $\zeta(\omega_1)$ as a consistency check between classical scattering theory and the results from our calculations. This comparison is made in figures 23 and 24 in the open and closed regime respectively. We observe that the integrands have exactly the same form, namely a peak at the chemical potential and outside of this region, a sharp decline to 0. This means that our model is consistent with scattering theory in the sense that frequencies around $\omega = \mu$ are the only contributing factor to the noise.

Naturally, we wish to calculate the integrals over ζ and σ in order to compare the classical result for the noise $S_{\text{scattering theory}}$ to the result of our calculations $\mathcal{T}_{1N}^1$ at zero frequency. This is done in figure 25(a) for the open regime at various temperatures in the non-interacting case. As expected, there is a linear dependence between the prediction of scattering theory and our results. However, once again we observe a scaling problem with regard to our implementation.

Figure 25(b) serves as a self-consistency check, namely that the calculation of the s-matrix through the retarded Greens function and the subsequent evaluation the classical integral in equation (41) matches the expected result $S_{\text{scattering theory}} = 4k_B T G$. The proportionality is well fulfilled, which is is the reason behind the fact that figures 22(a) and 25(a) look very similar.

Figure 23: Comparison between noise integrands predicted by (a) scattering theory ($\zeta(\omega_1)$) and our (b) model ($\sigma(\omega_1)$). The system is evaluated in the open regime ($\mu = -1.475$) at a temperature $T = 0.0008 = 1.6971 \cdot 10^{-2} \, \Omega_x$, with no magnetic field.
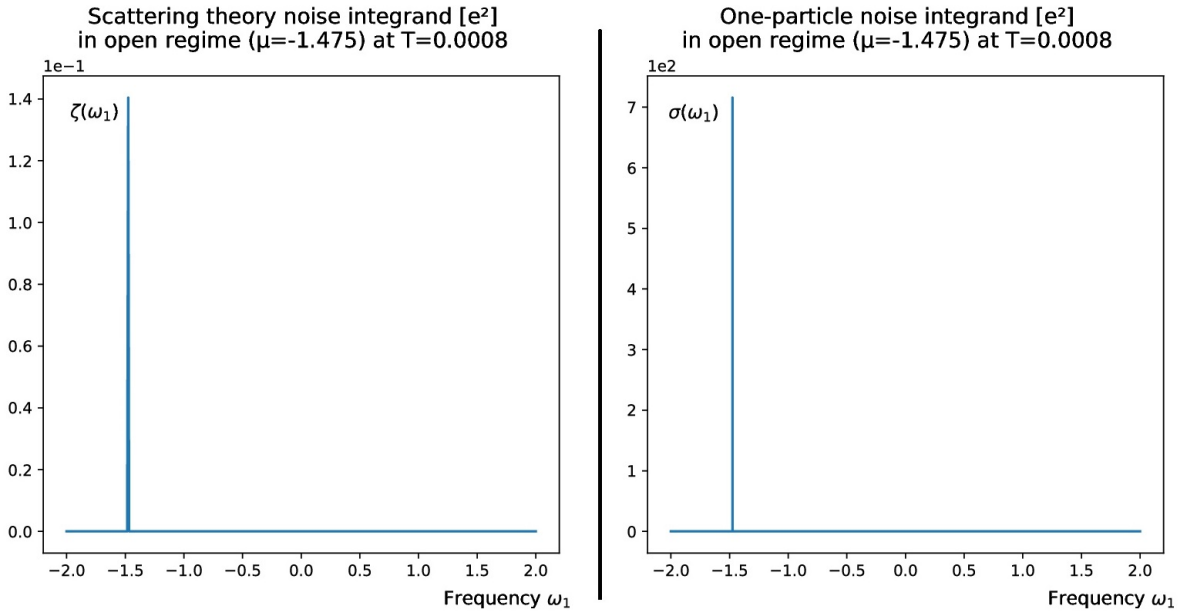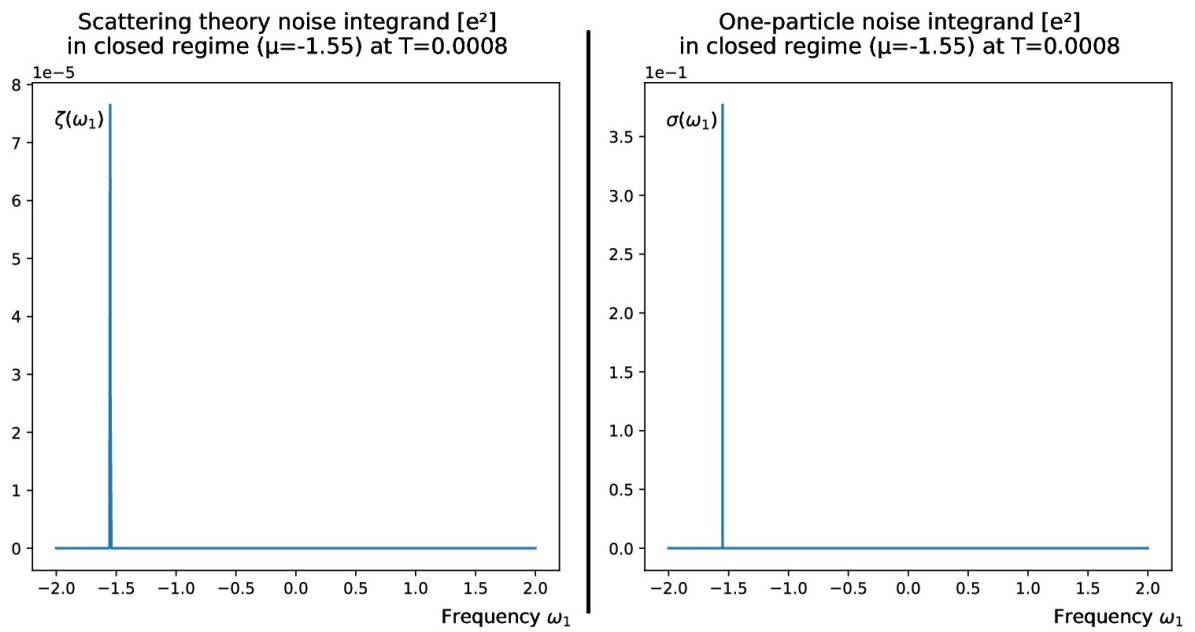
Figure 24: Comparison between noise integrands predicted by (a) scattering theory ($\zeta(\omega_1)$) and our (b) model ($\sigma(\omega_1)$). The system is evaluated in the closed regime ($\mu = -1.55$) at a temperature $T = 0.0008 = 1.6971 \cdot 10^{-2}\ \Omega_x$, with no magnetic field.
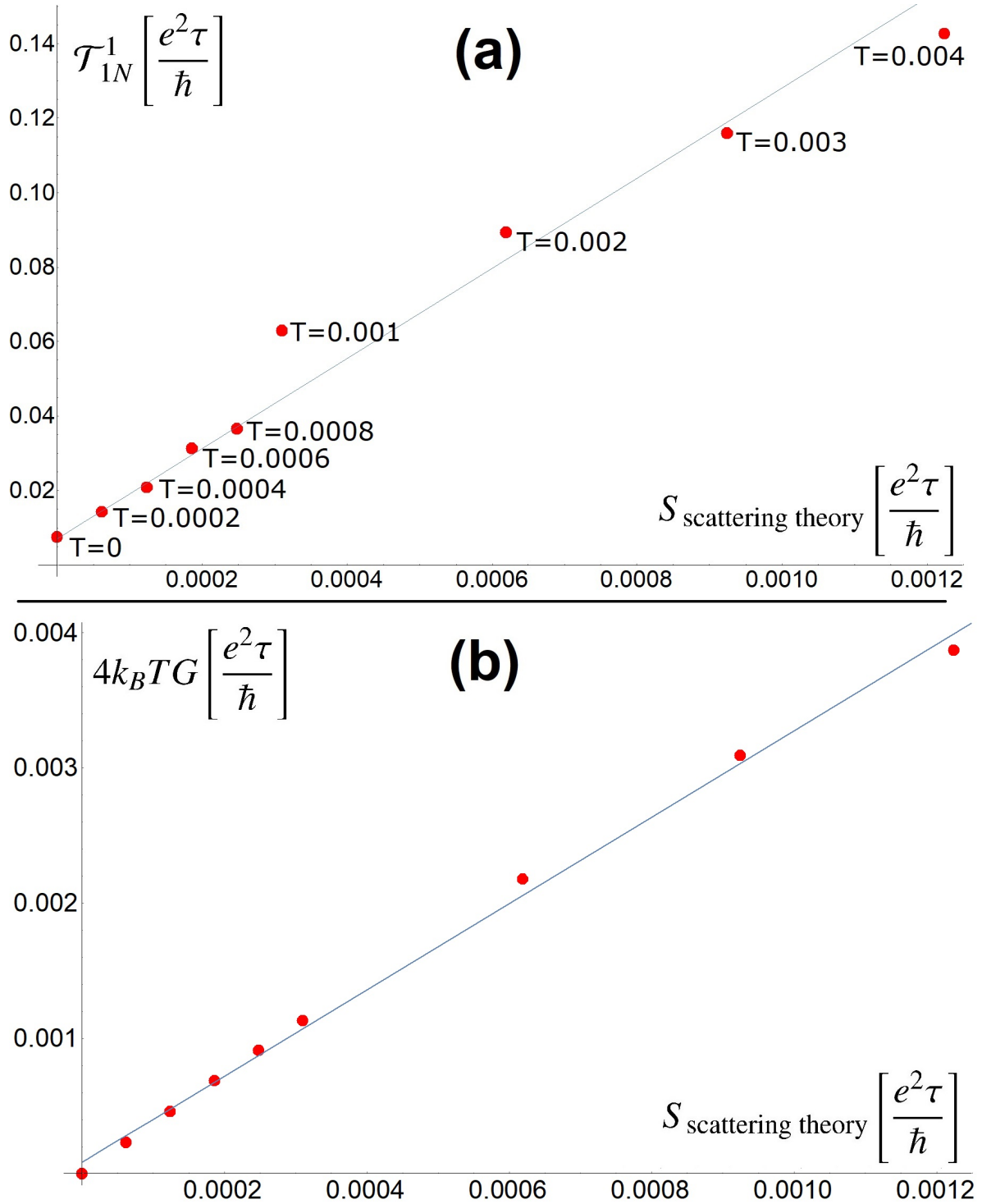
Figure 25: (a) Scatter plot of the zero frequency noise $\mathcal{T}_{1N}^1$ as a function of the noise predicted by scattering theory $S_{\text{scattering theory}}$ **in a strictly non-interacting system**. In this case, the system is in the open regime ($\mu = -1.475$) and the temperature is varied. In units of the curvature: $T = 0$, $0.42427 \cdot 10^{-2}\ \Omega_x$, $0.84854 \cdot 10^{-2}\ \Omega_x$, $1.2728 \cdot 10^{-2}\ \Omega_x$, $1.6971 \cdot 10^{-2}\ \Omega_x$, $2.1213 \cdot 10^{-2}\ \Omega_x$, $4.2427 \cdot 10^{-2}\ \Omega_x$, $6.3640 \cdot 10^{-2}\ \Omega_x$, $8.4854 \cdot 10^{-2}\ \Omega_x$, $10.607 \cdot 10^{-2}\ \Omega_x$. (b) Scatter plot of the product of conductance and temperature as a a function of the noise predicted by scattering theory $S_{\text{scattering theory}}$ **in a strictly non-interacting system**. The system is in the open regime ($\mu = -1.475$) and the temperature is varied as in (a).

6.5.2 Equilibrium noise: two-particle contribution

We consider the two-particle contribution to the noise $\mathcal{T}^2_{1N}(\omega)$, as given by equation (33). Evaluating this term for many frequencies is numerically very expensive, as mentioned before, which is the reason why we have been able to analyze the one-particle term to a greater extent.

Figure 26 is a plot of the one- and two-particle contributions to noise in the open regime at zero temperature. Note that the contribution of the two-particle term to zero-frequency noise vanishes, i.e. $\mathcal{T}^2_{1N}(0) = 0$. This is consistent with the fact that the contribution of the two-particle vertex to the conductivity in the zero-temperature limit vanishes, as predicted in [Ogu01] and [Kar06].

However, the fact that the imaginary part of the two-particle noise is nonzero and that it has the same magnitude as its real part is a contradiction to our theoretic expectation that equilibrium noise should be real and symmetric, as described in equation (38). This implies that there has either been a significant error with the fRG flow or in the utilization of its results to calculate the integrand of $\mathcal{T}^2_{1N}(\omega)$. Either way, this has to be subject of further investigations.
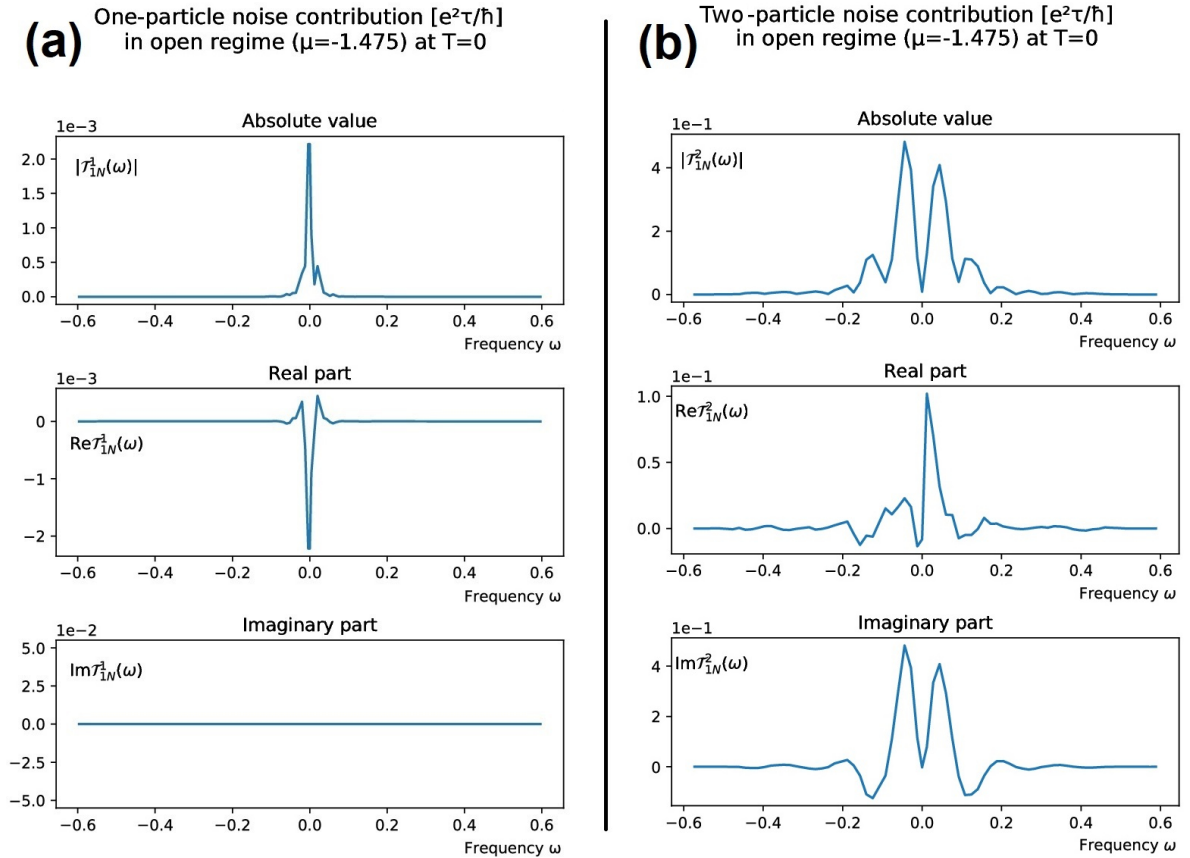

Figure 26: (a) One-particle noise contribution $\mathcal{T}^1_{1N}(\omega)$ in open regime ($\mu = -1.475$) at temperature $T = 0$ and with no magnetic field. (b) Two-particle noise contribution $\mathcal{T}^2_{1N}(\omega)$ in open regime ($\mu = -1.475$) at temperature $T = 0$ and with no magnetic field.

6.5.3   Non-equilibrium noise

The non-equilibrium case is more complicated to treat in many regards, as most symmetries of the system break down and the fluctuation dissipation theorem is no longer valid. Nevertheless, this section is dedicated to presenting the current results of the fRG flow as well as pointing out which areas are in need for improvement and further investigation.

6.5.3.1   Noise as a function of frequency

We consider the noise term $\mathcal{T}^1_{1N}(\omega)$ in figure 27 for $\Delta\mu > 0$ in the open and closed regime respectively. We make the following observations:

- The noise satisfies our expectation $\left[\mathcal{T}^1_{jk}(\omega)\right]^* = \mathcal{T}^1_{jk}(-\omega)$ (see equation (35)), which serves as a useful self-consistency check that the noise is indeed the Fourier transform of a real function.

- The noise is non-white, its absolute value is maximal around $\omega = 0$ and decreasing for large $|\omega|$; however this time far more slowly than in the equilibrium case. We have already discussed the fact that a classical consideration of shot noise predicts it to have the approximate form of a sinc-function (see equation (39)). This is well fulfilled by its real and imaginary part respectively; we can observe the same wave-like decreasing form as a sinc.
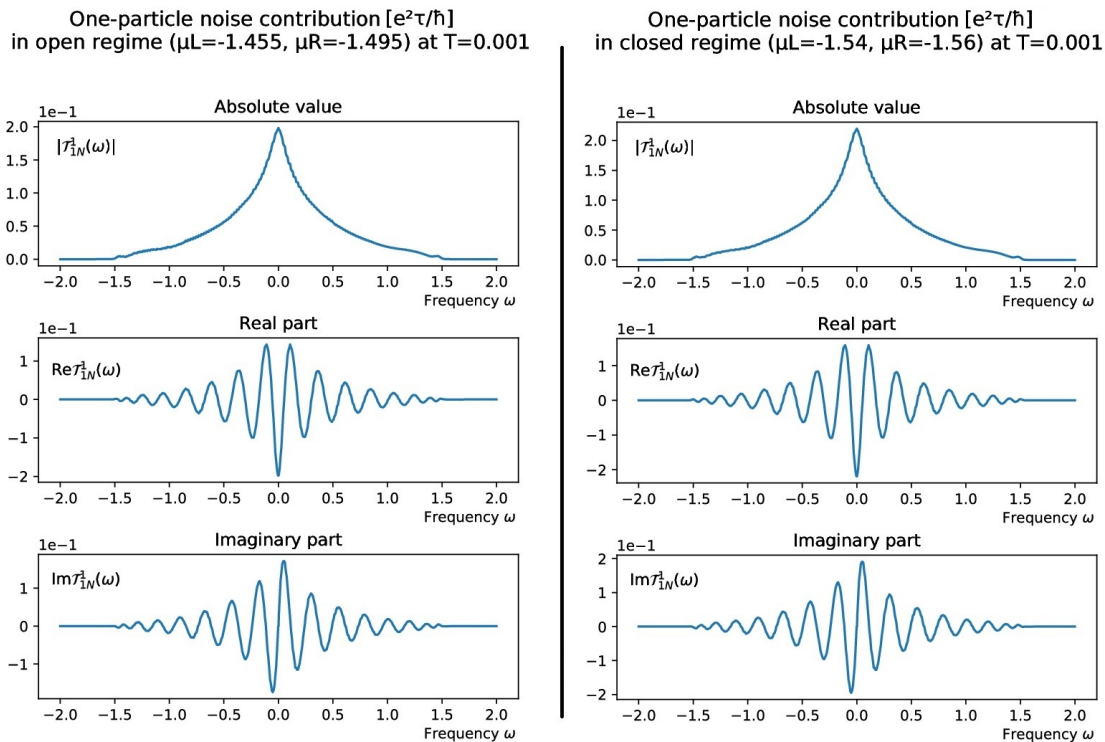

Figure 27: One-particle noise contribution $\mathcal{T}^1_{1N}(\omega)$ in the open regime ($\mu_L = -1.455, \mu_R = -1.495$) and the closed regime ($\mu_L = -1.54, \mu_R = -1.56$) respectively, evaluated at temperature $T = 0.001 = 1.4142 \cdot 10^{-2}\ \Omega_x$, with no magnetic field

6.5.3.2 Noise as a function of conductance

Recall the following results from scattering theory:

$$G = \frac{e^2}{2\pi\hbar}|t|^2 \text{ for } T \ll 1 \tag{4 revisited}$$

$$S = \frac{e^2}{\pi\hbar}\left[2k_BT|t|^2 + eV_{sd}\coth\left(\frac{eV_{sd}}{2k_BT}\right)|t|^2(1-|t|^2)\right] \tag{8 revisited}$$

By making the approximation $1 - |t|^2 \approx 1$ (which is fulfilled very well in the closed and subopen regimes) and by rewriting $\mathcal{N} := |t|^2/2$ we obtain

$$S - 4k_BTG = 2\frac{2e^2}{h}\mathcal{N}\left[eV_{sd}\coth\left(\frac{eV_{sd}}{2k_BT}\right) - 2k_BT\right] \tag{43}$$

This equation with $\mathcal{N}$ as the only free fitting parameter has been used in experimental measurements as a way to confirm scattering theory. For example, figure 28, originating from [DZM$^+$06], is such a fit of $\mathcal{N}$ as a function of the conductance G.
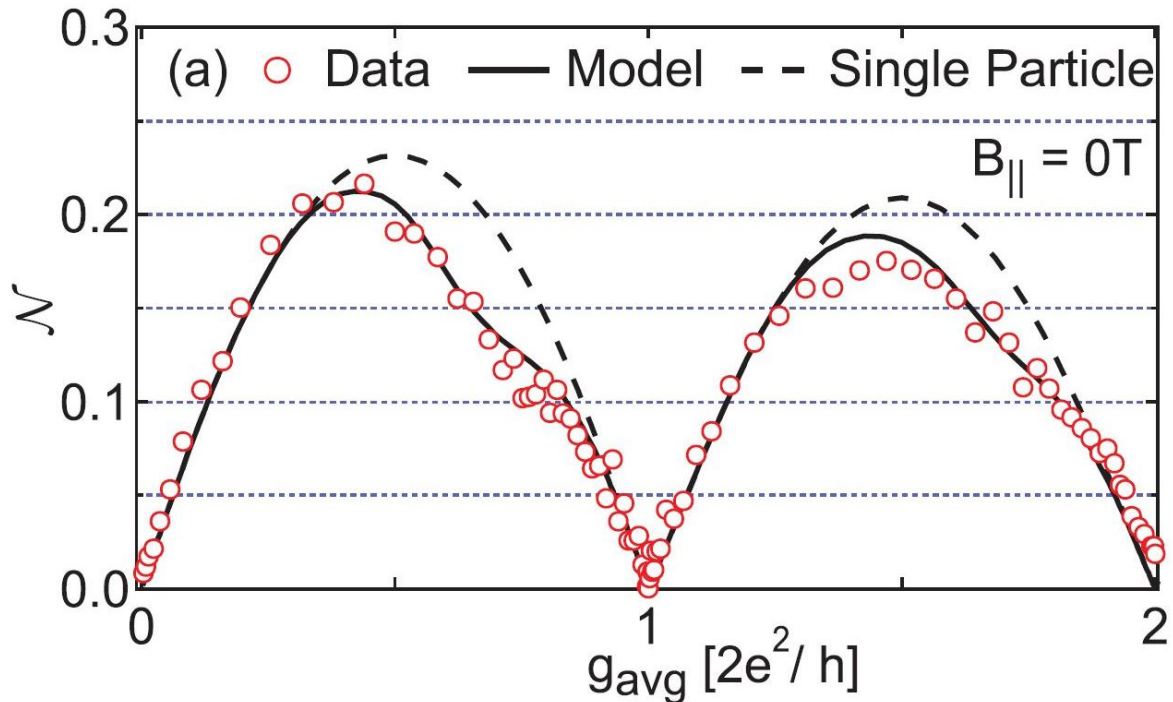
Figure 28: Experimental fit of the noise parameter $\mathcal{N}$ as a function of the measured conductance g_{avg} for various temperatures and chemical potentials with no magnetic field. [DZM$^+$06]

In an attempt to replicate the result above with the Keldysh fRG method, we obtained figure 29 as a plot of $\mathcal{N}$ to G, where the different points correspond to various $\Delta\mu$ and T. However, as one can see from the figure, the results are far too inaccurate at this point, so as to obtain a good fit matching the experimental results. There could be various reasons for this:

- The calculation of the local conductance is tackled in the fRG flow by differentiating the current with respect to μ_L and μ_R and then taking the average value. This is more

complicated than in the equilibrium case, where the chemical potentials are equal and the calculation of the conductance is comparatively more straightforward. This leads to a large discrepancy between the derivatives before they are averaged, which in turn leads to a high fluctuation of G from site to site, as one can see in figures 30 and 31. The fluctuation is as strong as 20% around the mean, which indicates a possible source of error.

- The neglect of the two-particle term $\mathcal{T}_{1N}^2(\omega)$ is not as easily justifiable in the non-equilibrium case, as interactions between electrons are more predominant.

- The fRG flow for the non-equilibrium case has not been perfected yet to the same degree as in the equilibrium case, which leads to high inaccuracies in some results.
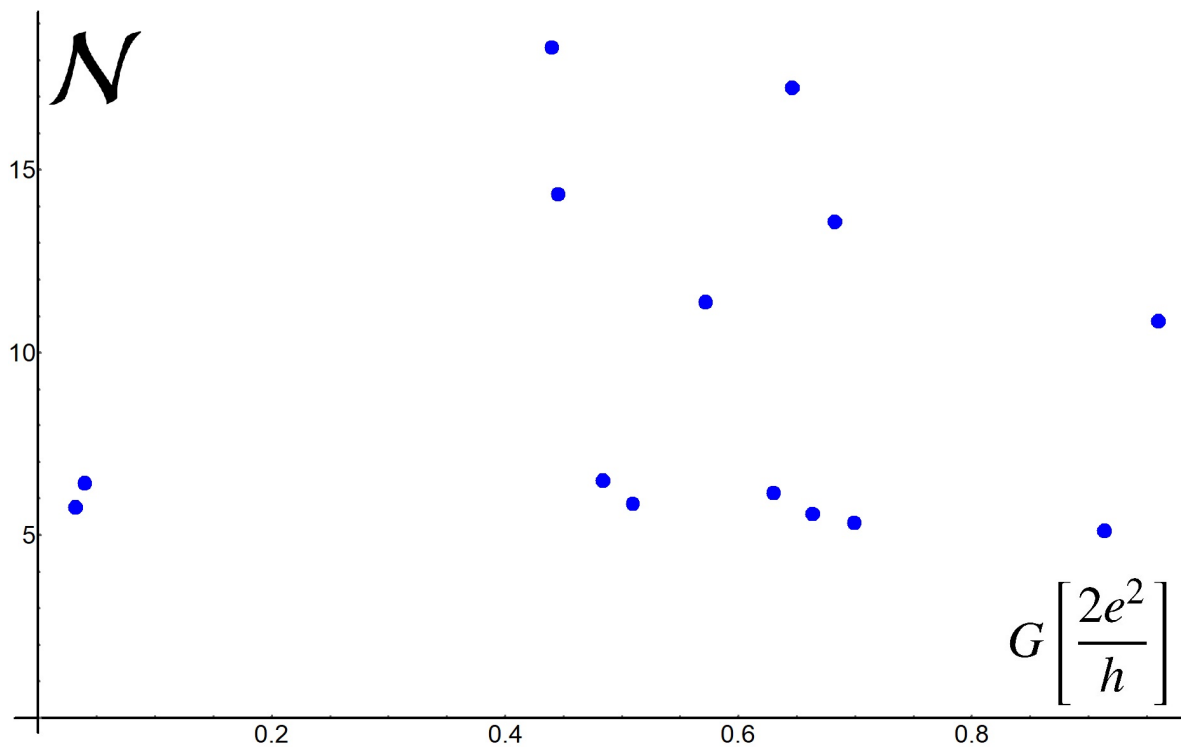
Figure 29: Our calculation of the noise parameter $\mathcal{N}$ as a function of the mean conductance G for various temperatures and chemical potentials with no magnetic field
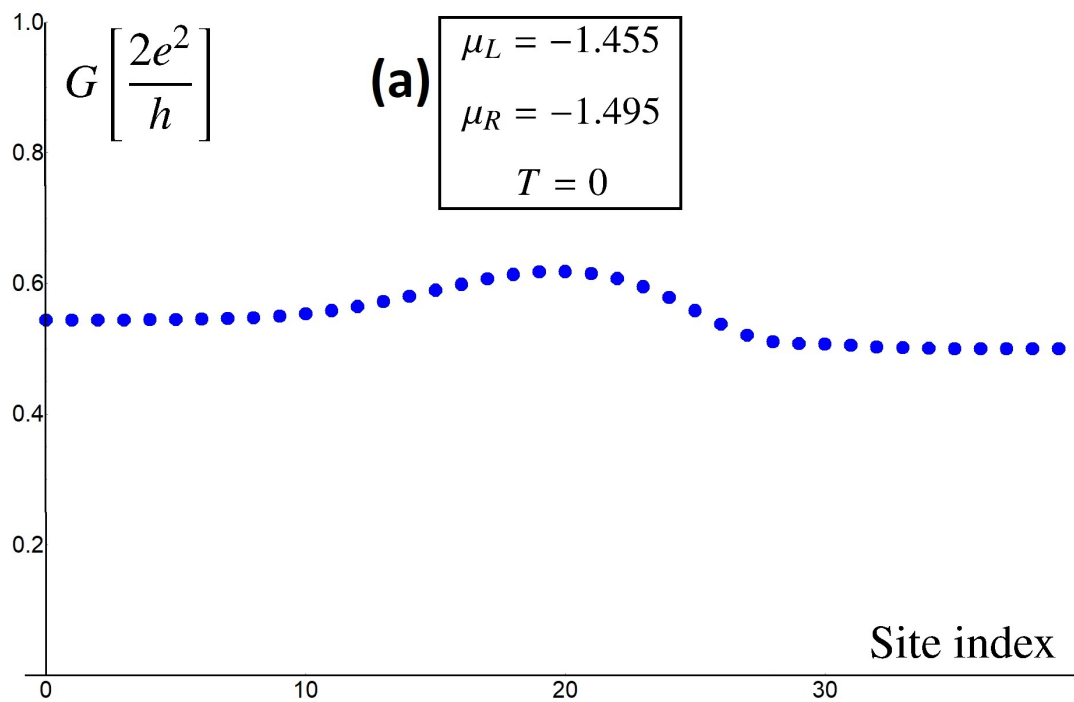
Figure 30: Local conductance G_j as a function of the site index j in the open regime ($\mu_L = -1.455, \mu_R = -1.495$) for temperature $T = 0$
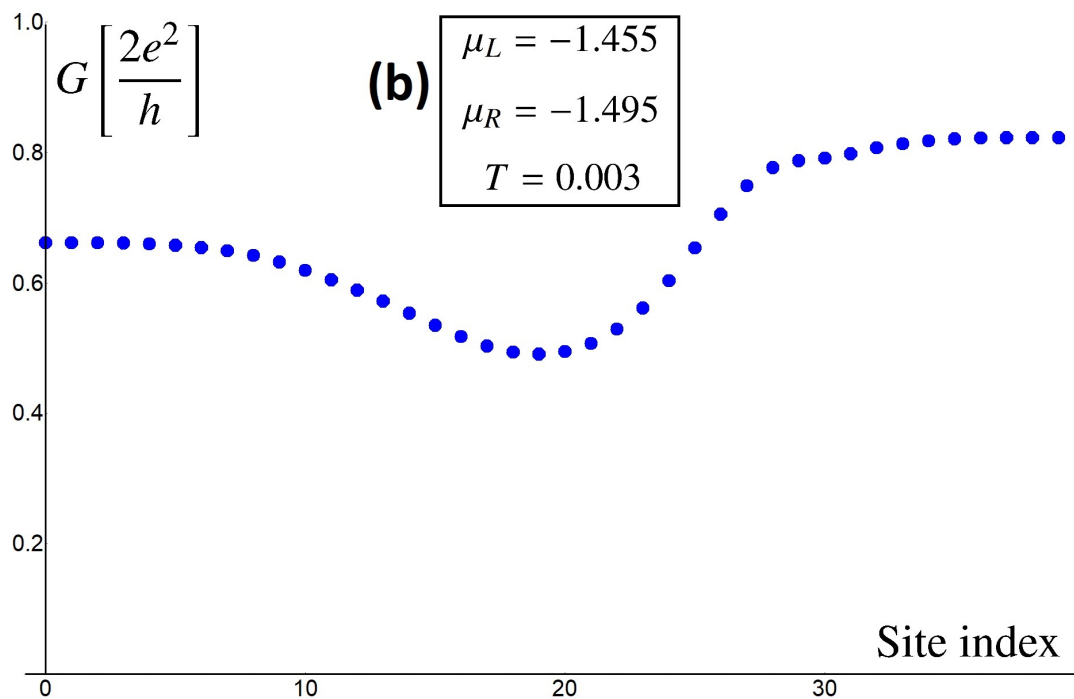
Figure 31: Local conductance G_j as a function of the site index j in the open regime ($\mu_L = -1.455, \mu_R = -1.495$) for temperature $T = 0.003 = 4.2427 \cdot 10^{-2}\Omega_x$

6.5.3.3 Comparison to scattering theory

Once again, we wish to compare the two noise integrands, one from scattering theory and the other from our Keldysh approach, in order the compare the results of the two theories. To that end, we are interested in plots of $\zeta(\omega_1)$ and $\sigma(\omega_1)$, which have been introduced in section 6.5.1.2 in the following way:

$$S = \int d\omega_1 \zeta(\omega_1)$$

$$\text{where } \zeta(\omega_1) := \frac{e^2}{2\pi} \sum_{\gamma\delta} A_{\gamma\delta}(\omega_1) A_{\delta\gamma}(\omega_1) \Big(f_\gamma(\omega_1)\big(1 - f_\delta(\omega_1)\big) + f_\delta(\omega_1)\big(1 - f_\gamma(\omega_1)\big) \Big)$$

(41 revisited)

$$\mathcal{T}^1_{jk}(0) = \int d\omega_1 \sigma(\omega_1)$$

$$\text{where } \sigma(\omega_1) := \frac{e^2 \tau_j \tau_k}{\hbar^2} \Big\{ G^{-|+}_{k+1|j+1}(\omega_1) G^{-|+}_{j|k}(\omega_1) + G^{-|+}_{k|j}(\omega_1) G^{-|+}_{j+1|k+1}(\omega_1)$$

$$- G^{-|+}_{k|j+1}(\omega_1) G^{-|+}_{j|k+1}(\omega_1) - G^{-|+}_{k+1|j}(\omega_1) G^{-|+}_{j+1|k}(\omega_1) \Big\} \qquad \text{(42 revisited)}$$

Figure 32: Comparison between noise integrands predicted by (a) scattering theory ($\zeta(\omega_1)$) and our (b) model ($\sigma(\omega_1)$). The system is evaluated in the open regime ($\mu_L = -1.455, \mu_R = -1.495$) at a temperature $T = 0.001 = 1.4142 \cdot 10^{-2} \, \Omega_x$ with no magnetic field.

The results have been plotted in figures 32 and 33. Both integrands are real within numerical accuracy, but ζ is only non-vanishing around the chemical potentials, while σ is non-vanishing for all frequencies between the chemical potentials and $\omega = 0$. Unfortunately, this result is discouraging in terms of finding a direct theoretical relation between ζ and σ, which constitutes a topic of high interest.

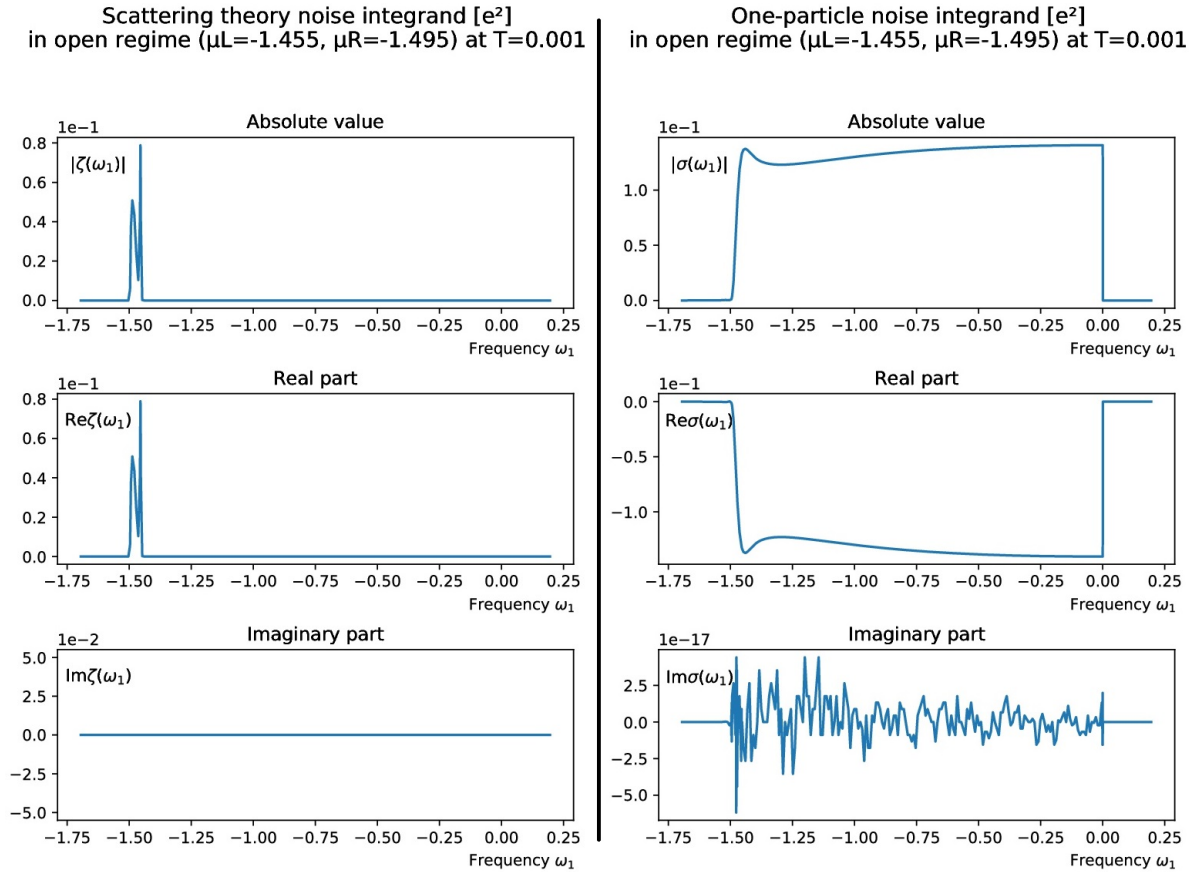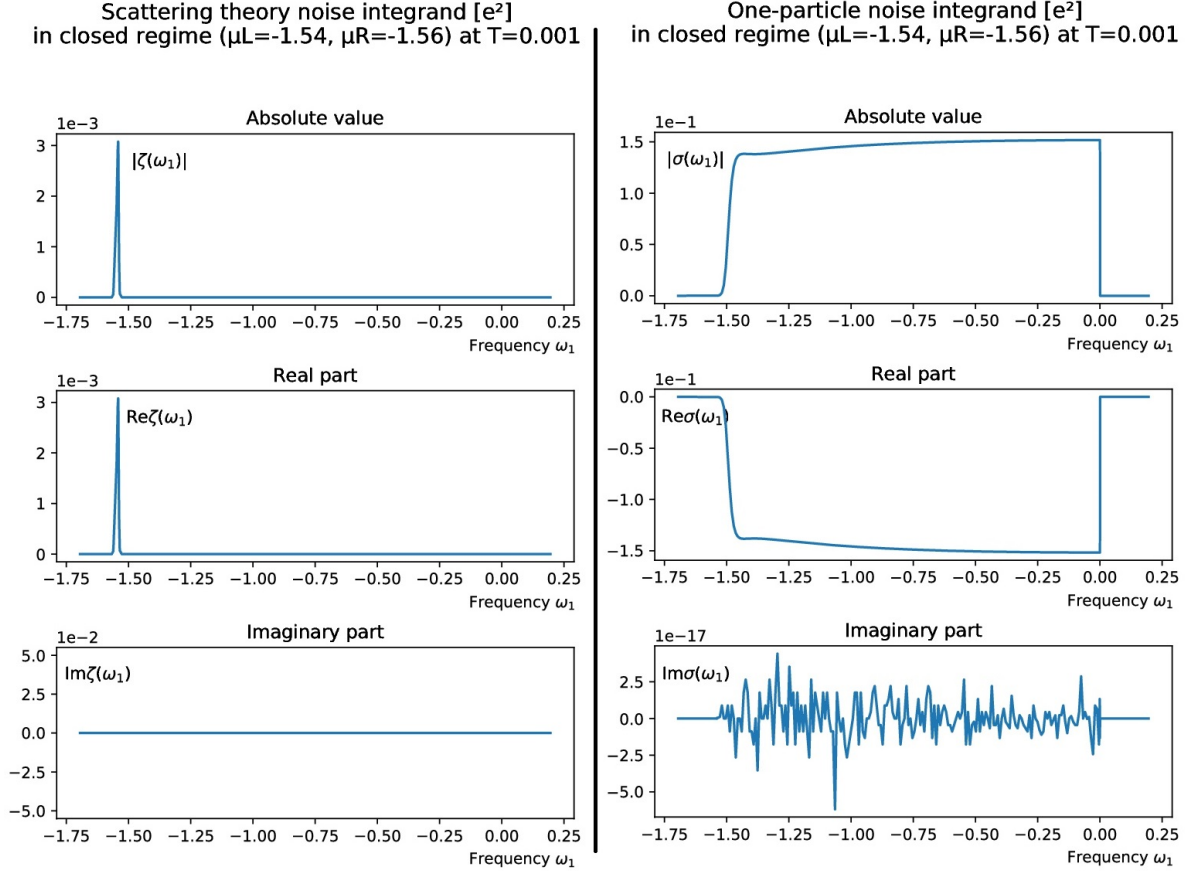Figure 33: Comparison between noise integrands predicted by (a) scattering theory ($\zeta(\omega_1)$) and our (b) model ($\sigma(\omega_1)$). The system is evaluated in the closed regime ($\mu_L = -1.54, \mu_R = -1.56$) at a temperature $T = 0.001 = 1.4142 \cdot 10^{-2}\ \Omega_x$ with no magnetic field.

7 Conclusion

7.1 Summary of results

This thesis demonstrates the feasibility of utilizing the Keldysh formalism to describe transport properties of strongly correlated many-body systems. We presented arguments for our description of the quantum point contact as a tight-binding chain and discretizing the Hamiltonian. Then we proceeded with deriving expressions for the current and noise within this formalism and investigating the properties of these observables. We split the noise S into two parts: a contribution arising from the dressed one-particle propagators and a two-particle contribution, which incorporates the two-electron vertex functions.

The main focus of the work leading up to this thesis lies within the numerical implementation of the model. As a starting point, previous results about the QPC as well as an implementation of the functional Renormalization Group flow equations have been used, which have been thoroughly referenced in the respective sections of this thesis. Building on these results, first of all, the system was modeled in both the equilibrium and the non-equilibrium case for various temperatures, chemical potentials and interaction strength parameters. Then we proceeded with the calculation of the full one- and two-particle propagators, as well as with the subsequent task of evaluating the numerically expensive integrals.

First, we treated the equilibrium case and visualized our results for the one-particle noise contributions. We showed that we obtain the best results and minimize non-physical artifacts of the discretization by considering terms that include a propagation across the entire length of the QPC instead of just small portions of it; or even worse, adjacent sites. We also showed that the one-particle noise terms fulfill many important identities, thus increasing our confidence in these results. Most importantly, we made numerous comparisons between our noise term and the theoretical predictions of scattering theory. Specifically, we showed that the two different approaches yield similar results in the low-temperature limit.

From this, two conclusions can be drawn. Firstly, the one-particle noise term fully suffices to describe certain transport phenomena in the low-temperature limit, as it outweighs the interaction term, which is only expected to become relevant at certain regimes or finite temperatures. Generally, the smaller the role of electron-electron interactions becomes, the more well justified the neglect of interaction terms is. This can be very useful, since interaction terms are usually more difficult and numerically expensive to compute. Secondly, the good correspondence between the results from scattering theory and our formalism allows us to consider the Keldysh method as a correction to the classical theory. Our approach is more exact, in theory, as it is more powerful and fully able to describe all features of a scattering approach, while dropping some of its basic assumptions, such as the unitarity of the s-matrix.

Then we proceeded to consider the two-particle contribution in the equilibrium case. Unfortunately, we have far fewer results here due to the expensive nature of the calculations. Additionally, this noise term fails to satisfy some basic identities, which lowers our confidence in the correctness of these results.

Going on, we considered the non-equilibrium case, whose fRG code is the most recent and a somewhat still experimental addition to our repository. Again, we confirmed that all one-particle noise terms satisfy some basic physical identities as a self-consistency check. We noticed that the form of the noise terms bears an interesting resemblance to some classical

results about shot noise, which can be seen as an another indicator that our approach is a more complete extension of previous classical considerations.

In the end, we compared our results in the non-equilibrium case to experimental measurements of noise in quantum point contacts and, again, to theoretical predictions from scattering theory. In both cases, the quality of the results is not as good as to justify definite conclusions, which means that a further investigation of this case is still needed.

7.2 Outlook and future endeavours

We were able to demonstrate the effectiveness of our approach in numerous cases surrounding noise phenomena. Furthermore, the pre-existing work about the Keldysh formalism and the functional Renormalization Group is well founded and has established the respective power and usefulness of the approaches. However, there is still some more research needed into questions, which have been left unanswered or which arose during research for this thesis that could serve as a starting point for further investigation down the road. Thus, here we present a brief overview over remaining problems:

- The scaling problem in this thesis needs to be addressed. While we have been able to demonstrate many results of qualitative nature, the slopes in some diagrams are off by up to two orders of magnitude from their expected value, which points us to some error or inconsistency in unit conventions that have been used throughout the implementation.

- The subopen regime has always been demonstrating the most anomalous and interesting features of the QPC, e.g. the 0.7 anomaly. In our case, our results concerning the subopen non-interacting system show a far greater deviation from scattering theory than the results in an interacting setting,[47] which still lacks a satisfactory explanation. A step-by-step investigation into this case is recommended.

- Both the on-site and the two-particle contributions to the noise violate basic identities.[48] The latter may point to an error in the fRG flow or to an error in the subsequent calculation of propagators from the results of said flow.

- All the non-equilibrium results are still experimental, since the fRG flow is newer and more inaccurate. There are still some obstacles, which have to be addressed, so that these results can be compared to both experimental measurements and scattering theory with sufficient confidence.

- Finally, one-loop fRG is known to have limitations, since the obtained results depend on the specific choice and implementation of the cutoff in the flow equations. Future work could aim to remedy this using multiloop fRG [Kv18].

---

[47]See figures 21(b) and 22(b).
[48]See figures 19, 20 and 26.

8 Appendix

8.1 Appendix A: Derivation of the free propagator

Here we derive the free propagator (see section 4.8). In the following steps, we are going to follow a similar approach as in [Kam11], which is recommended for further reading.

We are going to restrict ourselves to the fermionic case, since our goal is the description of electrons. Note that the bosonic case can be treated in a similar manner using bosonic statistics.

We have already shown in section 4 that

$$
\begin{aligned}
g^R_{s_1|s_2}(t_1|t_2) &= \theta(t_1 - t_2)\Big(g^{+|-}_{s_1|s_2}(t_1|t_2) - g^{-|+}_{s_1|s_2}(t_1|t_2)\Big) \\
&= -i\theta(t_1 - t_2)\Big\langle \mathbb{T}_C\Big(c^+_{s_1}(t_1)c^{-\,\dagger}_{s_2}(t_2) + c^{-\,\dagger}_{s_2}(t_2)c^+_{s_1}(t_1)\Big)\Big\rangle \\
&\propto \theta(t_1 - t_2)\delta_{s_1,s_2} \text{ by the anti-commutation rules} \\
g^A_{s_1|s_2}(t_1|t_2) &= \theta(t_2 - t_1)\Big(g^{-|+}_{s_1|s_2}(t_1|t_2) - g^{+|-}_{s_1|s_2}(t_1|t_2)\Big) \\
&= i\theta(t_2 - t_1)\Big\langle \mathbb{T}_C\Big(c^+_{s_1}(t_1)c^{-\,\dagger}_{s_2}(t_2) + c^{-\,\dagger}_{s_2}(t_2)c^+_{s_1}(t_1)\Big)\Big\rangle \\
&\propto \theta(t_2 - t_1)\delta_{s_1,s_2} \text{ by the anti-commutation rules}
\end{aligned}
$$

From the fluctuation dissipation theorem, we also obtain $g^K_{s_1|s_2}(t_1|t_2) \propto \delta_{s_1,s_2}$. Thus, it suffices to restrict the following considerations to the case of fermionic particles occupying a single quantum level. All quantum numbers s are assumed to be identical from here on.

Our approach is to calculate the above expectation values by deriving concrete expressions for the action and the partition function, which serves as the generating functional of correlation functions. This will be done in a discrete manner and we are going to consider the limit of continuous time.

8.1.1 Grassmann algebra and fermionic coherent states

According to the Pauli exclusion principle, one may have either zero or one fermion in such a single state. Thus, the entire many-body system is spanned by two orthonormal basis states $|0\rangle$ and $|1\rangle$. The fermionic creation and annihilation operators $c^\dagger$ and c fulfill following relations:

$$
c|0\rangle = 0, \quad c|1\rangle = |0\rangle, \quad c^\dagger|0\rangle = 1, \quad c^\dagger|1\rangle = 0
$$

For $n \in \{0, 1\}$ the following basic properties follow from the anti-commutation relations:

$$
c^\dagger c|n\rangle = n|n\rangle, \quad cc^\dagger + c^\dagger c = \mathbb{1}, \quad c^2 = (c^\dagger)^2 = 0
$$

We wish to introduce fermionic coherent states, which are eigenstates of the annihilation operator. To that end, one needs the Grassmann algebra; an algebra of anti-commuting numbers. The reasoning behind this is that a superposition of the two basis vectors of the Hilbert space with complex numbers does not suffice: in particular, for $x, y, \lambda \in \mathbb{C}$ we have $c(x|0\rangle + y|1\rangle) = y|0\rangle \neq \lambda(x|0\rangle + y|1\rangle)$, unless $y = \lambda = 0$.

The Grassmann algebra is defined by a set of generators $\{\psi_\alpha\}, \alpha = 1, 2, 3, \ldots, N$ for which there are the following available operations: they can be added, multiplied with complex

numbers and multiplied to each other. These generators anti-commute:

$$\psi_\alpha \psi_\beta + \psi_\beta \psi_\alpha = 0$$

In particular

$$\psi^2 = 0$$

Because of this property, any function f on the Grassmann algebra is fully defined by its first two Taylor expansion coefficients:

$$f(\psi) = f_0 + f_1 \psi$$

For example $e^\psi \equiv 1 + \psi$. Similarly, a function f of two variables is given by

$$f(\psi, \psi') = f_{00} + f_{10}\psi + f_{01}\psi' + f_{11}\psi\psi'$$

This allows us to introduce derivatives in a natural way with $\partial\psi/\partial\psi = 1$. Thus, $\partial f(\psi)/\partial\psi = f_1$. In practice, the definition of the derivative is identical to the one of the complex derivative, except for the fact that in order for $\frac{\partial}{\partial\psi}$ to act on ψ, ψ has to be anti-commuted through until it is adjacent to $\frac{\partial}{\partial\psi}$. This implies that derivatives anti-commute:

$$\frac{\partial}{\partial\psi}\frac{\partial}{\partial\psi'}f(\psi,\psi') = \frac{\partial}{\partial\psi}(f_{01} - f_{11}\psi) = -f_{11} = -\frac{\partial}{\partial\psi'}(f_{10} + f_{11}\psi') = -\frac{\partial}{\partial\psi'}\frac{\partial}{\partial\psi}f(\psi,\psi') \quad (44)$$

We also introduce the notion of an integral in the Grassmann algebra. It is defined as

$$\int d\psi\, 1 = 0, \qquad \int d\psi\, \psi = 1$$

The only non-vanishing integral is that of ψ, because it is not a derivative in contrast to 1.

Finally, we define that the creation and annihilation operator anti-commute with the Grassmann numbers, i.e.

$$c\psi + \psi c = 0, \qquad c^\dagger\psi + \psi c^\dagger = 0$$

We are now ready to construct coherent states. Given a Grassmann number ψ, consider a state characterized by this number

$$|\psi\rangle \equiv |0\rangle - \psi|1\rangle = (1 - \psi c^\dagger)|0\rangle = e^{-\psi c^\dagger}|0\rangle$$

Then $c|\psi\rangle = -c\psi|1\rangle = \psi c|1\rangle = \psi|0\rangle = \psi|0\rangle - \psi^2|1\rangle = \psi|\psi\rangle$, which means that $|\psi\rangle$ is an eigenstate of the fermionic annihilation operator with eigenvalue ψ. In an analogous way, one defines the left coherent state $\langle\psi|$ as a left eigenstate of $c^\dagger$ with eigenvalue $\bar\psi$, where $\bar\psi$ is a Grassmann number that is completely unrelated to ψ:

$$\langle\psi| \equiv \langle0| - \langle1|\bar\psi = \langle0|(1 - c\bar\psi) = \langle0|e^{-c\bar\psi}$$
$$\implies \langle\psi|c^\dagger = \langle0|(1 - c\bar\psi)c^\dagger = \langle0|\bar\psi = \langle\psi|\bar\psi$$

The set of coherent states is not orthonormal. The overlap of two coherent states is given by

$$\langle\psi|\psi'\rangle = \big(\langle0| - \langle1|\bar\psi\big)\big(|0\rangle - \psi|1\rangle\big) = 1 + \bar\psi\psi = e^{\bar\psi\psi}$$

Analogous to the completeness relation $\sum_{n=0,1} |n\rangle\langle n| = \mathbb{1}$, one can derive the resolution of unity in the fermionic coherent state representation:

$$\int d\bar{\psi} \int d\psi \, e^{-\bar{\psi}\psi}|\psi\rangle\langle\psi| = \mathbb{1} \tag{45}$$

This holds true because the term in the integral is equal to $(1 - \bar{\psi}\psi)|\psi\rangle\langle\psi|$. We obtain

$$
\begin{aligned}
(1 - \bar{\psi}\psi)|\psi\rangle\langle\psi| &= (1 - \bar{\psi}\psi)\big(|0\rangle - \psi|1\rangle\big)\big(\langle 0| - \langle 1|\bar{\psi}\big) \\
&= \big(|0\rangle - \psi|1\rangle - \bar{\psi}\psi|0\rangle\big)\big(\langle 0| - \langle 1|\bar{\psi}\big) \\
&= |0\rangle\langle 0| - |0\rangle\langle 1|\bar{\psi} - \psi|1\rangle\langle 0| - \bar{\psi}\psi\big(|0\rangle\langle 0| + |1\rangle\langle 1|\big) \\
&= |0\rangle\langle 0| - |0\rangle\langle 1|\bar{\psi} - \psi|1\rangle\langle 0| - \bar{\psi}\psi\mathbb{1}
\end{aligned}
$$

Performing the two integrations, all terms not containing $\bar{\psi}\psi$ vanish. The (-1) factor disappears because one has to anti-commute ψ to be next to $d\psi$ in order to evaluate the inner integral. This proves equation (45).

Last, we wish to calculate the trace of an operator in the coherent basis. To this end, we observe that every normally ordered[49] operator $\hat{H}$ fulfills

$$\langle\psi|\hat{H}(c^\dagger, c)|\psi'\rangle = \hat{H}(\bar{\psi}, \psi')\langle\psi|\psi'\rangle = \hat{H}(\bar{\psi}, \psi')e^{\bar{\psi}\psi'} \tag{46}$$

We obtain

$$
\begin{aligned}
\text{Tr}[\hat{O}] &= \sum_{n=0,1}\langle n|\hat{O}|n\rangle = \sum_{n=0,1}\iint d\bar{\psi}d\psi \, e^{-\bar{\psi}\psi}\langle n|\psi\rangle\langle\psi|\hat{O}|n\rangle \\
&= \iint d\bar{\psi}d\psi \, e^{-\bar{\psi}\psi}\sum_{n=0,1}\langle\psi|\hat{O}|n\rangle\langle n| - \psi\rangle \\
&= \iint d\bar{\psi}d\psi \, e^{-\bar{\psi}\psi}\langle\psi|\hat{O}| - \psi\rangle
\end{aligned}
\tag{47}
$$

where we used the resolution of unity for the orthonormal basis and the coherent states (equation (45)) and the fact that the minus sign in $|-\psi\rangle = |0\rangle + \psi|1\rangle$ comes from commuting the left and right coherent states.

8.1.2 Gaussian integrals

Given two sets of independent Grassmann variables, $\{\psi_j\}$ and $\{\bar{\psi}_j\}$, where $j = 1, 2, \dots, N$, we define the short notation

$$\mathbf{D}[\bar{\psi}_j, \psi_j] = \prod_{j=1}^{N}[d\bar{\psi}_j d\psi_j]$$

Given a complex invertible $N \times N$ matrix $\hat{A}$ and two additional independent sets of Grassmann variables, $\{\chi_j\}$ and $\{\bar{\chi}_j\}$, we wish to calculate the Gaussian integral

$$I[\chi, \bar{\chi}] = \int \mathbf{D}[\bar{\psi}_j, \psi_j]\exp\left\{-\sum_{i,j=1}^{N}\bar{\psi}_i\hat{A}_{ij}\psi_j + \sum_{j=1}^{N}[\bar{\psi}_j\chi_j + \bar{\chi}_j\psi_j]\right\}$$

---

[49]normally ordered: all creation operators are to the left, all annihilation operators are to the right

We observe that for $\chi = \bar{\chi} = 0$ the only non-vanishing contribution to the term in the integral comes from the N-th order expansion of the exponential function, i.e. $\left(- \sum \bar{\psi}_i \hat{A}_{ij} \psi_j \right)^N / N!$, because the number of variables has to be exactly equal to the number of integrals. In this expansion, only terms with all distinct ψ_j and $\bar{\psi}_j$ survive the integration. The surviving terms have signs which correspond to the parity of the permutations, because of the anti-commutation rules. This proves

$$I[0, 0] = \det(\hat{A})$$

Note that the result is not $1/\det(\hat{A})$, as one would expect from a Gaussian integral over complex numbers.

For general χ and $\bar{\chi}$, one notices that $\bar{\psi}\hat{A}\psi - \bar{\psi}\chi - \bar{\chi}\psi = (\bar{\psi} - \bar{\chi}\hat{A}^{-1})\hat{A}(\psi - \hat{A}^{-1}\chi) - \bar{\chi}\hat{A}^{-1}\chi$. The shift of integration variables $\psi \rightarrow \psi + \hat{A}^{-1}\chi$ and $\bar{\psi} \rightarrow \bar{\psi} + \bar{\chi}\hat{A}^{-1}$ works exactly like in ordinary integrals. We conclude

$$I[\chi, \bar{\chi}] = \det(\hat{A}) \exp \left\{ \sum_{i,j=1}^{N} \bar{\chi}_i (\hat{A}^{-1})_{ij} \chi_j \right\} \tag{48}$$

Now consider that we wish to find the average value of an arbitrary product of Grassmann variables $\psi_{a_1} \cdots \psi_{a_n} \bar{\psi}_{b_1} \cdots \bar{\psi}_{b_n}$ weighted with the factor $\exp\left(- \sum_{ij} \bar{\psi}_i \hat{A}_{ij} \psi_j \right)$. With the help of the result above, we find

$$\langle \psi_\alpha \bar{\psi}_\beta \rangle = \frac{1}{I[0, 0]} \frac{\partial^2 I[\chi, \bar{\chi}]}{\partial \chi_\beta \partial \bar{\chi}_\alpha} \bigg|_{\chi=0} = \hat{A}_{\alpha\beta}^{-1} \tag{49}$$

The factor $\frac{1}{I[0,0]}$ is necessary for the normalization of the average value with the given weight function. This can be continued for arbitrary n, for example,

$$\langle \psi_\alpha \psi_\beta \bar{\psi}_\gamma \bar{\psi}_\delta \rangle = \frac{1}{I[0, 0]} \frac{\partial^4 I[\chi, \bar{\chi}]}{\partial \chi_\delta \chi_\gamma \partial \bar{\chi}_\beta \partial \bar{\chi}_\alpha} \bigg|_{\chi=0} = -\hat{A}_{\alpha\gamma}^{-1} \hat{A}_{\beta\delta}^{-1} + \hat{A}_{\alpha\delta}^{-1} \hat{A}_{\beta\gamma}^{-1}$$

The minus sign in the last expression stems from the anti-commutativity of Grassmann derivatives (see equation (44)).

8.1.3 Partition function and action

Let us consider a single quantized state with energy ϵ_0. The Hamiltonian of this system has the form

$$\hat{H} = \epsilon_0 c^\dagger c$$

where c and $c^\dagger$ are the annihilation and creation operators of this state. Since we assumed that our system is in equilibrium at $-\infty$ and we do not consider interactions at this point, it suffices to choose the equilibrium density matrix ρ of the system, which is given by

$$\rho = \frac{e^{-\beta(\hat{H} - \mu\hat{N})}}{\text{Tr}\left[e^{-\beta(\hat{H} - \mu\hat{N})} \right]} = \frac{e^{-\beta(\hat{H} - \mu\hat{N})}}{\sum_{n=0,1} e^{-\beta(\epsilon_0 - \mu)n}} = \frac{e^{-\beta(\hat{H} - \mu\hat{N})}}{1 + e^{-\beta(\epsilon_0 - \mu)}}$$

Recall the time evolution operator $\hat{U}_C = \hat{U}(-\infty, +\infty)\hat{U}(+\infty, -\infty)$ along the closed time contour C $(-\infty \rightarrow \infty \rightarrow -\infty)$ from section (4.1).

The partition function (i.e. the generating functional of the correlation functions) is defined as

$$Z = \text{Tr}[\hat{U}_C \rho]$$

We have already observed that $\hat{U}_C = \mathbb{1}$ if the external fields on the forward branch are the same as the fields on the backwards branch of the contour. From this we obtain the normalization identity $Z = 1$ in our case, which is going to serve as a self-consistency check in the end.

Now we will attempt to calculate $\text{Tr}[\hat{U}_C \rho]$ as the limit of infinite discrete time steps along the contour C.

We divide the contour C into $(2N-2)$ infinitesimal time intervals of length δt, such that

$$-\infty = t_1 < t_2 < \ldots < t_{N-1} < t_N = +\infty = t_{N+1} > t_{N+2} > \ldots > t_{2N-1} > t_{2N} = -\infty$$

as shown in figure 34. Recall that the time evolution operator during δt in the positive (negative) direction is given by $\hat{U}_{\pm\delta t} = e^{\mp i \hat{H}(c^\dagger, c)\delta t} = e^{\mp i \hat{\epsilon}_0 c^\dagger c \delta t}$.
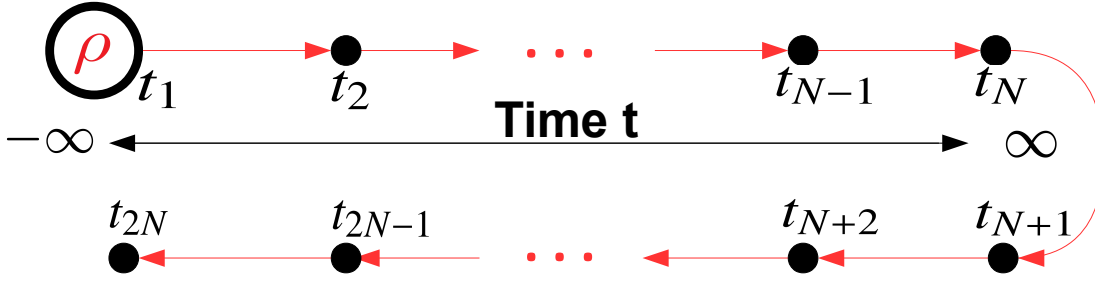
Figure 34: Graphic representation of the closed Keldysh contour with discrete time steps

We use the integral representation of the trace (equation (47)) to calculate $\text{Tr}[\hat{U}_C \rho]$. For example, for $N = 3$ one obtains

$$\text{Tr}[\hat{U}_C \rho] = \iint d\bar{\psi}_6 d\psi_6 \, e^{-\bar{\psi}_6 \psi_6} \langle \psi_6 | \hat{U}_C \rho | - \psi_6 \rangle$$

Now we insert the resolution of unity in the coherent state basis (equation (45)) at each point $j = 1, 2, \ldots, 2N - 1$ along the contour and obtain

$$\text{Tr}[\hat{U}_C \rho] = \int \prod_{i=1}^{2N} [d\bar{\psi}_i d\psi_i] \exp\left(-\sum_{j=1}^{2N} \bar{\psi}_j \psi_j\right) \langle \psi_6 | \hat{U}_{-\delta t} | \psi_5 \rangle \langle \psi_5 | \hat{U}_{-\delta t} | \psi_4 \rangle$$
$$\times \langle \psi_4 | \mathbb{1} | \psi_3 \rangle \langle \psi_3 | \hat{U}_{+\delta t} | \psi_2 \rangle \langle \psi_2 | \hat{U}_{+\delta t} | \psi_1 \rangle \langle \psi_1 | \rho | - \psi_6 \rangle$$

The generalization of this formula to arbitrary N is straightforward. By using equation

(46) we obtain

$$\langle \psi_{j+1}|\hat{U}_{\pm\delta t}|\psi_j\rangle = \langle \psi_{j+1}|\hat{e}^{\mp i\hat{\epsilon}_0 c^\dagger c\delta t}|\psi_j\rangle = e^{\mp i\hat{\epsilon}_0 \bar{\psi}_{j+1}\psi_j\delta t}e^{\bar{\psi}_{j+1}\psi_j} = e^{\bar{\psi}_{j+1}\psi_j(1\mp i\epsilon_0\delta t)}$$

$$\langle \psi_{N+1}|\mathbb{1}|\psi_N\rangle = e^{\bar{\psi}_{N+1}\psi_N}$$

$$\langle \psi_1|\rho| - \psi_{2N}\rangle = \frac{1}{1 + e^{-\beta(\epsilon_0-\mu)}}\langle \psi_1|e^{-\beta(\epsilon_0-\mu)c^\dagger c}| - \psi_{2N}\rangle$$

$$= \frac{1}{1 + e^{-\beta(\epsilon_0-\mu)}}\Big(\langle 0| - \langle 1|\bar{\psi}_1\Big)e^{-\beta(\epsilon_0-\mu)c^\dagger c}\Big(|0\rangle + \psi_{2N}|1\rangle\Big)$$

$$= \frac{1}{1 + e^{-\beta(\epsilon_0-\mu)}}\Big(\langle 0| - \langle 1|\bar{\psi}_1\Big)\Big(|0\rangle + \psi_{2N}e^{-\beta(\epsilon_0-\mu)}|1\rangle\Big)$$

$$= \frac{1 - \bar{\psi}_1\psi_{2N}e^{-\beta(\epsilon_0-\mu)}}{1 + e^{-\beta(\epsilon_0-\mu)}} = \frac{e^{-\bar{\psi}_1\psi_{2N}e^{-\beta(\epsilon_0-\mu)}}}{1 + e^{-\beta(\epsilon_0-\mu)}}$$

Thus, Z can be brought to the form

$$Z = \frac{1}{1 + e^{-\beta(\epsilon_0-\mu)}}\int \mathbf{D}[\bar{\psi}\psi]\exp\left(i\sum_{i,j=1}^{2N}\bar{\psi}_i\hat{g}_{ij}^{-1}\psi_j\right) \tag{50}$$

For example, for $N = 4$ we obtain

$$i\hat{g}^{-1} = \left[\begin{array}{cccc|cccc}
-1 & & & & & & & -e^{-\beta(\epsilon_0-\mu)} \\
1 - i\epsilon_0\delta t & -1 & & & & & & \\
& 1 - i\epsilon_0\delta t & -1 & & & & & \\
& & 1 - i\epsilon_0\delta t & -1 & & & & \\
\hline
& & & +1 & -1 & & & \\
& & & & 1 + i\epsilon_0\delta t & -1 & & \\
& & & & & 1 + i\epsilon_0\delta t & -1 & \\
& & & & & & 1 + i\epsilon_0\delta t & -1
\end{array}\right] \tag{51}$$

The determinant of this matrix is

$$\det(i\hat{g}^{-1}) = 1 + (1 - i\epsilon_0\delta t)^N(1 + i\epsilon_0\delta t)^N e^{-\beta(\epsilon_0-\mu)} = 1 + \Big(1 + \epsilon_0^2\delta t^2\Big)^N e^{-\beta(\epsilon_0-\mu)}$$

Because δt is infinitesimal, we can neglect all terms of higher order than linear in δt for $N \to \infty$. Thus $\det(i\hat{g}^{-1}) = 1 + e^{-\beta(\epsilon_0-\mu)}$. By using the Gaussian integral derived in equation (48), we obtain

$$Z = \frac{\det(i\hat{g}^{-1})}{1 + e^{-\beta(\epsilon_0-\mu)}} = 1$$

which confirms the expected result and underlines the self consistency of our calculation. Note that the existence of the upper right hand element of the matrix is essential for the normalization identity to hold true.

The partition function $Z = \text{Tr}[\hat{U}_C\rho]$ generates the correlation functions of our system and is thus connected to the action S_0 via

$$Z = \int \mathbf{D}[\bar{\psi}_j, \psi_j]\exp\left(iS_0[\bar{\psi}_j, \psi_j]\right) \tag{52}$$

where we have absorbed the constant factor $\frac{1}{1+e^{-\beta(\epsilon_0-\mu)}}$ into the integration measure $\mathbf{D}[\bar{\psi}_j, \psi_j]$. Thus, we can express the action through the matrix $\hat{g}^{-1}$ by using equation (50) and obtain

$$
\begin{aligned}
S_0[\bar{\psi}_j, \psi_j] &= \sum_{j=2}^{2N}\left(i\bar{\psi}_j\psi_j - i\bar{\psi}_j\psi_{j-1} - \epsilon_0\delta t_j\bar{\psi}_j\psi_{j-1}\right) + i\bar{\psi}_1\psi_1 + i\bar{\psi}_1\psi_{2N}e^{-\beta(\epsilon_0-\mu)} \\
&= \sum_{j=2}^{2N}\delta t_j\left(i\bar{\psi}_j\frac{\psi_j - \psi_{j-1}}{\delta t_j} - \epsilon_0\bar{\psi}_j\psi_{j-1}\right) + i\bar{\psi}_1\left(\psi_1 + \psi_{2N}e^{-\beta(\epsilon_0-\mu)}\right)
\end{aligned}
\tag{53}
$$

where $\delta t_j = t_j - t_{j-1} = \pm\delta t$ on the two branches of the contour respectively.

Now we take the limit $N \to \infty$ and use the continuum notation $\psi_j \to \psi(t)$. We write the partition function as

$$
Z = \int \mathbf{D}[\bar{\psi}\psi]\exp\left(iS_0[\bar{\psi}, \psi]\right)
$$

where the action takes the form

$$
S_0[\bar{\psi}, \psi] = \int_C dt\,\bar{\psi}\hat{g}^{-1}\psi
$$

Thus, taking equation (53) into account, in the continuum limit the operator $\hat{G}^{-1}$ is given by

$$
\hat{g}^{-1} = i\partial_t - \epsilon_0
$$

This equation can be understood to be an abbreviation of the large discrete matrix. Thus, the new compact notation has no additional meaning. In particular, in the continuum limit the boundary term $i\bar{\psi}_1\left(\psi_1 + \psi_{2N}e^{-\beta(\epsilon_0-\mu)}\right)$ of the action was discarded. However, we have already seen the importance of the upper right entry in the matrix G_{ij}^{-1} in ensuring the normalization $Z = 1$. We also observe that $(i\partial_t - \epsilon_0)$ is not an invertible operator because it has the eigenmode $e^{i\epsilon_0 t}$ with eigenvalue zero. As a result, one concludes that it is necessary to keep the boundary conditions in mind when handling this operator.

We split the integral along the closed time contour C into two components: the forward and the backward branch. By doing so, we split ψ into ψ^+ and ψ^- and we obtain

$$
S_0[\bar{\psi}, \psi] = \int_{-\infty}^{\infty} dt\left(\bar{\psi}^-(t)(i\partial_t - \epsilon_0)\psi^-(t) - \bar{\psi}^+(t)(i\partial_t - \epsilon_0)\psi^+(t)\right)
$$

The minus sign comes from the reversed direction of time on the backward (+) part of the contour. The ψ^+ and ψ^- fields are correlated because of the nonzero off-diagonal elements of $\hat{G}$, which makes the last equation somewhat incomplete / misleading. Thus, our goal is the development of a continuum notation which takes the normalization and proper correlations into account.

8.1.4 Greens functions

We define

$$
Z[\chi, \bar{\chi}] = \int \mathbf{D}[\bar{\psi}_j, \psi_j]\exp\left(i\sum_{i,j=1}^{2N}\bar{\psi}_i\hat{g}_{ij}^{-1}\psi_j + \sum_{j=1}^{N}[\bar{\psi}_j\chi_j + \bar{\chi}_j\psi_j]\right)
$$

where $Z[0,0] = Z = 1$. The correlator of the fermionic fields is given by

$$\langle \psi_\alpha \bar\psi_\beta \rangle = \int \mathbf{D}[\bar\psi_j, \psi_j] \psi_\alpha \bar\psi_\beta \exp^{iS_0[\bar\psi_j, \psi_j]} = \int \mathbf{D}[\bar\psi_j, \psi_j] \psi_\alpha \bar\psi_\beta \exp\left(i \sum_{i,j=1}^{2N} \bar\psi_i \hat{g}_{ij}^{-1} \psi_j \right)$$

$$= \left. \frac{\partial^2 Z[\chi, \bar\chi]}{\partial \chi_\beta \partial \bar\chi_\alpha} \right|_{\chi=0} = i\hat{g}_{\alpha\beta} Z[0,0] = i\hat{g}_{\alpha\beta}$$

where we have used our previous results about Gaussian integrals (equation (49)). Thus, we have to invert the matrix $\hat{g}^{-1}$ in order to obtain the correlators.

We first observe that $\hat{g}$ can be interpreted as a Greens function, since it is equal to the correlator of the fermionic fields (compare with equation (12)).

We define $h_\pm := 1 \pm \epsilon_0 \delta t$ and $\rho := -e^{-\beta(\epsilon_0 - \mu)}$. For $N = 4$ one can check by a simple multiplication that the inverse of the matrix (51) is given by

$$i\hat{g} = \frac{1}{\det[-i\hat{G}^{-1}]}
\left[
\begin{array}{cccc|cccc}
1 & \rho h_+^3 h_-^2 & \rho h_+^3 h_- & \rho h_+^3 & \rho h_+^3 & \rho h_+^2 & \rho h_+ & \rho \\
h_- & 1 & \rho h_+^3 h_-^2 & \rho h_+^3 h_- & \rho h_+^3 h_- & \rho h_+^2 h_- & \rho h_+ h_- & \rho h_- \\
h_-^2 & h_- & 1 & \rho h_+^3 h_-^2 & \rho h_+^3 h_-^2 & \rho h_+^2 h_-^2 & \rho h_+ h_-^2 & \rho h_-^2 \\
h_-^3 & h_-^2 & h_- & 1 & \rho h_+^3 h_-^3 & \rho h_+^2 h_-^3 & \rho h_+ h_-^3 & \rho h_-^3 \\
\hline
h_-^3 & h_-^2 & h_- & 1 & 1 & \rho h_+^2 h_-^3 & \rho h_+ h_-^3 & \rho h_-^3 \\
h_+ h_-^3 & h_+ h_-^2 & h_+ h_- & h_+ & h_+ & 1 & \rho h_+^2 h_-^3 & \rho h_+ h_-^3 \\
h_+^2 h_-^3 & h_+^2 h_-^2 & h_+^2 h_- & h_+^2 & h_+^2 & h_+ & 1 & \rho h_+^2 h_-^3 \\
h_+^3 h_-^3 & h_+^3 h_-^2 & h_+^3 h_- & h_+^3 & h_+^3 & h_+^2 & h_+ & 1
\end{array}
\right]$$

This can be generalized to arbitrary N. We switch to the fields $\psi_j^\pm$ which sit on the forward and backward branch of the contour respectively, From here on, $j = 1, 2, \ldots, N$. Thus the matrix is indexed as $1, 2, \ldots, N-1, N, N, N-1, \ldots, 2, 1$. We read out of the matrix:

$$\langle \psi_j^+ \bar\psi_{j'}^- \rangle \equiv i\hat{g}_{j|j'}^{+|-} = \frac{\rho h_+^{j'-1} h_-^{j-1}}{\det[-i\hat{g}^{-1}]}$$

$$\langle \psi_j^- \bar\psi_{j'}^+ \rangle \equiv i\hat{g}_{j|j'}^{-|+} = \frac{h_+^{N-j} h_-^{N-j'}}{\det[-i\hat{g}^{-1}]}$$

$$\langle \psi_j^- \bar\psi_{j'}^- \rangle \equiv i\hat{g}_{j|j'}^{-|-} = \frac{h_+^{j'-j}}{\det[-i\hat{g}^{-1}]} \times
\begin{cases}
\rho(h_+ h_-)^{N-1}, & j > j' \\
1, & j \le j'
\end{cases}$$

$$\langle \psi_j^+ \bar\psi_{j'}^+ \rangle \equiv i\hat{g}_{j|j'}^{-|-} = \frac{h_-^{j-j'}}{\det[-i\hat{g}^{-1}]} \times
\begin{cases}
1, & j \ge j' \\
\rho(h_+ h_-)^{N-1}, & j < j'
\end{cases}$$

We define Hermitian conjugation † intuitively as complex conjugation along with the interchange of indices (in this case this corresponds to an interchange in time arguments). By noticing that $h_+^* = h_-$, we observe that

$$(\hat{g}^{-|+})^\dagger = -\hat{g}^{-|+} \quad , \quad (\hat{g}^{+|-})^\dagger = -\hat{g}^{+|-} \quad , \quad (\hat{g}^{+|+})^\dagger = -\hat{g}^{-|-}$$

Now we take the limit $N \to \infty$, while keeping $N\delta t$ constant and denoting $t = j\delta t, t' = j'\delta t$. We observe

$$(h_+ h_-)^{N-1} = (1 + \epsilon_0^2 \delta t^2)^{N-1} \xrightarrow{N \to \infty} 1$$

$$h_\pm^j = (1 \pm i\epsilon_0 \delta t)^j = \left(1 \pm \frac{i\epsilon_0 t}{j}\right)^j \xrightarrow{N\to\infty} e^{\pm i\epsilon_0 t}$$

$$h_+^{N-j} h_-^{N-j'} = (h_+ h_-)^{N-1} h_+^{1-j} h_-^{1-j'} \xrightarrow{N\to\infty} e^{-i\epsilon_0(t-t')}$$

We observe that the fermionic distribution function n_F is given by

$$n_F(\epsilon_0) = \frac{1}{e^{\beta(\epsilon_0-\mu)}+1} = \frac{-\rho(\epsilon_0)}{1-\rho(\epsilon_0)} = -\frac{\rho(\epsilon_0)}{\det[-i\hat{g}^{-1}]}$$

Thus, we obtain in the continuum limit

$$\langle \psi^+(t)\bar{\psi}^-(t')\rangle = i\hat{g}^{+|-}(t|t') = -n_F(\epsilon_0)e^{-i\epsilon_0(t-t')}$$
$$\langle \psi^-(t)\bar{\psi}^+(t')\rangle = i\hat{g}^{-|+}(t|t') = (1-n_F(\epsilon_0))e^{-i\epsilon_0(t-t')}$$
$$\langle \psi^-(t)\bar{\psi}^-(t')\rangle = i\hat{g}^{-|-}(t|t') = \theta(t'-t)i\hat{g}^{-|+}(t|t') + \theta(t-t')i\hat{g}^{+|-}(t|t')$$
$$\langle \psi^+(t)\bar{\psi}^+(t')\rangle = i\hat{g}^{+|+}(t|t') = \theta(t-t')i\hat{g}^{-|+}(t|t') + \theta(t'-t)i\hat{g}^{+|-}(t|t')$$

Essentially, up to now we have calculated the contour-indexed Greens functions and now wish to perform a Keldysh rotation in order to eliminate the redundant degree of freedom (one can check that the new Greens functions satisfy exactly the same redundancy as in equation (13)). The new fermionic fields are defined as

$$\psi_1(t) = \frac{1}{\sqrt{2}}\left(\psi^+(t) + \psi^-(t)\right) \quad , \quad \psi_2(t) = \frac{1}{\sqrt{2}}\left(\psi^+(t) - \psi^-(t)\right)$$

By convention the bar fields transform in a different manner:

$$\bar{\psi}_1(t) = \frac{1}{\sqrt{2}}\left(\bar{\psi}^+(t) - \bar{\psi}^-(t)\right) \quad , \quad \bar{\psi}_2(t) = \frac{1}{\sqrt{2}}\left(\bar{\psi}^+(t) + \bar{\psi}^-(t)\right)$$

In literature, the terms 'quantum' and 'classical' are being avoided in the case of Grassman variables because the have no classical physical meaning and are always integrated out in practical calculations. The resulting Greens functions are highly dependent on the convention of the chosen transformation. In this case we obtain

$$\hat{g}^R(t-t') \equiv \hat{g}^R(t|t') \equiv \hat{g}^{1|1}(t|t') = -i\langle\psi_1(t)\bar{\psi}_1(t')\rangle = -i\theta(t-t')e^{-i\epsilon_0(t-t')}$$
$$\hat{g}^A(t-t') \equiv \hat{g}^A(t|t') \equiv \hat{g}^{2|2}(t|t') = -i\langle\psi_2(t)\bar{\psi}_2(t')\rangle = i\theta(t'-t)e^{-i\epsilon_0(t-t')}$$
$$\hat{g}^K(t-t') \equiv \hat{g}^K(t|t') \equiv \hat{g}^{1|2}(t|t') = -i\langle\psi_1(t)\bar{\psi}_2(t')\rangle = -i\left(1-2n_F(\epsilon_0)\right)e^{-i\epsilon_0(t-t')}$$
$$\hat{g}^{2|1}(t|t') = -i\langle\psi_2(t)\bar{\psi}_1(t')\rangle = 0$$

We notice that $[\hat{G}^R]^\dagger = \hat{G}^A$ and $[\hat{G}^K]^\dagger = -\hat{G}^K$. By taking the Fourier transform with respect to time $(t-t')$, we obtain the free propagators in frequency space:

$$\hat{g}^R(\epsilon) = \frac{1}{\epsilon - \epsilon_0 + i0}$$
$$\hat{g}^A(\epsilon) = \frac{1}{\epsilon - \epsilon_0 - i0}$$
$$\hat{g}^K(\epsilon) = -2\pi i(1 - 2n_F(\epsilon_0))\delta(\epsilon - \epsilon_0)$$

We inserted the infinitesimal terms $\pm i0$ as a prescription for calculations involving integration through the residue theorem, since one has to keep in mind that $\hat{g}^R$ is only nonzero for positive times (i.e. closing of the contour in the upper half of the complex plain), while $\hat{g}^A$ is nonzero for negative times.

To sum up, we have expressed the free propagator

$$\hat{g}_{\alpha\beta}(t|t') = -i \int \mathbf{D}[\bar{\psi}\psi]\psi_\alpha(t)\bar{\psi}_\beta(t') \exp^{iS_0[\bar{\psi},\psi]}$$

in terms of the bare action

$$S_0[\bar{\psi}, \psi] = \int_C dt\, \bar{\psi}(i\partial_t - \epsilon_0)\psi$$

and calculated it.

8.2   Appendix B: Interaction action

We formally treat the action in the interacting case with the goal of calculating the exact propagator (see section 4.8). The notation used in this section is the same as in Appendix A.

In the case of the exact propagator, interactions can no longer be neglected, as observables and correlation functions are affected by them. Thus, it no longer suffices to only consider the bare action S_0, which does not include any interactions. Instead, the interaction action S_{int} which stems from the interaction Hamiltonian has to be added to the total action.

For example, let us consider a normally ordered interaction Hamiltonian of the form

$$\hat{H}_{\text{int}} = A \sum_{k_1,k_2,k_3} c^\dagger_{k_1} c^\dagger_{k_2} c_{k_1-k_3} c_{k_2+k_3}$$

where c_k is an annihilation operator corresponding to an electron with wave number vector k and energy $\epsilon_k = k^2/(2m)$. The corresponding action takes the form

$$S_{\text{int}} = -A \sum_{k_1,k_2,k_3} \int_C dt\, \bar{\psi}(k_1,t)\bar{\psi}(k_2,t)\psi(k_1 - k_3, t)\psi(k_2 + k_3, t)$$

or in continuum notation

$$S_{\text{int}} = -A \int dk^3 \int_C dt\, (\bar{\psi}\psi)^2 = -A \int dk^3 \int_{-\infty}^{\infty} dt\, \left[(\bar{\psi}^+\psi^+)^2 - (\bar{\psi}^-\psi^-)^2\right]$$

We can finally apply a Keldysh rotation to the last term, as we have done before, in order to express the interaction action in terms of the fields ψ_1, ψ_2, $\bar{\psi}_1$ and $\bar{\psi}_2$.

Once again, it is useful to interpret the terms in the action as Feynman diagrams. For example, the term $(\bar{\psi}^+\psi^+)^2$ in the integral above can be considered a vertex with two incoming $+$ lines, two outgoing $+$ lines and vertex factor A. This allows us to calculate expressions such as $\left\langle \mathbb{T}_C S_{\text{int}}^n \right\rangle$ by using Wick's theorem, i.e. evaluating all possible Feynman diagrams of order n.

The exact propagator is then given by:

$$\hat{G}_{\alpha\beta}(t|t') = -i \int \mathbf{D}[\bar{\psi}\psi]\psi_\alpha(t)\bar{\psi}_\beta(t') \exp^{iS_0[\bar{\psi},\psi]+iS_{\text{int}}[\bar{\psi},\psi]}$$

We can evaluate this expression by expanding the exponent in powers S_{int}. The remaining integration with the remaining action S_0 is performed by applying Wick's theorem. We thus obtain an infinite sum of terms, which can be represented as Feynman diagrams. Each such diagram has exactly two external legs: one incoming (representing the contraction between ψ_α and a $\bar{\psi}$-field) and one outgoing (representing the contraction between $\bar{\psi}_\beta$ and a ψ-field).

Note that no disconnected diagrams contribute to this infinite sum. This can be seen in the following way: the partition function

$$Z = \int \mathbf{D}[\bar{\psi}_j, \psi_j] \exp\left(iS_0[\bar{\psi}_j, \psi_j] + iS_{\text{int}}[\bar{\psi}_j, \psi_j]\right)$$

still has to fulfill to normalization identity $Z = 1$,[50] which implies that all terms in the expansion of Z vanish expect the term of zeroth order in S_{int}, which is equal to 1, as shown before. This implies that all expansions of S_{int} vanish if they are not contracted with ψ_α and $\bar{\psi}_\beta$.

8.3 Appendix C: On-site noise

The noise term for equal site indices is calculated here (see section 5.3):

$$
\begin{aligned}
S_{kk} =& \left\langle \hat{I}_k \hat{I}_k \right\rangle - \left\langle \hat{I}_k \right\rangle\left\langle \hat{I}_k \right\rangle = -\frac{e^2 \tau_k^2}{\hbar^2} \left\langle (c_k c_{k+1}^\dagger - c_{k+1} c_k^\dagger)(c_k c_{k+1}^\dagger - c_{k+1} c_k^\dagger) \right\rangle - \left\langle \hat{I}_k \right\rangle^2 \\
=& -\frac{e^2 \tau_k^2}{\hbar^2} \left\langle c_k c_{k+1}^\dagger c_k c_{k+1}^\dagger + c_{k+1} c_k^\dagger c_{k+1} c_k^\dagger - c_k c_{k+1}^\dagger c_{k+1} c_k^\dagger - c_{k+1} c_k^\dagger c_k c_{k+1}^\dagger \right\rangle - \left\langle \hat{I}_k \right\rangle^2 \\
=& -\frac{e^2 \tau_k^2}{\hbar^2} \left\langle c_k c_{k+1}^\dagger c_k c_{k+1}^\dagger + c_{k+1} c_k^\dagger c_{k+1} c_k^\dagger - c_k c_k^\dagger c_{k+1}^\dagger c_{k+1} - c_k^\dagger c_{k+1} c_{k+1}^\dagger c_k \right\rangle - \left\langle \hat{I}_k \right\rangle^2 \\
=& -\frac{e^2 \tau_k^2}{\hbar^2} \left\langle c_k c_{k+1}^\dagger c_k c_{k+1}^\dagger + c_{k+1} c_k^\dagger c_{k+1} c_k^\dagger + c_k^\dagger c_{k+1}^\dagger c_{k+1} c_k + c_k^\dagger c_{k+1}^\dagger c_{k+1} c_k - c_{k+1}^\dagger c_{k+1} - c_k^\dagger c_k \right\rangle - \left\langle \hat{I}_k \right\rangle^2 \\
=& \frac{e^2 \tau_k^2}{\hbar^2} \left\langle c_{k+1}^\dagger c_{k+1}^\dagger c_k c_k + c_k^\dagger c_k^\dagger c_{k+1} c_{k+1} - c_k^\dagger c_k^\dagger c_{k+1} c_k - c_k^\dagger c_{k+1}^\dagger c_{k+1} c_k + c_{k+1}^\dagger c_{k+1} + c_k^\dagger c_k \right\rangle - \left\langle \hat{I}_k \right\rangle^2 \\
=& \frac{e^2 \tau_k^2}{\hbar^2} \left\langle \mathbb{T}_C \left(c_{k+1}^{+\dagger} c_{k+1}^{+\dagger} c_k^- c_k^- + c_k^{+\dagger} c_k^{+\dagger} c_{k+1}^- c_{k+1}^- - c_k^{+\dagger} c_{k+1}^{+\dagger} c_{k+1}^- c_k^- - c_k^{+\dagger} c_{k+1}^{+\dagger} c_{k+1}^- c_k^- + c_{k+1}^{+\dagger} c_{k+1}^- + c_k^{+\dagger} c_k^- \right) \right\rangle \\
& - \left\langle \hat{I}_k \right\rangle^2 \\
=& \frac{e^2 \tau_k^2}{\hbar^2} \left\langle \mathbb{T}_C \left(c_k^- c_k^- c_{k+1}^{+\dagger} c_{k+1}^{+\dagger} + c_{k+1}^- c_{k+1}^- c_k^{+\dagger} c_k^{+\dagger} - 2 c_k^{+\dagger} c_{k+1}^{+\dagger} c_{k+1}^- c_k^- + c_{k+1}^{+\dagger} c_{k+1}^- + c_k^{+\dagger} c_k^- \right) \right\rangle - \left\langle \hat{I}_k \right\rangle^2 \\
=& \frac{e^2 \tau_k^2}{\hbar^2} \left\langle \mathbb{T}_C \left(c_k^- c_k^- c_{k+1}^{+\dagger} c_{k+1}^{+\dagger} + c_{k+1}^- c_{k+1}^- c_k^{+\dagger} c_k^{+\dagger} + 2 c_k^{+\dagger} c_{k+1}^- c_{k+1}^{+\dagger} c_k^- + c_{k+1}^{+\dagger} c_{k+1}^- - c_k^{+\dagger} c_k^- \right) \right\rangle - \left\langle \hat{I}_k \right\rangle^2 \\
=& \frac{e^2 \tau_k^2}{\hbar^2} \left\langle \mathbb{T}_C \left(c_k^- c_k^- c_{k+1}^{+\dagger} c_{k+1}^{+\dagger} + c_{k+1}^- c_{k+1}^- c_k^{+\dagger} c_k^{+\dagger} - 2 c_{k+1}^- c_k^- c_k^{+\dagger} c_{k+1}^{+\dagger} - c_{k+1}^{+\dagger} c_{k+1}^- - c_k^{+\dagger} c_k^- \right) \right\rangle - \left\langle \hat{I}_k \right\rangle^2 \\
=& \frac{e^2 \tau_k^2}{\hbar^2} \left\langle \mathbb{T}_C \left(c_k^- c_k^- c_{k+1}^{+\dagger} c_{k+1}^{+\dagger} + c_{k+1}^- c_{k+1}^- c_k^{+\dagger} c_k^{+\dagger} + c_{k+1}^- c_k^- c_{k+1}^{+\dagger} c_k^{+\dagger} + c_k^- c_{k+1}^- c_k^{+\dagger} c_{k+1}^{+\dagger} \right) \right\rangle \\
& + \frac{e^2 \tau_k^2}{\hbar^2} \left\langle \mathbb{T}_C \left(- c_{k+1}^{+\dagger} c_{k+1}^- - c_k^{+\dagger} c_k^- \right) \right\rangle - \left\langle \hat{I}_k \right\rangle^2
\end{aligned}
$$

---

[50]We have argued in previous sections that $Z = 1$ is always true unless we insert a potential which acts differently on the forward and backward branch of the contour.

$$
= \frac{e^2 \tau_k^2}{\hbar^2} \Big\langle \mathbb{T}_C \Big(c_{k+1}^- c_k^- c_{k+1}^{+\dagger} c_k^{+\dagger} + c_k^- c_{k+1}^- c_k^{+\dagger} c_{k+1}^{+\dagger} - c_k^- c_k^- c_{k+1}^{+\dagger} c_{k+1}^{+\dagger} - c_{k+1}^- c_{k+1}^- c_k^{+\dagger} c_k^{+\dagger} \Big) \Big\rangle - \Big\langle \hat{I}_k \Big\rangle^2
$$

$$
+ \frac{e^2 \tau_k^2}{\hbar^2} \Big\langle \mathbb{T}_C \Big(2 c_k^- c_k^- c_{k+1}^{+\dagger} c_{k+1}^{+\dagger} + 2 c_{k+1}^- c_{k+1}^- c_k^{+\dagger} c_k^{+\dagger} - c_{k+1}^{+\dagger} c_{k+1}^- - c_k^{+\dagger} c_k^- \Big) \Big\rangle
$$

$$
= \text{previous } + \frac{e^2 \tau_k^2}{\hbar^2} \Big\langle \mathbb{T}_C \Big(2 c_k^- c_k^- c_{k+1}^{+\dagger} c_{k+1}^{+\dagger} + 2 c_{k+1}^- c_{k+1}^- c_k^{+\dagger} c_k^{+\dagger} - c_{k+1}^{+\dagger} c_{k+1}^- - c_k^{+\dagger} c_k^- \Big) \Big\rangle
$$

$$
= \text{previous } + \frac{e^2 \tau_k^2}{\hbar^2} \Big\langle \mathbb{T}_C \Big(c_{k+1}^- c_{k+1}^{+\dagger} + c_k^- c_k^{+\dagger} - 2 \Big) \Big\rangle
$$

$$
= \text{previous } + \frac{e^2 \tau_k^2}{\hbar^2} \Big(i G_{k|k}^{-|+} + i G_{k+1|k+1}^{-|+} - 2 \Big)
$$

Note that we used $c_k c_k = 0$ (due to the anti-commutation rules of fermionic operators) several times. In this context, 'previous' refers to the term in equation (29), where j is set equal to k, specifically:

$$
\text{previous } \equiv - \frac{e^2 \tau_k^2}{\hbar^2} \Big(G_{k+1,k|k,k+1}^{--|++} + G_{k,k+1|k+1,k}^{--|++} - G_{k,k|k+1,k+1}^{--|++} - G_{k+1,k+1|k,k}^{--|++} \Big)
$$

$$
- \frac{e^2 \tau_k^2}{\hbar^2} \Big(G_{k|k+1}^{-|+} - G_{k+1|k}^{-|+} \Big) \Big(G_{k|k+1}^{-|+} - G_{k+1|k}^{-|+} \Big)
$$

9 References

[Bü92]   M. Büttiker. Scattering theory of current and intensity noise correlations in con-
            ductors and wave guides. *Phys. Rev. B*, 46:12485–12507, Nov 1992.

[BB00]   Ya.M. Blanter and M. Büttiker. Shot noise in mesoscopic conductors. *Physics
            Reports*, 336(1):1 – 166, 2000.

[BGG+05]   H. Bouchiat, Y. Gefen, S. Guéron, G. Montambaux, and J. Dalibard.
            *Nanophysics: Coherence and Transport: Lecture Notes of the Les Houches Sum-
            mer School 2004*. Les Houches. Elsevier Science, 2005.

[BHS+13]   Florian Bauer, Jan Heyder, Enrico Schubert, David Borowsky, Daniela Taubert,
            Benedikt Bruognolo, Dieter Schuh, W. Wegscheider, Jan von Delft, and Stefan
            Ludwig. Microscopic origin of the '0.7-anomaly' in quantum point contacts.
            Nature, 501:73–78, 2013.

[BHvD14]   Florian Bauer, Jan Heyder, and Jan von Delft. Functional renormalization
            group approach for inhomogeneous interacting fermi systems. *Phys. Rev. B*,
            89:045128, Jan 2014.

[CLGG+02] S. M. Cronenwett, H. J. Lynch, D. Goldhaber-Gordon, L. P. Kouwenhoven,
            C. M. Marcus, K. Hirose, N. S. Wingreen, and V. Umansky. Low-temperature
            fate of the 0.7 structure in a point contact: A kondo-like correlated state in an
            open system. *Phys. Rev. Lett.*, 88:226805, May 2002.

[DZM+06]   L. DiCarlo, Y. Zhang, D. T. McClure, D. J. Reilly, C. M. Marcus, L. N. Pfeiffer,
            and K. W. West. Shot-noise signatures of 0.7 structure and spin in a quantum
            point contact. *Phys. Rev. Lett.*, 97:036810, Jul 2006.

[FW03]   A.L. Fetter and J.D. Walecka. *Quantum Theory of Many-particle Systems*. Dover
            Books on Physics. Dover Publications, 2003.

[GPM07]   R. Gezzi, T. Pruschke, and V. Meden. Functional renormalization group
            for nonequilibrium quantum many-body problems. *Physical Review B*,
            75(4):045324, January 2007.

[Jak10]   Severin Georg Jakobs. *Functional renormalization group studies of quantum
            transport through mesoscopic systems*. PhD thesis, RWTH Aachen, 2010.

[JPS10a]   S. G. Jakobs, M. Pletyukhov, and H. Schoeller. Nonequilibrium functional
            renormalization group with frequency-dependent vertex function: A study of
            the single-impurity Anderson model. *Phys. Rev. B, 81.195109*, 81(19):195109,
            May 2010.

[JPS10b]   S. G. Jakobs, M. Pletyukhov, and H. Schoeller. TOPICAL REVIEW: Proper-
            ties of multi-particle Green's and vertex functions within Keldysh formalism.
            Journal of Physics A Mathematical General, 43(10):103001, March 2010.

[Kam11]   Alex Kamenev. *Field Theory of Non-Equilibrium Systems*. Cambridge University Press, 2011.

[Kar06]   C. Karrasch. Transport Through Correlated Quantum Dots – A Functional Renormalization Group Approach. *eprint arXiv:cond-mat/0612329*, December 2006.

[KBH+00]   A Kristensen, Henrik Bruus, Adam Hansen, J B. Jensen, Poul Lindelof, C J. Marckmann, J Nygard, C Sørensen, F Beuscher, A Forchel, and M Michel. Bias and temperature dependence of the 0.7 conductance anomaly in quantum point contacts. *Physical review. B, Condensed matter*, 62, 06 2000.

[Kv18]   F. B. Kugler and J. von Delft. Multiloop functional renormalization group for general models. 97(3):035162, February 2018.

[Lan57]   R. Landauer. Spatial variation of currents and fields due to localized scatterers in metallic conduction. *IBM Journal of Research and Development*, 1957.

[Mar05]   T. Martin. Noise in mesoscopic physics. *eprint arXiv:cond-mat/0501208*, January 2005.

[Mic11]   A. P. Micolich. What lurks below the last plateau: experimental studies of the 0.7 $\times 2e^2$/h conductance anomaly in one-dimensional systems. *Journal of Physics Condensed Matter*, 23:443201, November 2011.

[Neg18]   J.W. Negele. *Quantum Many-particle Systems*. CRC Press, 2018.

[Ogu01]   A. Oguri. Transmission Probability for Interacting Electrons Connected to Reservoirs. *Journal of the Physical Society of Japan*, 70:2666, September 2001.

[Sch18]   Dennis Schimmel. *Transport through inhomogeneous interacting low-dimensional systems*. PhD thesis, LMU Munich, January 2018.

[Tay12]   J.R. Taylor. *Scattering Theory: The Quantum Theory of Nonrelativistic Collisions*. Dover Books on Engineering. Dover Publications, 2012.

[TNS+96]   K. J. Thomas, J. T. Nicholls, M. Y. Simmons, M. Pepper, D. R. Mace, and D. A. Ritchie. Possible spin polarization in a one-dimensional electron gas. *Phys. Rev. Lett.*, 77:135–138, Jul 1996.

[vHB05]   H. van Houten and C. W. J. Beenakker. Quantum point contacts. *eprint arXiv:cond-mat/0512609*, December 2005.

[vKv+88]   B. J. van Wees, L. P. Kouwenhoven, D. van der Marel, H. von Houten, and C. W. J. Beenakker. Quantized conductance of point contacts in a two-dimensional electron gas. *Physical Review Letters*, 60:848–850, February 1988.

[WBvD17]   Lukas Weidinger, Florian Bauer, and Jan von Delft. Functional renormalization group approach for inhomogeneous one-dimensional fermi systems with finite-ranged interactions. *Phys. Rev. B*, 95:035122, Jan 2017.

10 Acknowledgements

I would like to sincerely thank Prof. Jan von Delft for supervising me in my Bachelor project and suggesting this topic, thereby giving me this excellent opportunity to participate in research and significantly broaden my knowledge.

Furthermore, I would like to extend a very warm thank you to my direct supervisor, Lukas Weidinger, for the introduction to the software and theoretical background, the countless discussions we had and the many hours, which he spared for me - filled with providing suggestions, engaging in mutual problem solving and supporting me throughout the project.

Finally, I am grateful to the members of the department of Theoretical Solid State Physics at the LMU Munich, who were very friendly to me and with whom I engaged in some very interesting conversations throughout my time at the faculty.

11   Declaration

I hereby declare that I have written the present work independently and that I have not used any sources or resources other than those specified in the work.

Hiermit erkläre ich, die vorliegende Arbeit selbständig verfasst zu haben und keine anderen als die in der Arbeit angegebenen Quellen und Hilfsmittel benutzt zu haben.

Munich, November 22, 2018

Andreas Tsevas